NTNU – Trondheim
Norwegian University of
Science and Technology

Frequency Response Presentation of Power System Components

Olav Westeng Alstad

Master of Energy and Environmental Engineering
Submission date: June 2015
Supervisor: Kjetil Uhlen, ELKRAFT
Co-supervisor: Steinar Danielsen, Jernbaneverket

Norwegian University of Science and Technology
Department of Electric Power Engineering

Problem Description

After the introduction of advance electric traction vehicles, the electric traction system has experienced problems related to low frequency power oscillations. To solve this, the dynamics of a vehicle can be modeled as a set of frequency responses. These frequency responses gives the relation between dq transformed currents and voltages, seen from an input-output approach of the vehicle.

To reveal the frequency responses of the vehicle, a set of tests has been performed. However, there are some issues related to achieving the correct frequency responses, and further implement the frequency responses in stability analysis:

- How does the test infrastructure affect the test results?
- During the tests, the excitation voltage was deviating from its test specifications. Why?
- How truthful will the developed frequency responses be?
- How can the resulting frequency responses be applied for stability analysis?

Abstract

This master thesis presents a method for stability analysis. The dynamics of an electric system are described through frequency dependent impedances and admittances. This is presented with the basis of an electric traction vehicle. The frequency responses of the vehicle are revealed and verified through tests, compensations and analyzes of test measurements.

After the introduction of advance electric traction vehicles, the electric traction system has experienced problems related to low frequency power oscillations. To solve these problems the dynamics of the vehicle is modeled. This is conducted from an input-output approach at the interface of the vehicle seen from the rest of the system. The input and output are small changes in voltage and current from a linearized operation point. The vehicle is presented as a set of four admittances in the dq system. These admittances are functions of the oscillation frequency, further referred to as frequency responses.

A description of an electric oscillating system can be done by using modulated signals. In this thesis, current and voltage are described as amplitude- and phase modulated components. Calculations with modulated components requires an extension of the phasor system. This extension, and relevant calculation rules and examples, are presented in this thesis.

Further, tests to reveal the frequency responses of the vehicle is presented. Measurements from the tests show deviations from the specified excitation voltage. Analysis of the test measurements explains some of these deviations. Since the frequency responses do not depend on the excitation voltage, the tests are verified as sufficient for their purpose. After compensating for the test topology, a set of frequency responses for the vehicle are found. They are considered as correct, but have limitations. The numeric frequency responses are extracted to transfer functions. At last, usage of the transfer functions in stability analysis with several vehicles is presented.

Sammendrag

Denne oppgaven vil presentere en metode for stabilitetsanalyser. Her blir dynamikken til et elektrisk system beskrevet gjennom frekvensavhengige impedanser og admittanser. Dette blir gjort med utgangspunkt i ett elektrisk tog. Togets frekvensresponser avdukes og verifiseres gjennom tester, kompensering, og analyser av måledata.

Etter innføringen av avanserte elektriske tog har jernbanenettet opplevd problemer med lavfrekvente energisvingninger. For å løse disse problemene bør togenes indre dynamikk modelleres. Dette kan gjøres ved å se på forholdet mellom inngang og utgang på togets grensesnitt til resten av systemet. Inngang og utgang er små endringer i spenning og strøm fra et linearisert arbeidspunkt. Toget representeres her som et sett med fire admittanser i dq-systemet. Disse admittansene er funksjoner av svingefrekvensen, heretter kalt frekvensresponser.

En beskrivelse av et svingende elektrisk system kan gjøres ved hjelp av modulerte signaler. I oppgaven beskrives strøm og spenning som amplitude- og fasemodulerte størrelser. Beregninger med modulerte størrelser krever en utvidelse av visersystemet. En slik utvidelse, med tilhørende regneregler og eksempler på anvendelse, er presentert i oppgaven.

Videre i oppgaven presenteres tester for å avdekke togets frekvensresponser. Måledata fra testene viser at eksiteringsspenningen avviker fra testspesifikasjonene. Analyser av måledata forklarer noe av dette avviket. Siden frekvensresponsene ikke avhenger av eksiteringsspenningen blir testene verifisert som tilstrekkelig gode. Etter kompensasjon for testtopologi, blir ett sett med frekvensresponser funnet. Disse ansees som riktige, men har sine begrensninger. De numeriske frekvensresponsene blir så ekstrahert til transferfunksjoner. Oppgaven avsluttes med å vise hvordan disse kan brukes i stabilitetsanalyser av et system med flere tog.

Acknowledgments

First, I want to thank Jernbaneverket for providing data and documents, and giving me the opportunity for studies in interesting topics. I want to thank Stanislav Pika for showing great interest in my work, answering technical questions, providing data, and participating in interesting discussions. Further, I want to thank my supervisors, Prof. Kjetil Uhlen, and Dr. Steinar Danielsen, for their guidance, interesting discussions, and wisely advises. Thanks to my sister, Bjørg Elise Alstad, and my friend Jørgen Viken, for being of great support during the writing of this thesis. Finally, thanks to all my fellow students and employees at NTNU for these last five years. They have been great!

Contents

Chapter 1

Introduction

This chapter gives motivation, relevant background information with relevant reference, scope of work and the outline of the thesis. Further, this chapter presents methods and limitation.

1.1 Motivation

The motivation of this master thesis is contribute to solve the problem of low frequency oscillations in the Norwegian electric traction system. This might be conducted through stability analysis in a system including an electric traction vehicle, a line and a converter. Thus, the dynamic behavior of these components needs to be known. Modern electric traction vehicles are demanding to model due to the usage of power electronics and advance digital control. In addition, the inner topology of the electric vehicles is often hidden for the system operator(s), due to company secrets.

By modeling the vehicle by an input-output approach, the inner topology of the vehicle can be ignored. This approach make use of frequency dependent impedances and admittances. In case of admittances, the relation of small changes in current due to a small changes of voltage is given as a function of the oscillating frequency. The impedances and admittances can be found by specific tests on the components. Therefore, this method is beneficial for modeling components where the inner topology is hidden or challenging to model.

However, there might be several issues during calculations of the frequency responses from a set of measurements. This is the case for tests performed by Jernbaneverket. These issues

are related to the interaction of other parts of the system, and the complexity of achieving the correct frequency responses. It is important for further stability analysis to solve these issues, obtain the correct frequency responses, and apply these frequency responses correctly.

1.2 Background

In this section, the background of the work during this master thesis will be given. The major references at each field are presented continuously.

1.2.1 Stability in the electric traction system

The Norwegian electric traction system is a 15 kV, 16 2/3 Hz, single phase power system. The power system is mainly supplied through rotating converters connected to the 50 Hz national utility grid.

After the introduction of modern electric vehicles, equipped with power electronics and digital control, low frequency instability has become an issue in electric traction systems. Especially in the Norwegian traction system consisting of long radial lines with high impedance.

S. Danielsen's[2] PhD concerns electric traction stability, and gives an introduction to electric traction systems. For further details about electric traction systems, see Kiessling, et al.[7], Steimel[19] or Östlund[14].

1.2.2 "DQ approach" to the stability of an electric traction system

The dynamics of an electric traction vehicle can be modeled by an input-output approach of the vehicle. These inputs and outputs are small changes of currents and voltages at the interface at the vehicle. The change of current and voltage are given as dq-transformed components. The input-output are given by frequency dependent admittances or impedances. The dynamic behavior of the electric traction vehicle is then described at the interface to the rest of the system without any information about the inner topology. This approach was first suggested by Menth and Meyer[10], and further developed by e.g. Danielsen[2] and Pika[17]. This approach is called the "DQ approach" as suggested by Pika.

1.2.3 The "DQ tests"

The admittance or impedance of a component can be measured by performing tests on its interface. The component's behavior during excitation by an oscillating voltage is measured. The oscillating voltage has an increasing oscillating frequency, such that the frequency response can be achieved. To fully reveal the dynamic behavior of the vehicle, two voltage sweeps has to be performed: One direct modulated voltage sweep and one quadrature modulated voltage sweep[1].

The process for achieving the frequency responses of an electric vehicle is roughly illustrated by Figure 1.1. The method is further called the "DQ test". This test are close connected to the "DQ approach", thus the same references yields.

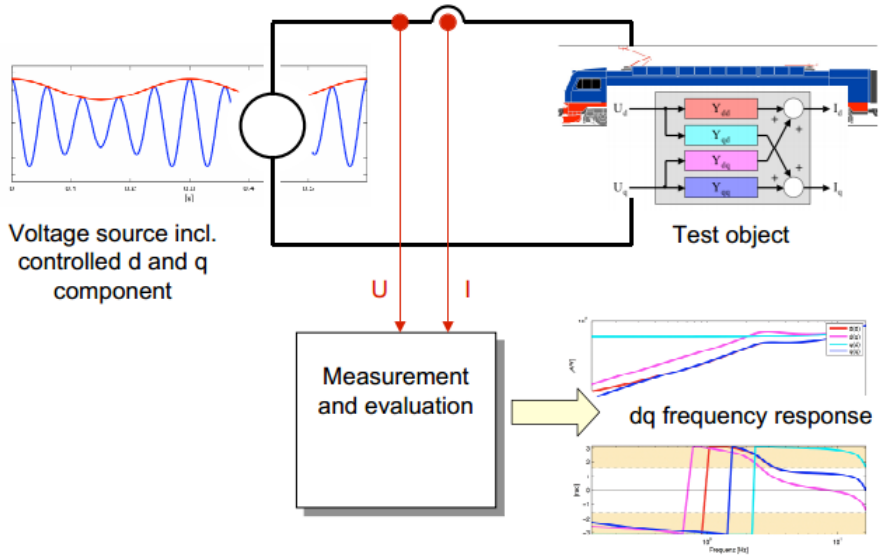

Figure 1.1: From "DQ tests" to frequency responses. Markus Meyer[12]

1.2.4 "DQ tests" at Alnabru

"DQ tests" on an electric traction vehicle are performed as a part of a joint research program of Jernbaneverket, Trafikverket, ABB and Emkamatik[16]. The tests were conducted on June 27 and 28, 2014 at Alnabru converter station, Norway. The tests were conducted in island mode with a static converter. The test topology is given in Figure 1.2. Tests for several operations were

[1]Later in this thesis, it is shown that these sweeps do not have to be exactly direct- and quadrature modulated

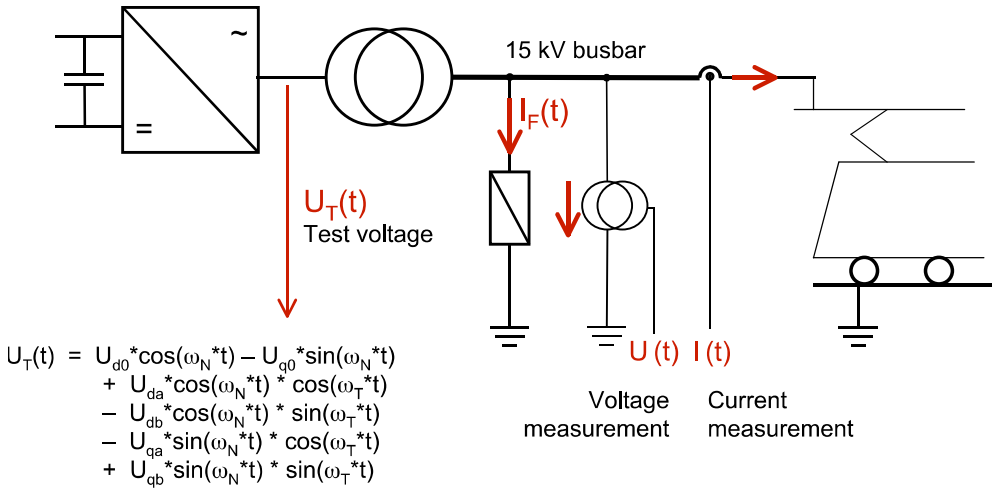

Figure 1.2: Setup for the "DQ tests". Menth and Meyer[9]

performed. This thesis will study tests were the vehicle is in idle mode; ID33d and ID33q.

More information about the test can be found in the test report by Pika[16], and further in this thesis. Reports of achiving the frequency response of the electric traction vehicle is conducted by Danielsen and Pika[3] and by Emkamatikk[9]. These "DQ tests" was one of the topics of the authors project from fall 2014[1].

There are several issues related to the "DQ tests" at Alnabru. Since the vehicle can not be fully isolated, the frequency responses might be affected by other parts of the topology, seen in Figure 1.2. The reference of the voltage sweeps is located in the static converter, thus not the same place as the point of measurements. In addition, the measured excitation voltage deviates from the test specification. These issues are the basis of this thesis' research questions, which are presented in Section 1.3.

1.3 Research questions

- How does the test infrastructure affect the test results?
- During the tests, the excitation voltage was deviating from its test specifications. Why?
- How truthful will the developed frequency responses be?
- How can the resulting frequency responses be applied for stability analysis?

1.4 Outline of report

- Chapter 1 gives motivation, relevant background information with references, scope of work and the outline of the thesis. Further, this chapter presents methods and limitation.

- Chapter 2 introduces direct and quadrature modulated signals. These signals are applied for description of currents and voltages in an oscillating system. Studies of these signals are conducted in order to establish rules for calculations regarding stability analysis using the "DQ approach". These studies includes detailed information of the dq transformation and phasor representation.

- Chapter 3 introduces a method for stability analysis where the dynamics of the system are presented through frequency dependent admittances and impedances. A modification of the classic description of this method is suggested. Further, the analytic frequency responses of some components are established. At last, application of these responses in electric systems is presented.

- Chapter 4 gives a summary of the project from fall 2014. The project includes calculations and methods to establish the frequency responses of a system from measurements from "DQ tests". Further, the frequency responses of an electric traction vehicle is established through analytically compensation for a line and a cable.

- Chapter 5 presents analysis of the voltage measurements from the "DQ tests" at Alnabru. These analyzes explain some of the unexpected measurements, and is necessary in order to verify the test results. These analysis includes a wide presentation of the measurements from different views, calculation of the voltage drop over a transformer, and representation of the results in both the modulation domain, fundamental domain and time domain.

- Chapter 6 discuss how imperfect "DQ tests" affects the resulting frequency responses. The mathematical description of the system states that imperfect tests are sufficient for achieving the correct frequency responses. However, the excitation voltage can not be in conflict with the linearization point.

- Chapter 7 presents a set of extracted transfer functions from the numeric frequency response of the electric traction vehicle. Application of these transfer functions in a larger electric system during stability analysis is presented.

- Chapter 8 makes conclusions of the discoveries made in this thesis. Later, proposals to further work is suggested.

1.5 Methods

The research questions of Section 1.3 is investigated using the following methods:

- Literature studies of mainly the electric traction system, stability analysis of electric traction systems, dq transformation, the "DQ approach", and the "DQ test". All the major references are given in 1.2

- Investigations on the data from the "DQ tests" at Alnabru. This data includes both time domain data and dq transformed data. The investigations are mainly performed by studying plots which reveals different relations and approaches to the topic. Some of these plots are presented in Section 5

- Analysis on direct and quadrature modulated signals. These analysis has been performed by studying the mathematically description (Equation 2.3) with corresponding plots of different combinations of signals.

- Time to dq transformation of both measured data and articicial signals. This dq transformation is performed by a function developed by M. Meyer[11].

- Application and studies of linear states spaces.

- All calculations are performed by using MATLAB[2].

[2]MATLAB, The MathWorks, Inc., Natick, Massachusetts, United States.

1.6 Limitations

The limitation of this thesis is divided into limitation of the model, and limitation of the performance of the studies:

1.6.1 Limitation of the model

- A set of frequency responses is related to one specific operation point and linearized of amplitude of the disturbances.

1.6.2 Limitation of the performance

Some issues according to the limitations of data, software, and models have decreased the progression of the studies. If the following things have been available, the progression of the thesis would been faster:

- Available dq transformed components a bit earlier. A lot of effort were but since the authors frequency response did not match other available numeric frequency responses. The author did not know that this error was due to poor preconditioning of the time data.
- Available analytic frequency responses of the vehicle and the static converter. These data might be available through existing models. However, the effort of extracting frequency responses of old models with unknown simulation tools was considered as to large.
- A-time-to-fundamental function had been very nice.
- Measurements on the terminal of the static converter

Chapter 2

Direct- and quadrature modulated signals

This chapter introduces direct and quadrature modulated signals. These signals are applied for description of currents and voltages in an oscillating system. Studies of these signals are conducted in order to establish rules for calculations regarding stability analysis using the "DQ approach". These studies includes detailed information of the dq transformation and phasor representation.

2.1 The dq-transformation

The direct–quadrature–zero (dq0)transformation (from now on called dq transformation) is a mathematical transformation used to simplify dynamic analysis of electric systems. The dq transformation was developed by Park in 1929[15] for simplified analysis of electric machines, and is also known as Park transformation.

2.1.1 Motivation

The dq transformation results in a system where the phase and amplitude can be treated as two decoupled components: the direct component and the quadrature component. These values will in regular steady state operation appear as DC values. As dynamics in the system appear, these DC-values will start oscillating. This is beneficial from a control theoretical view. The dq transformation is widely used in control of energy converters, which is used in traction- vehicles and power supply.

2.1.2 dq transformation in three phase systems

The dq transformation is mainly used on three phase systems. If the three phase system is balanced, the transformation reduces the three AC quantities to two DC quantities. Simplified calculations can then be carried out on these DC quantities. The inverse transformation on the resulting DC quantities will recover the actual three phase AC results.

2.1.3 dq transformation in single phase systems

For single phase quantities in steady state, the dq transformation has much in common to the phasor system:

dq transformation vs phasor representing

- *A phasor* is a complex representation of a sinusoidal signal where amplitude, frequency and phase are time-invariant. A voltage phasor can be represented in two ways: $U = U_{eff}\angle\theta_{phase}$ and $U = U_{Re} + jU_{Im}$.

- By letting the orthogonal *dq-frame* rotate in the same speed as the fundamental frequency, a steady state signal is described by two DC values related to the amplitude and the time deviation; U_d and U_q.

The references of these two systems can both be defined arbitrary. If the reference of the two systems are the same, and the signal to be described are the same, the two representation are quite equal: The DC terms of the dq transformation, is equal the imaginary and complex projection of the phasor representation. This is shown by Equation 2.1 (dq transformation) and Equation 2.2 (phasor):

$$U = \begin{bmatrix} U_d \\ U_q \end{bmatrix} \tag{2.1}$$

$$U = U_d + jU_q \tag{2.2}$$

For *steady state operation*; representation of single phase sinusoidal signals as phasors is well developed. Therefore dq transformation on single phase steady state signals is also well developed. More details about the phasor system, can be found from an electric approach (e.g. Nilsson and Riedel[13]) or a mathematically approach (e.g. Kreyszig[8]).

The dq transformation for dynamic analysis

The phasor system can only be applied for steady state systems. Therefore, the dq transformation can be considered as an extended version of the phasor system, valid for dynamic electrical systems.

To transform a single phase component to dq components might not be easy for dynamic cases. This can be understood by considering a measurement for a infinite short period: In the case of single phase signal, the measurement results in one single scalar that gives the instant value of the signal. From only this value, it is impossible to to find the total amplitude or the phase of the signal. For the three phase case, the measurement gives three scalar values. If each phase is symmetric[1], these three values reveals both the phase and the amplitude of the three phase signals. The infinite short time periode must be considered in order to do the transformation for dynamic systems. Since the system is dynamic, the dq components vary and the specific values for an instant moment can not be based on measurements of a spanning time period. However, methods are developed for doing dq transformation for single phase systems, e.g. by introducing an artificial perpendicular component to the single phase component[5].

2.2 Voltage modulation

In this master thesis, the system is excited with modulated voltage. In addition to the fundamental sinusoidal voltage, the voltage is modulated so the amplitude and/or phase of the fundamental voltage vary sinusoidally with a modulation frequency. An example of a modulated signal is shown in Figure 2.1.

[1]The dq transformation only makes sense for symmetric systems. In non-symmetric systems the state of the system can not be described by just two variables.

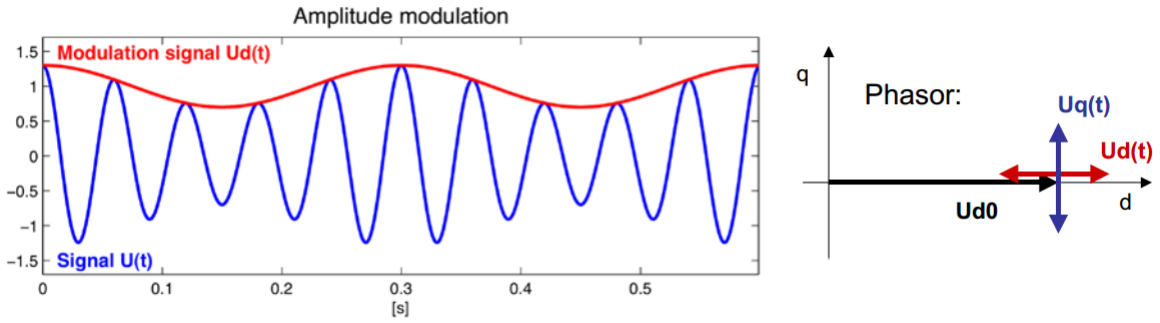

Figure 2.1: To the left: $U(t)$ is the modulated signal. It is direct modulated by the modulation signal Ud(t) in red so the direct component of U(t) vary with time. An eventual quadrature modulated component is not visible in this figure in the time frame. To the right: Phasor representation: U_{d0} is constant, $U_q(t)$ and $U_d(t)$ varies with time in range illustrated by the phasors. Figure by M. Meyer[12]

2.2.1 Motivation

In order to perform stability analysis, the dynamic behavior of the system must be known. To detect the dynamic behavior, the system can be excited with dynamic signals. One way of doing this excitation is to excite the component with modulated signals, where the modulation specifications vary.

2.2.2 Description in the time domain

The mathematically description of a fundamental signal, that is modulated in the direct- and quadrature direction, is given by Equation 2.3:

$$\begin{aligned} u(t) &= U_{d0}\cos(\omega_N t) - U_{q0}\sin(\omega_N t) \\ &+ U_{da}\cos(\omega_N t)\cos(\omega_T t) - U_{db}\cos(\omega_N t)\sin(\omega_T t) \\ &- U_{qa}\sin(\omega_N t)\cos(\omega_T t) + U_{qb}\sin(\omega_N t)\sin(\omega_T t) \end{aligned} \tag{2.3}$$

Equation 2.3 gives the modulated signal. The description is made as a sum of six terms. The six terms are divided in three pairs: fundamental, direct modulation and quadrature modulation:

- $U_{d0}\cos(\omega_N t) - U_{q0}\sin(\omega_N t)$ describes the fundamental signal.

- $U_{da}\cos(\omega_N t)\cos(\omega_T t) - U_{db}\cos(\omega_N t)\sin(\omega_T t)$ describes the modulation of amplitude component, or the direct component.

- $-U_{qa}\sin(\omega_N t)\cos(\omega_T t) + U_{qb}\sin(\omega_N t)\sin(\omega_T t)$ desribes the modulation of the phase component, or the quadrature component.

As seen, the fundamental part, the direct modulated part, and the quadrature modulated part, are all described with two constant. This is necessary in order to determine both the phase and amplitude of each part. It might be confusing that the direct- and quadrature modulation also need to be defined by a phase. This is of great importance for further investigations in this master thesis, and is discussed in in Section 2.2.3.

2.2.3 "Phase of modulation" and "direction of modulation"

A signal can both be quadrature modulated and direct modulated. In the fundamental phasor frame, the direct and quadrature components are orthogonal. The term "direction of modulation" is used in this thesis to express how the modulation is distributed between direct- and quadrature modulation. Or in other words: The direction of modulation shows how the modulation span in the fundamental phasor frame.

From the time domain description in Equation 2.3, it is seen that both the direct modulation and quadrature modulation is determined by two scalars. It must be given to derermine the "phase of each modulation", in addition to the amplitude. The phase of the modulation is illustrated in Figure 2.2. This illustration shows that the modulation signal shifts in the time axis as the phase of each of the components change.

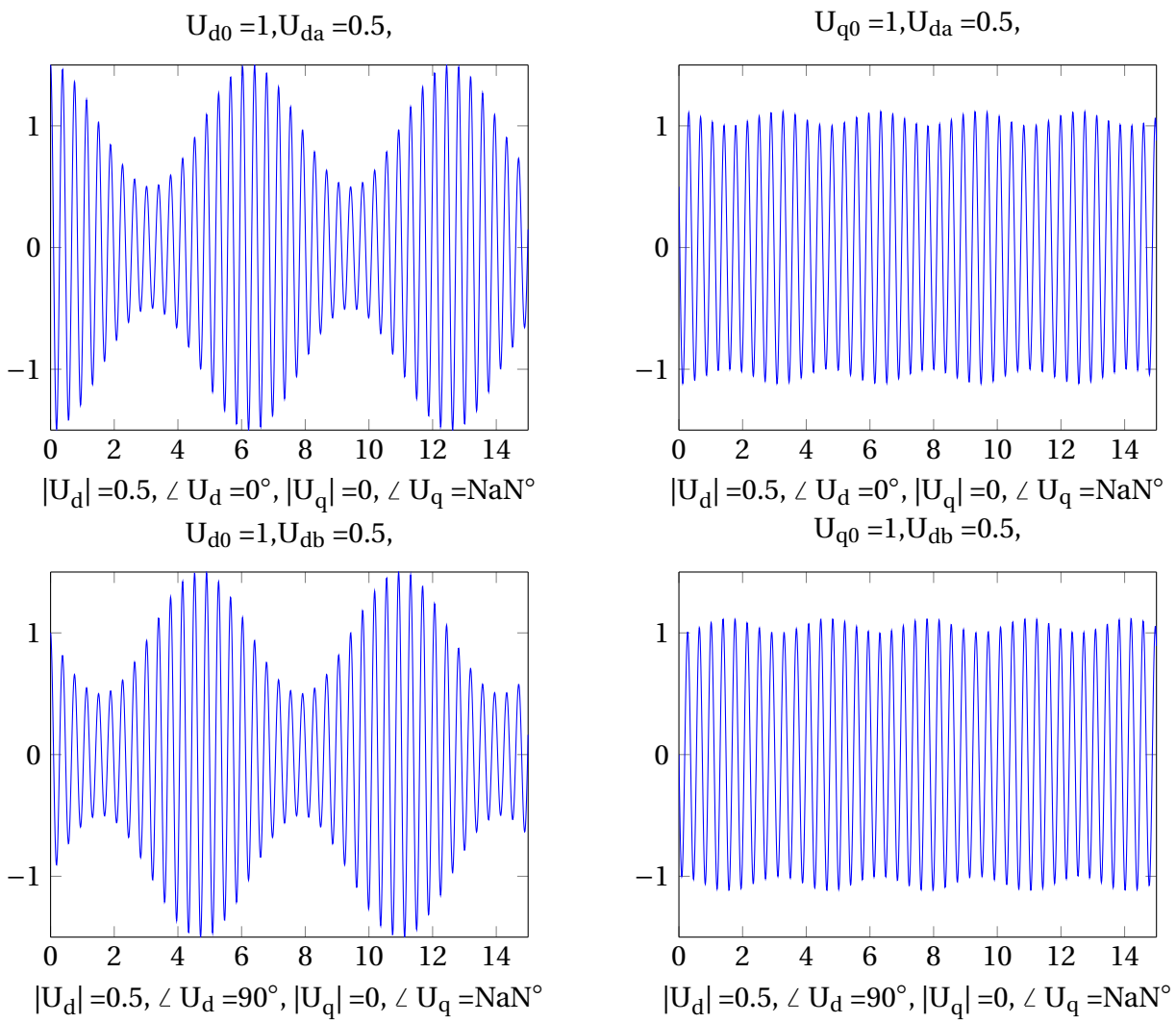

Figure 2.2: Demonstration of the phase of both the direct modulation and quadrature modulation. The time domain parameters (from Equation 2.3) are given in the upper title line. Time domain parameters which is not displayed equals zero. The phasors for the direct- and quadrature modulation (Equation 2.5) are given in the lower title line.

2.2.4 The modulation signal has four degrees of freedom

The modulation signal is described by four parameters: Two for the direct modulated signal and two for the quadrature modulated signal. This differs from the dq transformation of fundamental signals: This transformation gives scalar components for the direct and quadrature components. In other words: the fundamental frequency is described by two values, and the

sum of the modulation signals is described by four values. From this, the following question is posed: Do the sum of the modulation signals have four degrees of freedom?

To test if the modulation signal really have four degrees of freedom, two signals are plotted in Fig. 2.3, by randomizing the constants in Equation 2.3:

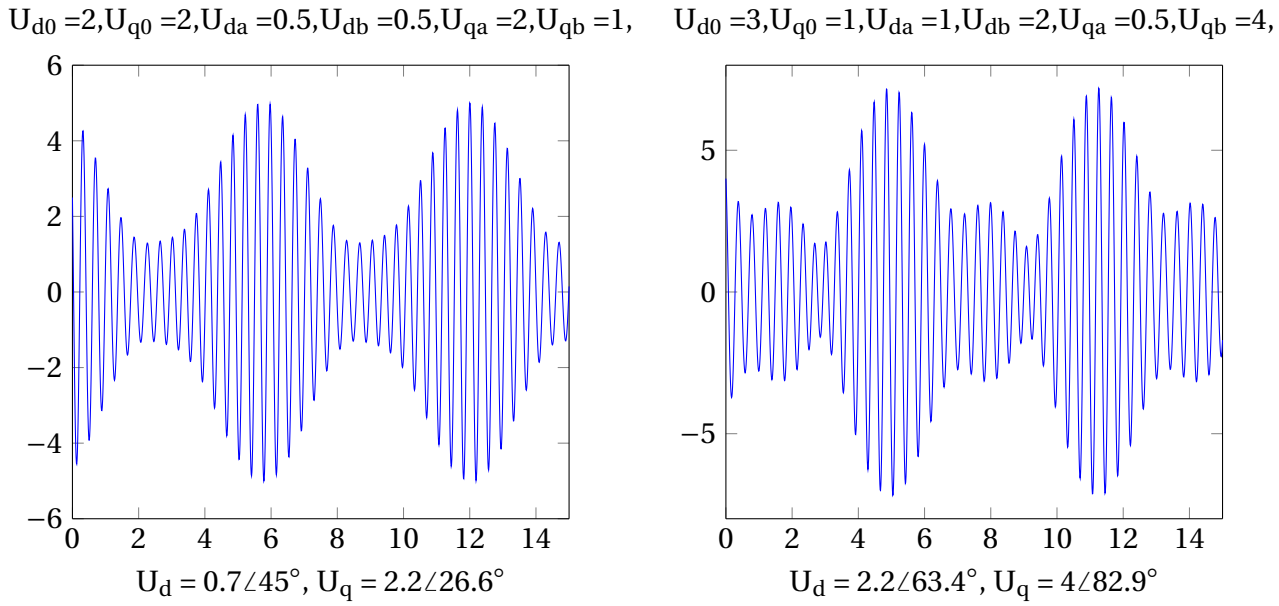

Figure 2.3: Demonstration of the modulation signal Equation 2.3. The time domain parameters are given in the upper title line. The phasors for the direct- and quadrature modulation (Equation 2.5) are given in the lower title line. The signal is quite complex behavior and the sum of the modulation needs four degrees of freedom to precisely be described.

By consider the right-handed subplot of Fig. 2.3 it is quite clear that the modulation signal do have more than two degrees of fredom. Mathematically identities related to trigonometry, given by e.g. Kreyszig[8], do also state that Equation 2.3 can not be reduced to fewer than four terms. Thus, it is confirmed that the modualtion signal do have four degrees of freedom, and the direct- and quadrature modulation must be given as phasors, not scalars.

2.2.5 Description in the frequency domain

The transformation from time domain to the frequency domain must be performed for each of the three signals. The result is one phasor for the fundamental signal, one phasor for the direct modulated signal, and one phasor for the quadrature modulated signal. These components are given in relation to the time domain description (Equation 2.3) in Equation 2.4 and Equation 2.5:

$$U = U_{0d} + iU_{0q} \tag{2.4}$$

$$\begin{aligned} U_d &= U_{da} + jU_{db} \\ U_q &= U_{qa} + jU_{qb} \end{aligned} \tag{2.5}$$

Notice that imaginary operators for the fundamental and modulation description is different. i for the fundamental description determines 90 fundamental degrees. j for the modulation description determines 90 modulation degrees. The two operators must not be mixed, as shown in the next section.

2.2.6 Direct and quadrature components connected in the complex plane

Fundamental signals have two degrees of freedom, and can therefore be visualized in the complex plane, which span in two dimensions. In other words; the direct and quadrature components of a fundamental signal is visualized by letting them span orthogonally in the complex plane. The direction can be defined arbitrary, but is often defined such that the direct component spans in the real dimension and the quadrature component spans in the imaginary dimension.

Since $U_0 = U_{0d} + jU_{0q}$ yields for fundamental components, maybe $U = U_d + jU_q$ is valid for representing the modulation signals? This is *not* the case: The complex plane is applied to representing the phase of the modulation, and can not be applied again to represent the direction of the modulation. This is obvious since modulation signals have four degrees of freedom, and can not be represented as a phasor in a two dimensional space. This is illustrated by figure 2.4

and stated by Equation 2.6 and Equation 2.7:

$$U \neq U_d + jU_q \tag{2.6}$$

$$U = \begin{bmatrix} U_d \\ U_q \end{bmatrix} \tag{2.7}$$

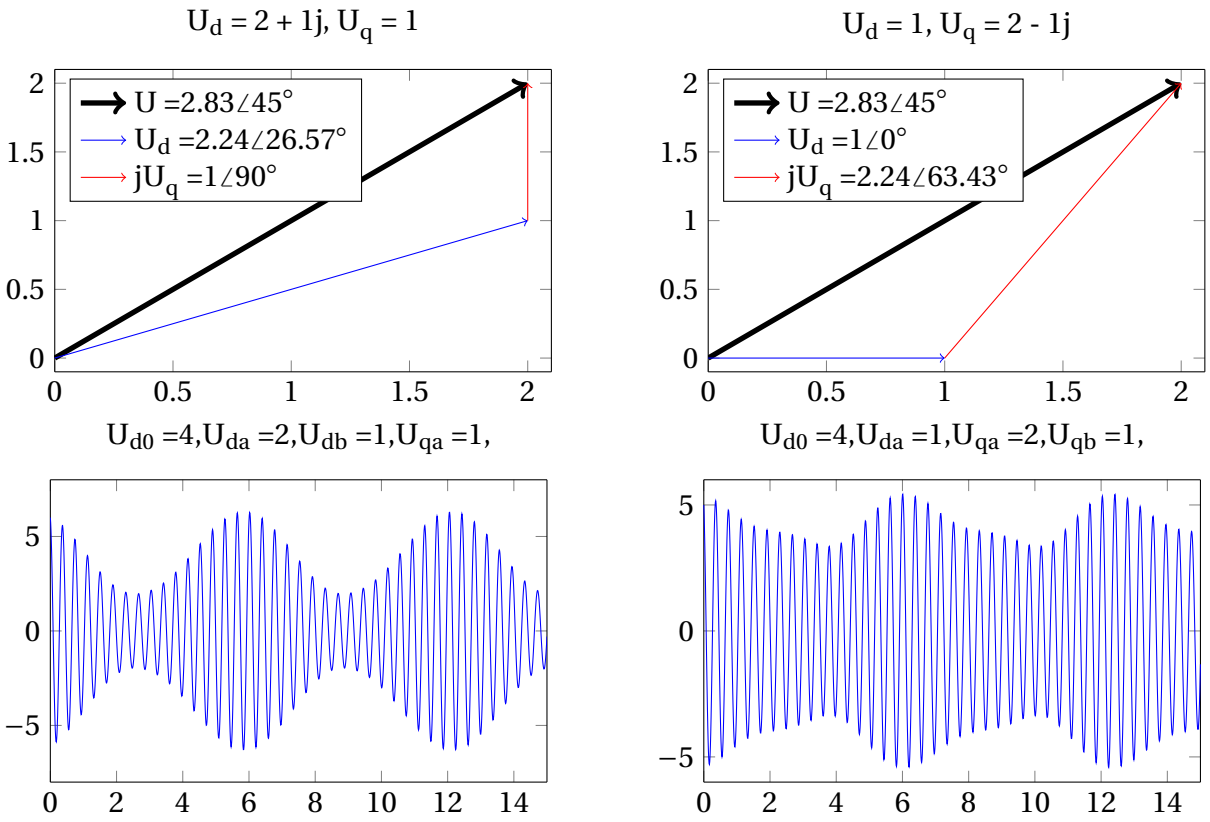

Figure 2.4: If suming phasors like this is valid, the combination of U_d and U_q to the left should be equal the combination of U_d and U_q to the right. The time domain plots do not give the same result. Conclusion: Phasor sumation of direct and quadrature components, in the complex plane, do not make senses. $U \neq U_d + jU_q$

2.2.7 Time to dq transformation

The relation between the output and input of the transformation is important knowledge further in this thesis, and will be presented here. The performance of the time to dq transformation is not the scope of this thesis and will not be presented.

Regular time to dq transformation

In case of modulated voltage in steady state, such that described by Equation 2.3, a general dq transformation (power invariant), which rotate with the fundamental frequency (ω_N) will give the following components:

- The fundamental quantities ($U_{d0}\cos(\omega_N t) - U_{q0}\sin(\omega_N t)$) gives pure DC quantities.
- The direct modulate quantities ($U_{da}\cos(\omega_N t)\cos(\omega_T t) - U_{db}\cos(\omega_N t)\sin(\omega_T t)$) gives AC components with a frequency equal the modulation frequency (ω_T).
- The quadrature modulated quantities ($-U_{qa}\sin(\omega_N t)\cos(\omega_T t) + U_{qa}\sin(\omega_N t)\sin(\omega_T t)$) gives AC components with a frequency equal the modulation frequency (ω_T).

Time to dq transformation used at Alnabru

The time to dq transformation performed on the measurements at Alnabru are a bit modified compared to regular time to dq transformation. These modifications are now described:

The components from a regular time to dq transformation are still given in the time frame although they are transformed to the dq-domain. At the "DQ tests" at Alnabru, only steady state[2] data is transformed. Thus, the output of the transformation do not have to be given the time domain. The output of the dq transformation is given in the frequency domain where the direct- and quadrature modulated components are given as phasors. The modulation frequency and the fundamental frequency can therefore not be detected from the frequency domain data, but have to be given in advance. The phase of the phasor system is defined by the fundamental voltage: It is orientated such that the fundamental voltage is in the direct direction ($U_{d0} \neq 0$ and $U_{q0} = 0$). As the test wants to reveal the dynamic behavior of the electric traction vehicle, the

[2] Steady state in terms of constant amplitudes, phases and frequencies of the fundamental components, direct modulated components and quadrature modulated components.

fundamental components are not of interest. They are therefore removed from the output of the transformation. Therefore, no information about the operating point can be detected from the frequency data.

The result of the dq transformation is therefore the modulation components of the signal, given as phasors, as explained by Equation 2.5. Figures that describes this is already given: In Figure 2.2 and Figure 2.3, artificial signals are plotted in the time frame, according to Equation 2.3. The constants of this Equation is given in head of each subplot. The modulation components, and thus the output of time to dq transformation, is given in the bottom of each subplot.

Naming conventions

The output of the time to dq transformation are described by different terms, depending on usage and the author. Some of them are:

- Direct modulated and quadrature modulated components: Mainly used in this thesis.
- Modulation components: Used in this theses
- Oscillation components
- Subharmonics
- Frequency components
- Low frequency components
- Disturbance components

Chapter 3

Application of modulated signals in electric systems

This chapter introduces a method for stability analysis where the dynamics of the system are presented through frequency dependent admittances and impedances. A modification of the classic description of this method is suggested. Further, the analytic frequency responses of some components are established. At last, application of these responses in electric systems is presented.

3.1 The "DQ approach"

In this section, a simple electric system exposed to modulated voltage, is described. As the modulated voltage can not be described by a singel phasor, the description of the system must be extended. Such a description is given by S. Pika[17], which the following section is inspired by. The same description was made first by Menth and Meyer[10] and further by e.g. Danielsen[2]. These three presentations are quite similar, but with minor differences in syntax. In the next section a brief presentation of the newest approach, by S. Pika[17] is given.

3.1.1 Simple electric traction power system

In Figure 3.1, a simple electric system is presented. This consists of one voltage source in series with a distribution system and an electric traction vehicle. The vehicle is modeled as impedance in parallel with a current source. The current source describes the conducted current due to steady state operation. The current through the impedance represents the conducted vehicle current due to dynamics in the system .

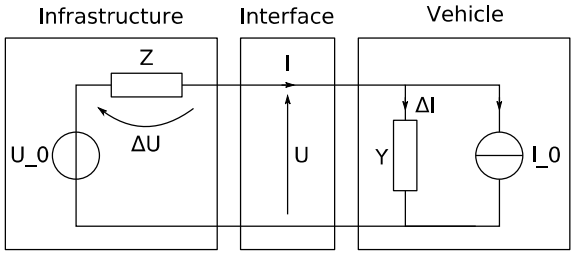

Figure 3.1: An simple model for interaction between a power supply unit and an electric vehicle. S. Pika[16]

In Figure 3.2 the same electric system is presented by use of blocks that give the relations between input and output. The system creates a closed loop system.

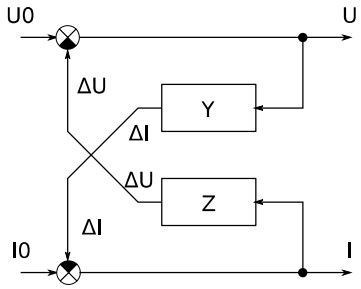

Figure 3.2: A simple circuit with load and supply is represented with transfer functions. This configuration is a closed loop system. S. Pika[16].

3.1.2 MIMO-systems

The system is exposed for modulated voltage. Therefore, the currents and voltages in the system must be described by two phasors each: One phasor for the direct modulation, and one phasor

for the quadrature modulation. As both voltage and current are described by two phasors, the admittance and impedance of Figure 3.2 has two inputs and two outputs, which requires four blocks for describing one impedance/admittance, as shown in Fiure. 3.3:

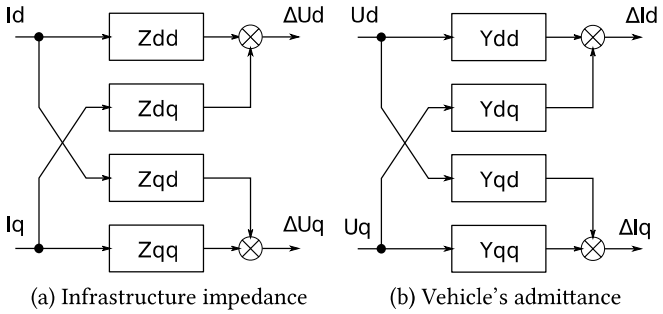

(a) Infrastructure impedance (b) Vehicle's admittance

Figure 3.3: The impedance and admittance of components have to be given by four blocks. S Pika[16]

The admittance of the load and the impedance of the source is then given as 2×2-matrices in Equation 3.1 and Equation 3.2:

$$Y = \begin{bmatrix} Y_{dd} & Y_{dq} \\ Y_{qd} & Y_{qq} \end{bmatrix} \tag{3.1}$$

$$Z(s) = \begin{bmatrix} Z_{dd}(s) & Z_{dq}(s) \\ Z_{qd}(s) & Z_{qq}(s) \end{bmatrix} \tag{3.2}$$

When the two components in Figure 3.3 are combined in the model for the electric system from Figure 3.2, the result is a multiple input multiple output (MIMO) system with two feedback loops:

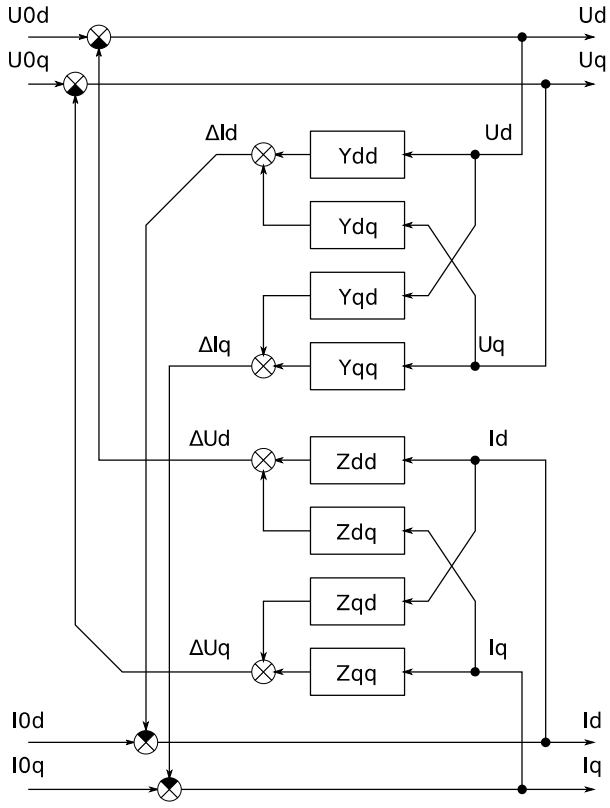

Figure 3.4: Model with one supply and one loads represented by transfer functions in the dq-frame. The system has a double feedback loop with cross couplings. S. Pika[16]

The resulting dependency between the current through , voltage, and admittance is given by Equation 6.1:

$$\begin{bmatrix} \Delta I_d \\ \Delta I_q \end{bmatrix} = \begin{bmatrix} Y_{dd} & Y_{dq} \\ Y_{qd} & Y_{qq} \end{bmatrix} \begin{bmatrix} U_d \\ U_q \end{bmatrix} \tag{3.3}$$

3.2 Suggested modification of the "DQ approach"

The "DQ approach" is based on small changes related to the dynamic behavior of the system. The current source represent a constant current due to the static operation. The current source is therefore suggested to be removed. This is explained in more details throughout this section. The consequences of this modification is also presented in this section.

3.2.1 The model describe the dynamics

The goal of the system description, is to describe the dynamic behavior of the electric traction vehicle with frequency dependent admittances. Each admittances give a small change of current given a small change of voltage. These small changes are the modulated components of the voltage and current.

3.2.2 Phasors of different systems can not be summed

As the fundamental components are presented as phasors in another system than the modulation components, they can not be summed. The phasor system of the fundamental components are based on the fundamental frequency, and the phasor system of the modulation components are based on the modulation frequency.

3.2.3 Representation in the time domain

Modulation components and fundamental components can be summed in the time domain. This is explained by investigating Equation 2.3: The direct modulation components, the quadrature modulation components and the fundamental components are summed. Therefore, it is suggested to illustrate the concepts of modeling the vehicle as a current source and a frequency dependent admittance, in the time domain. In Figure 3.5, such a Figure is illustrated.

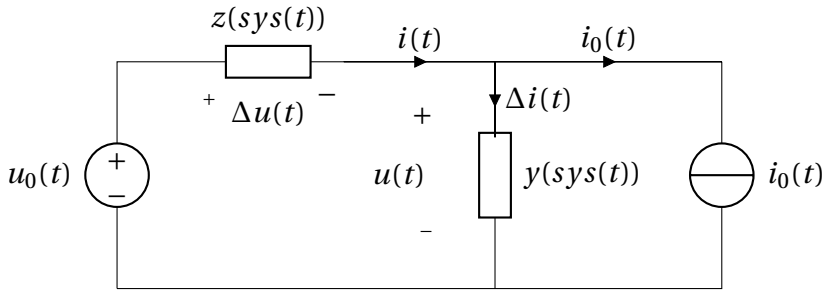

Figure 3.5: Time domain

Further in Figure 3.6, the voltage and current are explained by plots. It is now clear that $i_0(t)$ is just related to the fundamental current, and $\Delta i(t)$ is related to the modulation current. This

is according to the idea of the model: The current source models the steady state operation, the admittance models the dynamic.

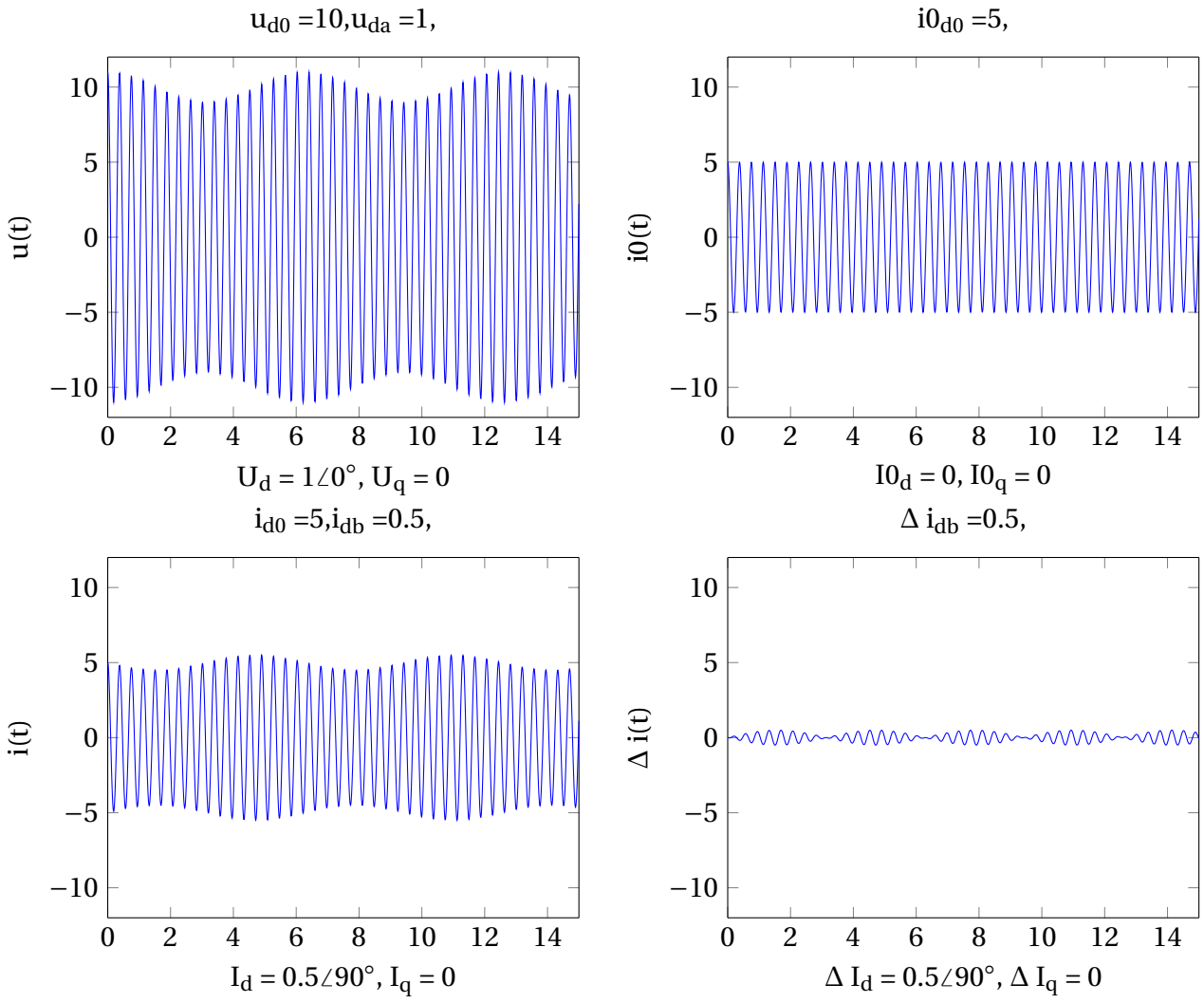

Figure 3.6: $i(t) = i0(t) + \Delta i(t)$. $i0(t)$ includes just fundamental components. $i(t)$ includes both modulation components and fundamental components. $\Delta i(t)$ includes just modulation components.

3.2.4 Result of suggested modification

When the concept of dividing the vehicle into a dynamic component (the admittance) and a steady state component (the current source), is illustrated by phasors, the modulation compo-

nents is suggested to be separated from the fundamental components. ΔI is therefore suggested to be separated from I_0. This is shown by Figure 3.7. The subscript d and q, means direct- and quadrature modulated components, respectively. The subscript f means fundamental component. The modulation circuit(s) and the fundamental circuit are decoupled. In spite of same physical path, the different electric components might have different influence on the modulation components and the fundamental components. The components can not be mixed, without dedicated rules, as they are in different domains.

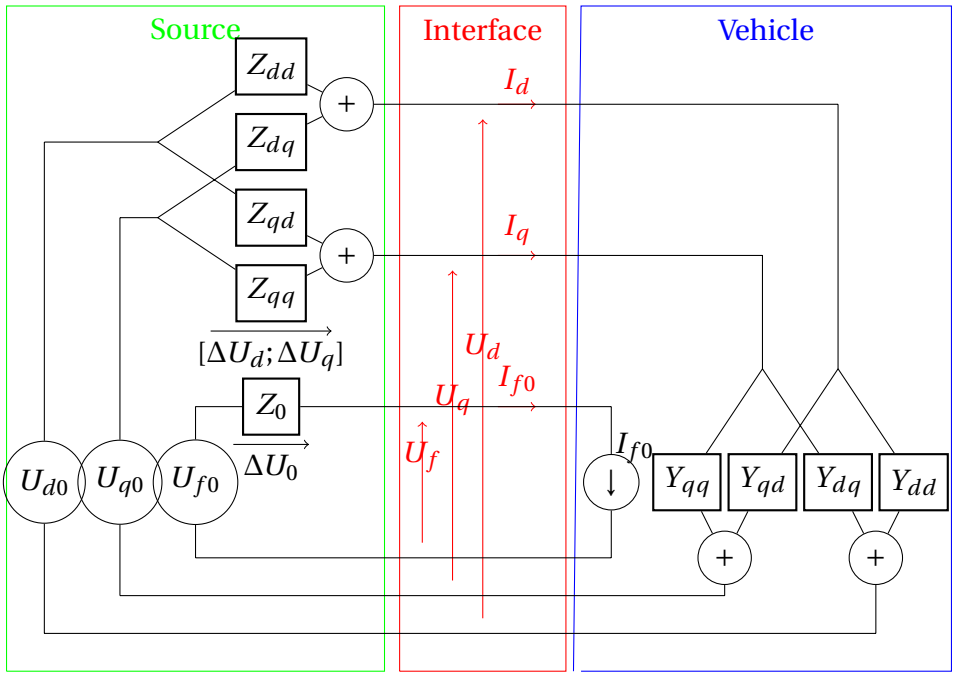

Figure 3.7: System where the direct modulated components (subscript d), quadrature modulated components (subscript q), and fundamental components (subscript f) are separated. This scheme is not strictly correct as it combines block scheme and phasor circuit scheme. The block scheme has to be included to illustrate the cross couplings of the modulation impedance and modulation admittance.

As seen from Figure 3.7, the modulation circuits are decoupled from the fundamental circuit. As the dynamics are of further interest, the fundamental circuit is removed from the model, as it is (partly) done in the traditional "DQ approach" deviation. The result from the suggested modification is almost equal to the traditional, from Figure 3.4. However, it is suggested to remove

I_0, or set I_0 equal zero, $I_0 \equiv 0$, which results in the following equations:

$$\Delta I = I \tag{3.4}$$

$$\begin{bmatrix} I_d \\ I_q \end{bmatrix} = \begin{bmatrix} Y_{dd} & Y_{dq} \\ Y_{qd} & Y_{qq} \end{bmatrix} \begin{bmatrix} U_d \\ U_q \end{bmatrix} \tag{3.5}$$

All equations represented in the traditional "DQ approach", Section 3.1 are still valid, but $I0$ is removed. However, usage of the traditional "DQ approach", will result in removing $I0$. This is because $I0$ is filtered out of the time to dq transformation, which only keeps modulation components. So the numeric results of the modified "DQ approach" will be exactly the same as the traditional.

3.3 Derivation of the impedance for some simple components

In Section 3.1.2 it is shown that the impedances and admittances of components has to be described by 2×2-matrices. These matrices are frequency dependent, both as a function of the fundamental frequency and the modulation frequency. In this section, the impedance for a resistor, an inductor and a capacitor, on the (2×2)-matrix format, are derived.

The impedance for a resistor and an inductor is presented by e.g. Harnefoss[6], but the author has not seen any derivation by others. However, derivations of the impedances of these components has been conducted before by the author in the prject from fall 2014[1]. This will be presented in this section with some corrections.

3.3.1 Frequencies

The impedances of electric components are often frequency dependent. This is e.g. the case for a capacitor and an inductor as shown by Equation 3.6 and Equation 3.7, respectively.

$$Z = \frac{1}{j\omega C} \tag{3.6}$$

$$Z = j\omega L \tag{3.7}$$

Equation (3.6) and Equation (3.7) yields in the phasor domain, and has its origin from corresponding equations in the time domain; Equation 3.8 and Equation 3.9.

$$i(t) = C\frac{du(t)}{dt} \tag{3.8}$$

$$u(t) = L\frac{di(t)}{dt} \tag{3.9}$$

For a system exposed with modulated voltage, the system has to deal with two frequencies; the fundamental frequency and the modulation frequency. The derivative of the voltage, and thus the derivative of the current, is dependent on both frequencies. Therefore both frequencies must be evaluated in the mathematical description of the system:

- The fundamental frequency, f_N, is static and equals $16^2/_3$ Hz in the Norwegian electric traction system. Since the fundamental frequency is static, as described by Alstad[1], it is evaluated directly in the impedance/admittance matrices, and not implemented as a variable.

- The modulation frequency, f_T, is not locked to any foreknown size, so it must be included as a variable in the mathematically description of the system.

For applying well known phasor operations on both frequencies, it is necessary to do a frequency translation: $s' \rightarrow s + j\omega_s$, $s = j\omega_{modulation}$. This frequency translation is shown by Harnefoss[6]. It is quite intuitive as the total angular velocity is the sum of the fundamental angular velocity and the modulation angular velocity.

3.3.2 Derivation of the impedance of an inductor

The derivation involves mixing with components as phasors, components in the dq system, and components as both phasors and in the dq system. Therefore, vector notation is used for "vectors" in the dq system ($\vec{U} = \begin{bmatrix} U_d \\ U_q \end{bmatrix}$), phasors notation for phasors ($\overline{U} = U_{re} + jU_{im}$), and both

phasor- and vector notation is used for modulated sizes which requires usage of phasors in the dq system ($\vec{\bar{U}} = \begin{bmatrix} \bar{U}_d \\ \bar{U}_q \end{bmatrix}$).

The voltage drop over an inductor is given by $\bar{U} = s' L\bar{I}$, where $s' = j\omega$. By splitting the voltage- and current phasors into real and imaginary components; $\bar{U} = U_d + jU_q$ and $\bar{I} = I_d + jI_q$, the voltage drop is described by $U_d + jU_q = s'L(I_d + jI_q)$. Notice that the dq system is not introduced yet, only phasors where the real and imaginary components are determined by the subscripts d and q. Now, the modulation frequency is introduced in addition to the fundamental frequency. This requires the frequency transformation: $s' \rightarrow s + j\omega_s$, $s = j\omega_{modulation}$. The voltage drop is now $U_d + jU_q = L(s + j\omega_s)(I_d + jI_q)$. This expression is reorganized by multiplying the factors and using the definition of the imaginary numer; $j^2 \equiv -1$. The final expression for the voltage drop is then given by Equation 3.10:

$$U_d + jU_q = (sLI_d - \omega_s LI_q) + j(sLI_q + \omega_s LI_d), \quad s = \omega_{osc} \tag{3.10}$$

Further, the real and imaginary terms of Equation 3.10, is separated into $U_d = sLI_d - \omega_s LI_q$ and $jU_q = j(sLI_q + \omega_s LI_d)$. These equations are given by a matrix equation in Equation 3.11:

$$\begin{bmatrix} U_d(s) \\ U_q(s) \end{bmatrix} = \begin{bmatrix} Ls & -\omega_s L \\ \omega_s L & Ls \end{bmatrix} \begin{bmatrix} I_d(s) \\ I_q(s) \end{bmatrix}, s = \omega_{osc} \tag{3.11}$$

Equation 3.11 is still in the phasor domain, and is limited to a description of fundamental voltage and fundamental current: $\bar{U} = U_d + jU_q$ and $\bar{I} = I_d + jI_q$. This yields in spite of the introduction a modified frequency: $f = f_s + f_{modulation}$. Equation 3.11 will now be extended, to describe the modulation components, $\bar{U}_d$ and $\bar{U}_q$, of a system where the voltage is modulated. This is done by introducing the dq-system where the modulation voltage is given by $\vec{\bar{U}} = \begin{bmatrix} \bar{U}_d \\ \bar{U}_q \end{bmatrix}$ and the modulation current by $\vec{\bar{I}} = \begin{bmatrix} \bar{I}_d \\ \bar{I}_q \end{bmatrix}$. Equation 3.11 is then extended from the phasor system to the dq system where the dq-components are described by phasors. This operation is

described in detail in Appendix E, and the result is shown in Equation 3.12:

$$\begin{bmatrix} \bar{U}_d(s) \\ \bar{U}_q(s) \end{bmatrix} = \begin{bmatrix} Ls & -\omega_s L \\ \omega_s L & Ls \end{bmatrix} \begin{bmatrix} \bar{I}_d(s) \\ \bar{I}_q(s) \end{bmatrix} = \begin{bmatrix} Z_{dd}(s) & Z_{dq}(s) \\ Z_{qd}(s) & Z_{qq}(s) \end{bmatrix} \begin{bmatrix} \bar{I}_d(s) \\ \bar{I}_q(s) \end{bmatrix}, s = \omega_{osc} \tag{3.12}$$

The derivation of the impedance of an inductor is now completed and the result is the same as presented by e.g. Harnefoss[6].

3.3.3 Derivation of the impedance of a capacitance

The derivation of the impedance of a capacitance is done in the exact same way as for the inductor. A compilation of the derivation is given by Equation 3.13:

$$\begin{aligned} U_d + jU_q = \\ (\frac{1}{j\omega_s C} + \frac{1}{Cs})(I_d + jI_q) = \\ -j\frac{I_d}{\omega_s C} + \frac{I_q}{\omega_s C} + \frac{I_d}{Cs} + j\frac{I_q}{Cs} = \\ (\frac{1}{Cs}I_d + \frac{1}{\omega_s C}I_q) + j(\frac{-1}{\omega_s C}I_d + \frac{1}{Cs}I_q), \\ s = j\omega_{osc} \end{aligned} \tag{3.13}$$

Further, the modulation voltage and modulation current is introduced and (3.13) is given in form of a matrix in Equation 3.14:

$$\begin{bmatrix} \bar{U}_d(s) \\ \bar{U}_q(s) \end{bmatrix} = \begin{bmatrix} \frac{1}{Cs} & \frac{1}{\omega_s C} \\ -\frac{1}{\omega_s C} & \frac{1}{Cs} \end{bmatrix} \begin{bmatrix} \bar{I}_d(s) \\ \bar{I}_q(s) \end{bmatrix} = \begin{bmatrix} Z_{dd}(s) & Z_{dq}(s) \\ Z_{qd}(s) & Z_{qq}(s) \end{bmatrix} \begin{bmatrix} \bar{I}_d(s) \\ \bar{I}_q(s) \end{bmatrix}, s = j\omega_{osc} \tag{3.14}$$

The impedance for the capacitance (Equation 3.14) is not found in literature by the author. However, the result is considered as correct for several reasons:

- The resulting dq-impedance of the capacitor and the resulting dq-impedance of the inductor correspond to the well known relation between the impedance of an inductor ($Z = j\omega L$) and a capacitor ($Z = \frac{1}{j\omega C}$). The dq-impedance of an inductor is found in the

litteratur by e.g. Harnefoss[6] (3.13). Since the final equation was successfully derived for the line, it is assumed successfully derived for the capacitor as well.

- The usage of the expression is successfully conducted. This usage involves circuit calculations performed further in this thesis. The result from this usage is discussed in Section 4.3.2 and Section 5.4.4

3.3.4 Derivation of the impedance of a resistance

The derivation of the impedance of a resistance is quite fast:

$$U_d + jU_q = R(I_d + jI_q) \tag{3.15}$$

Further, the modulation voltage and current is introduced and Equation 3.15 is given in matrix form in Equation 3.16:

$$\begin{bmatrix} \overline{U}_d(s) \\ \overline{U}_q(s) \end{bmatrix} = \begin{bmatrix} R & \\ & R \end{bmatrix} \begin{bmatrix} \bar{I}_d(s) \\ \bar{I}_q(s) \end{bmatrix} = \begin{bmatrix} Z_{dd}(s) & Z_{dq}(s) \\ Z_{qd}(s) & Z_{qq}(s) \end{bmatrix} \begin{bmatrix} \bar{I}_d(s) \\ \bar{I}_q(s) \end{bmatrix}, s = j\omega_{osc} \tag{3.16}$$

3.4 Example of usage, and rules for calculation

The "DQ approach", presented in Section 3.1, models each components as independent from the rest of the system. The inputs and outputs are clearly defined by the components four frequency responses. This is the same principle as traditional linear state space modeling. Thus, the same rules are applicable. The "DQ approach" deals with just two types of blocks; the admittance block and the impedance block. Both blocks are MIMO systems with two inputs and two outputs. The inputs and outputs are uniquely given by $\begin{bmatrix} I_d \\ I_q \end{bmatrix}_{out} = \begin{bmatrix} Y_{dd} & Y_{dq} \\ Y_{qd} & Y_{qq} \end{bmatrix} \begin{bmatrix} U_d \\ U_q \end{bmatrix}_{in}$ for the admittance, and $\begin{bmatrix} U_d \\ U_q \end{bmatrix}_{out} = \begin{bmatrix} Z_{dd} & Z_{dq} \\ Z_{qd} & Z_{qq} \end{bmatrix} \begin{bmatrix} I_d \\ I_q \end{bmatrix}_{in}$ for the impedance. Further, $\begin{bmatrix} Z_{dd} & Z_{dq} \\ Z_{qd} & Z_{qq} \end{bmatrix} = \begin{bmatrix} Y_{dd} & Y_{dq} \\ Y_{qd} & Y_{qq} \end{bmatrix}^{-1}$ yields. The equations for the impedance of a capacitor, an inductor and a resistance, presented in Section 3.3, is applicable. Also other state space models can be included as

long as their inputs/outputs are in accordance with the state variables of the system. These state space models might be of larger system, which can be extracted from measurements or analytic models.

An example of usage is illustrated in Figure 3.8. This is a model of a vehicle in series with a line and a cable. The line is modeled as a series of a resistance and a inductor. The cable is modeled by a π-equivalent. The analogous circuit representation is given to the right of the point of measurements in Figure 4.2. In order to make this model regular circuit rules are applied on matrix form. These rules are $Z_{1+2+...} = Z_1 + Z_2 + ...$ for components in series, $Y_{1+2+...} = Y_1 + Y_2 + ...$ for components in parallel, and the fact that the admittance is the inverse of the impedance, $Y = inv(Z)$.

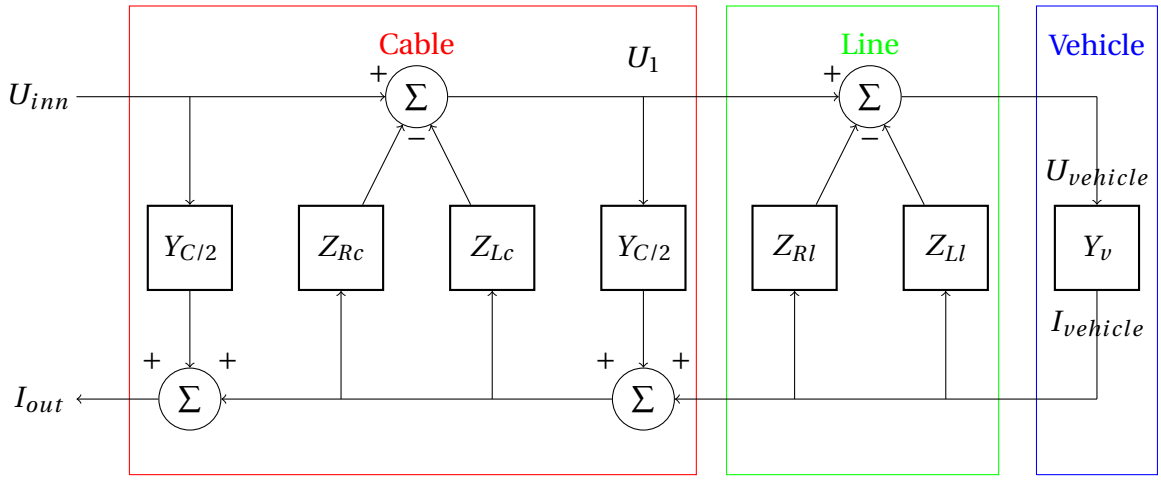

Figure 3.8: A vehicle, a line and a cable in series, represented by blocks extracted from the "DQ approach". All the blocks are 2×2-transfer systems.

Chapter 4

Summary of project, fall 2014

This chapter gives a summary of the project from fall 2014. The project includes calculations and methods for establishing the frequency responses of a system from "DQ tests". Further, the admittance of an electric traction vehicle is established through analytically compensation for a line and a cable.

4.1 Research Objecvtives

The research objectives of the project was to develop the frequency response of the electric traction vehicle from the measurements at Alnabru[16]. To achieve this objective, several smaller objective was established:

- Gain the required knowledge to develop the admittance of the electric traction vehicle from measurements at Alnabru[16]
- Obtain the numeric frequency responses of the electric system seen from the point of measurements.
- Obtain an overview of which components are involved in the frequency response
- Obtain the analytic frequency response of simple components. Further reveal mathematically rules of how these components can be involved in the electric system.

- Achieve the correct frequency response of the electric traction vehicle by compensating for the line and the cable in the test topology.

4.2 From measurements to frequency responses

The process of achieving the frequency responses were illustrated by Figure 1.1. The process involves conditioning of the measurements, time to dq transformation, and solving the system of equations. This steps will be explained in this section.

The background theory of the test at Alnabru was described in Section 1.2.4, and the topology is illustrated in Figure 1.2.

4.2.1 Conditioning the measurements

Conditioning of the time domain measurements is important for the accuracy of the time to dq transformation. Some theory of conditioning of signals is presented in Section 5.5.1. Some conditioning of the measurements were conducted, such as splitting the signals dependent on the frequency, measuring the frequencies and avoiding transient behavior. However, this conditioning was to poor as the author did not know about the strict requirements of the length of the signal. This poor conditioning resulted in an inaccurate frequency response.

4.2.2 Time to dq transformation

The time to dq transformation was performed with a Matlab function written by M. Meyer[11]. This function gives the output specified in Section 2.2.7

4.2.3 Solving the system of equations

From the "DQ approach" of e.g. S. Pika[17], presented in Section 3.1, the admittance of the electric vehicle is given by $\begin{bmatrix} \Delta I_d \\ \Delta I_q \end{bmatrix} = \begin{bmatrix} Y_{dd} & Y_{dq} \\ Y_{qd} & Y_{qq} \end{bmatrix} \begin{bmatrix} U_d \\ U_q \end{bmatrix}$. As discussed in the same section; ΔI was not measured. The measured components where $i(t) = i_0(t) + \Delta i(t)$. The time to dq transformation of $i(t)$ gives I, not ΔI. However, the time to dq transformation of $i_0(t)$ gives $I_0 = 0$

since $i_0(t)$ do not include any modulated components. Therefore ΔI and I are equal and measured time to dq transformation could be used to finding the admittance of the system: $\begin{bmatrix} I_d \\ I_q \end{bmatrix} = \begin{bmatrix} Y_{dd} & Y_{dq} \\ Y_{qd} & Y_{qq} \end{bmatrix} \begin{bmatrix} U_d \\ U_q \end{bmatrix}$.

As this matrix equation gives two equations, but has four unknown variables, the matrix equation must be applied two times. One time for the d-sweep and one time for the q-sweep, as shown in Equation 4.1

$$\begin{bmatrix} I_{d,d-sweep}(j\omega) & I_{d,q-sweep}(j\omega) \\ I_{q,d-sweep}(j\omega) & I_{q,q-sweep}(j\omega) \end{bmatrix} = \begin{bmatrix} Y_{dd}(j\omega) & Y_{dq}(j\omega) \\ Y_{qd}(j\omega) & Y_{qq}(j\omega) \end{bmatrix} \begin{bmatrix} U_{d,d-sweep}(j\omega) & U_{d,q-sweep}(j\omega) \\ U_{q,d-sweep}(j\omega) & U_{q,q-sweep}(j\omega) \end{bmatrix} \tag{4.1}$$

Equation 4.1 gives four equations and includes four unknown, so the system is solvable as long as the equations are linear independent. The linear independency is disscused more in Section 6.1.2. As the system is solvable, linear algebra is applied, and the final explicit expression of the admittance of the system, is given by Equation 4.2

$$\begin{bmatrix} Y_{dd}(j\omega) & Y_{dq}(j\omega) \\ Y_{qd}(j\omega) & Y_{qq}(j\omega) \end{bmatrix} = \begin{bmatrix} I_{d,d-sweep}(j\omega) & I_{d,q-sweep}(j\omega) \\ I_{q,d-sweep}(j\omega) & I_{q,q-sweep}(j\omega) \end{bmatrix} \begin{bmatrix} U_{d,d-sweep}(j\omega) & U_{d,q-sweep}(j\omega) \\ U_{q,d-sweep}(j\omega) & U_{q,q-sweep}(j\omega) \end{bmatrix}^{-1} \tag{4.2}$$

4.2.4 Result

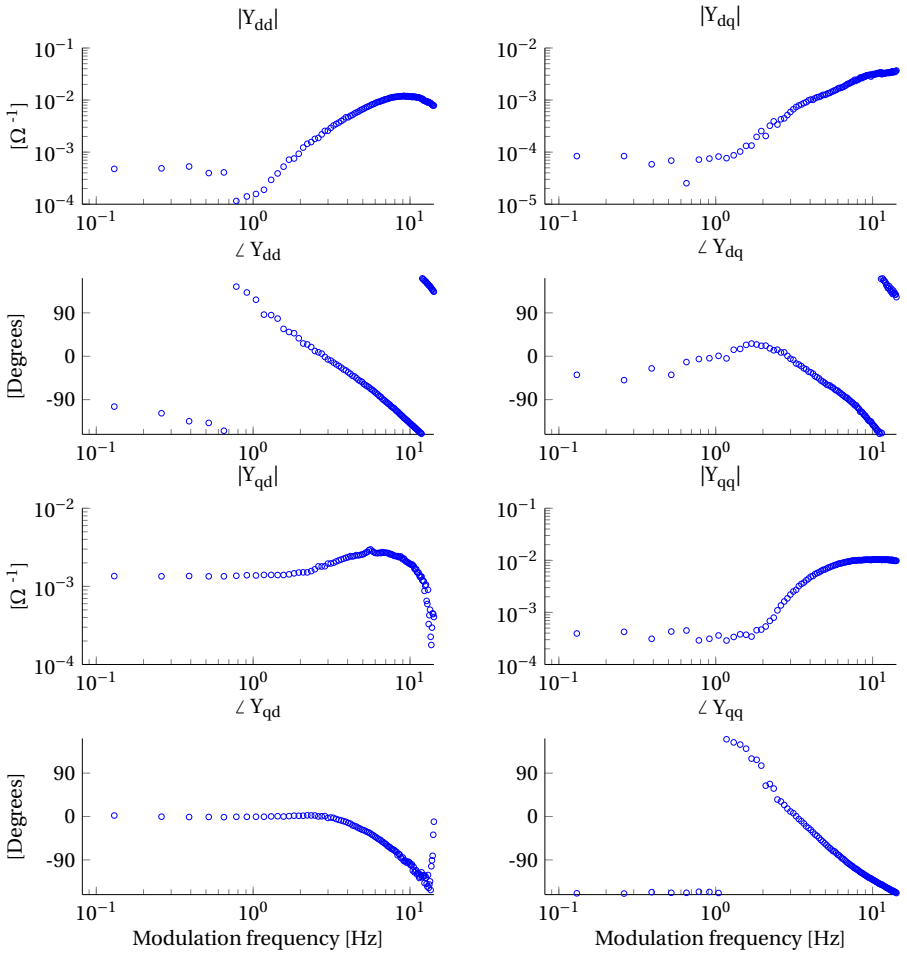

Figure 4.1: Y calculated direct from measurements.

4.2.5 Physical interpretation of the result

This section will presented a physical interpretation of the resulting frequency response of the vehicle, presented in Figure 4.1. The response is not corrected for the other topology yet, but the same interpretation is still valid.

The physical interpretation on the admittance is easiest described by considering the Y_{dd}-component. Y_{dd} determines the change in current amplitude (direct component of current) in response to the change of voltage amplitude (direct component of voltage). This is seen through studies of Equation 6.1. The voltage over the DC link of the electric vehicle must follow the oscillation of the line voltage in order to keep the current constant. When the oscillating frequency

increase, it is harder for the system to follow the line voltage. By the term system, every inner component of the vehicle that affect the dynamics is included. This is mainly measurements, controllers, PLL(s), PWM(s) and the DC-link. When the system can not follow the faster oscillating voltage, the system starts to lag. This will cause a voltage difference between the line voltage, and the not perfect regulated DC-link voltage. The voltage difference cause conducted current. The conducted current is visible as increasing $|Y_{dd}|$ for increasing modulation frequency. The lagging system is visible as increasing $\angle Y_{dd}$ for increasing modulation frequencies.

4.3 Compensating for cable and Line

The objective of this section is to develop an expression of the admittance of the electric vehicle. To achieve this objective, the following subtask is conducted:

- Make a model for the topology.
- Determine which components affect the obtained frequency response.
- Strategy for calculation.
- Find the required parameters for the components which are involved.
- Find the analytical frequency responses of the components in the model.
- Performing calculations with the frequency responses of the components.

Model

In addition to the components given in Figure 1.2, the test setup at Alnabru includes a line and a cable in series with the electric traction vehicle. The cable is modeled as a π-equivalent. The line is modeled as a inductor and resistor in series. The transformer and grid filter are just given as unknown blocks as they probably are not needed to be further explored in order to achieve the correct frequency response of the vehicle. The model is given in Figure 4.2:

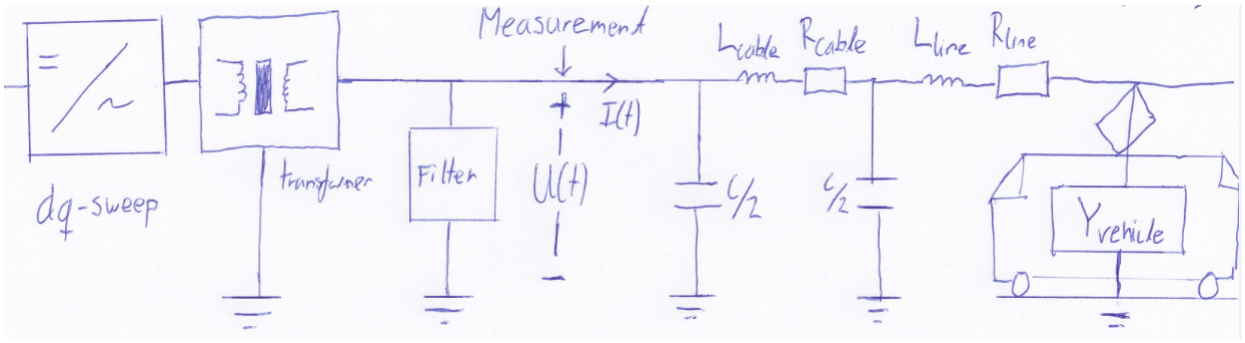

Figure 4.2: The topology used for compensating for the cable and line.

Which components affect the total frequency response

The calculated admittance from 4.2 is the admittance of the series of the line, cable and vehicle, as shown in Figure 4.3:

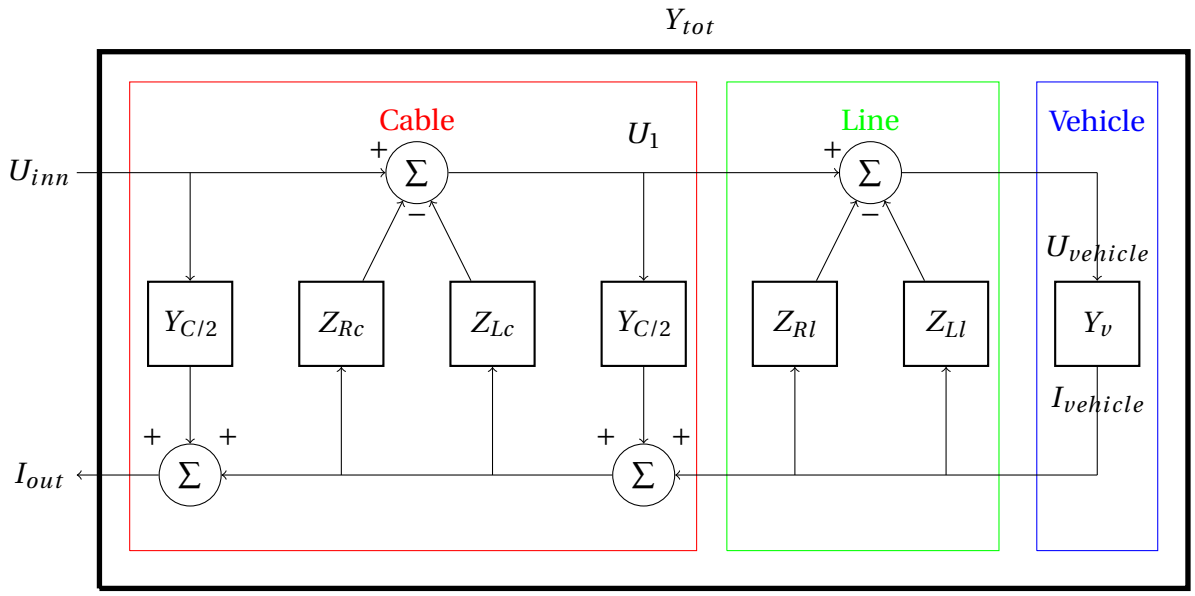

Figure 4.3: The measured admittance, Y_{tot}, includes more than the vehicle.

This statement is true as the measured voltage is equal the voltage over the interface, and modulation component of the measured current is equal the modulation components of the current at the interface. The importance of specifying *the modulation component* of the current has its background from I_0, discussed in Section 3.2.

To perform the calculations for achiving the admittance of the vehicle, the source compo-

nents of Figure 4.2 do not take part in this calculations. This is in accordance with the model description; the "DQ approach", presented in Section 3.1.

Frequency response of the components and calculations

Since the cable and line are modeled as a set of resistors, inductances and capacitances, the frequency response can be achieved by using the formulas presented in Section 3.3.2.

Calculation

Further, rules for calculations of impedances and admittances in the power system describing modulation components is used. These rules are presented and discussed in Section 3.4. The admittance of the vehicle is implicitly given by Equation 4.3. Equation 4.4 isolate the admittance of the electric vehicle through iterative calculations.

$$Z_{tot} = Z_{C/2}||(Z_{RL,cable} + [Z_{C/2}||(Z_{RL,line} + Z_{vehicle})]) \tag{4.3}$$

$$\begin{aligned}
Y_{(tot-C/2)} &= Y_{tot} - Y_{C/2} \\
Z_{(tot-C/2)} &= inv(Y_{(tot-C/2)}) \\
Z_{(vehicle+line+C/2)} &= Z_{(tot-C/2)} - Z_{RL,cable} \\
Y_{(vehicle+line+C/2)} &= inv(Z_{(vehicle+line+C/2)}) \\
Y_{(line+vehicle)} &= Y_{(vehicle+line+C/2)} - Y_{C/2} \\
Z_{(line+vehicle)} &= inv(Y_{(line+vehicle)}) \\
Z_{vehicle} &= Z_{(line+vehicle)} - Z_{RL,line} \\
Y_{vehcile} &= inv(Z_{vehcile})
\end{aligned} \tag{4.4}$$

4.3.1 Result

The compensation of the line and the cable, have a small effect on the admittance. This effect is so small that it is not noticeable through full size plot. To make the effect noticeable, the frequency response is zoomed very much and ploted in Figure 4.4. Notice that this compensation

was performed with a set of frequency responses that is not up to date. The frequency response will therefore differ a bit from the updated set of frequency responses.

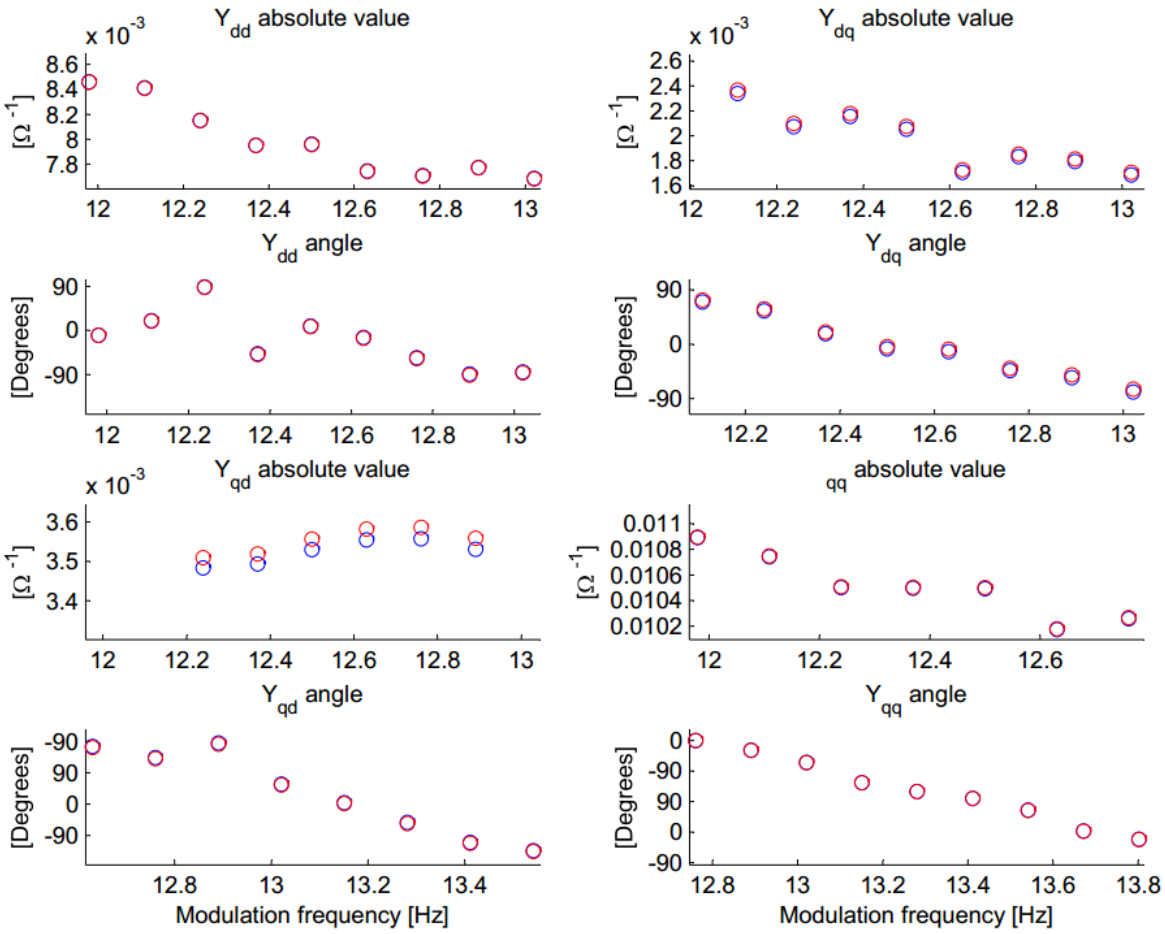

Figure 4.4: $Y(j\omega)_{tot}$ in red, and $Y(j\omega)_{vehicle}$ in blue. Since the two responses are almost exactly equal, the responses is zoomed in for make the difference visible.

4.3.2 Discussion

Since the lengths of the cable and line are short (510 m + 500 m), the effect of the compensation is expected to be low. This is also explained by simple circuit analysis: The conducted current through the shunt capacitance of the cable is low due to the high impedance to earth. The series impedance is just a bit larger due to the low series impedance of the cable and line, and the quite large impedance of the admittanc of the vehicle. So, both the series impedance and shunt impedance has a small impact of the of the total admittance. The series impedance and

shunt impedance will actually have opposite effect on the amplitude of the current conducted through the system. However, they will have the same effect on the phase. Therefore, as seen in Figure 4.4, the effect on the admittance matrix is larger on the cross coupled components (Y_{dq} and Y_{qd}) than in the direct coupled components (Y_{dd} and Y_{qq}).

In addition to the expected result, the method and performance of the method (MATLAB-script) are strengthen through testing. This testing includes boosting of parameters and some simple hand calculations. Therefore the method are considered to be sufficiently accurate to draw the following conclusion: The impact of the cable and line on the total admittance is small. It is so small that the effect of the cable and line are hardly noticeable in any conceivable scenarios. In further calculations, the admittance of the electric vehicle can be assumed to be equal the admittance conducted directly from the measurements.

Chapter 5

Analysis of voltage measurements

This chapter presents analysis of the voltage measurements from the tests presented in Chapter 4. These analysis explain some of the unexpected measurements, and is necessary in order to verify the test results. These analysis includes a wide presentation of the measurements from different views, calculation of the voltage drop over a transformer, and representation of the results in both the modulation domain, fundamental domain and time domain.

5.1 Background

A description of modulated signals in the electric system, through an impedance/admittance approach, is quite complex: The currents and voltages are not described by one phasor any more, but by two phasors. The impedance or admittance of electric components are not described by one phasor any more, but by four. To fully understand the behavior of these components, a deeper knowledge about the system is needed to:

- Verify results from measurements and calculations.
- Improve the performance of the "DQ test".
- Analyze the resulting frequency responses of the electric components.
- Be aware of limitations related to the "DQ tests" and stability analysis, performed by using frequency dependent components.

In this chapter, such knowledge is gained through a close look at the voltage measurements. The voltage measurements are chosen for a deeper analysis due to their close relation to the voltage specifications for the "DQ tests". Thus, the voltage measurements have expected values, and the analysis might be less complex than e.g. analyzing the current, as the current is less predictable. Fundamental knowledge about the excitation (voltage) of the system should be gained before analyzing the response (current) of the system.

Another motivation of performance of the voltage analysis is that voltage measurements differs from expected values. More specific: The voltage measurements on the 15 kV line differ from the voltage specifications for the output on the static converter. This chapter will explain some of the reasons of the deviation from the expected values.

5.2 Presentation of measurements

In this section, the voltage measurements from test ID33d and test ID33q will be presented. In order to give a wider presentation of the measurements, they will be presented in four ways: The amplitude and modulation phase as frequency responses, as phasors in the modulation phase domain, as phasors in the 'modulation-direction' domain, and in the time domain. The different presentation methods of the measurements will hopefully give a wider understanding of the system. The presentation methods will be discussed continuously during this section. The measurements themselves will be discussed in later sections of this chapter.

Data

All data is collected from test ID33d and test ID33q, at the "DQ tests", performed at Alnabru[16]. The time domain data was received from S. Pika at Jernbaneverket, Oslo, 29th of October. The dq transformed data by S. Pika was recived by mail 4th of May. All plots and calculations are done by the author of this thesis.

5.2.1 Frequency response of amplitude and phase

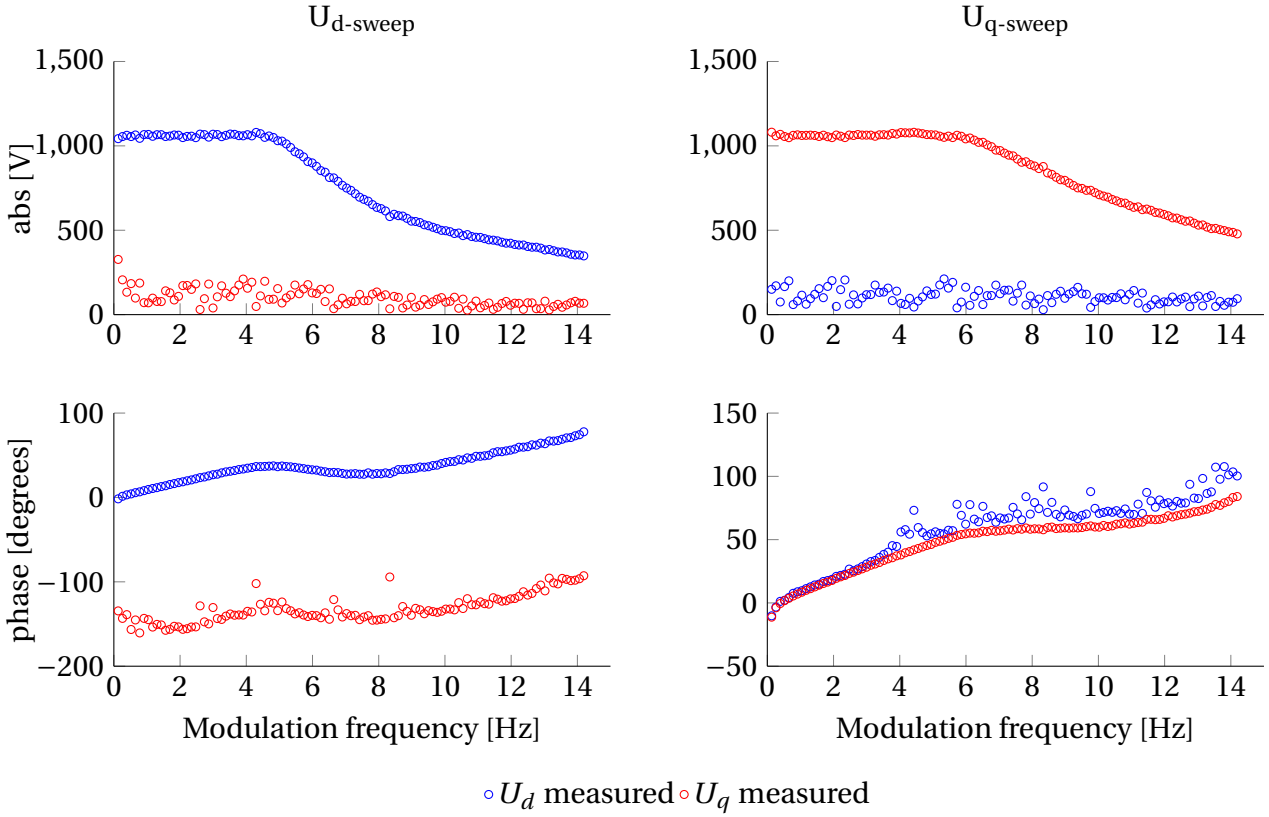

Figure 5.1: Frequency response of the modulation voltages in the dq-frame on the 15-kV line during sweep ID33d and ID33q.

5.2.2 Phasors

In Figure 5.3 and Figure 5.4, the voltage measurements are presented as phasors for some chosen frequencies. The same frequencies are also chosen in the time domain presentation in Figure 5.5. Both direct- and quadrature components of the voltages, for both the direct and qudrature sweeps, are presented in each plot.

Since the direct and quadrature modulated voltage have more than four degrees of freedom, phasor presentations in two dimensions must involve some compromises. The 'modulation-direction' is highlighted in Figure 5.3. The 'modulation-phase' is highlighted in Figure 5.4. The 'modulation-direction' and the modulation phase were discussed in Section 2.2.3.

'Modulation-direction' of the voltages

The phasor plots in Figure 5.3 highlight the 'modulation-direction'. The voltage for the d-sweep and q-sweep are both described as $U = |U_d| + j|U_q|$. These plots are in the fundamental frame, which means that the imaginary operator, j, corresponds to a movement of 90 fundamental degrees. The total voltage phasor is the sum of U_0 and $U_{d-sweep}(t)$ for the d-sweep, and the sum of U_0 and $U_{q-sweep}(t)$ for the q-sweep. The phasor U_0 is static. The phasors $U_{d-sweep}(t)$ and $U_{d-sweep}(t)$ depends on the time, but their direction is static, only the amplitudes vary. The modulation amplitude vary with time (t), illustrated in Figure 5.2:

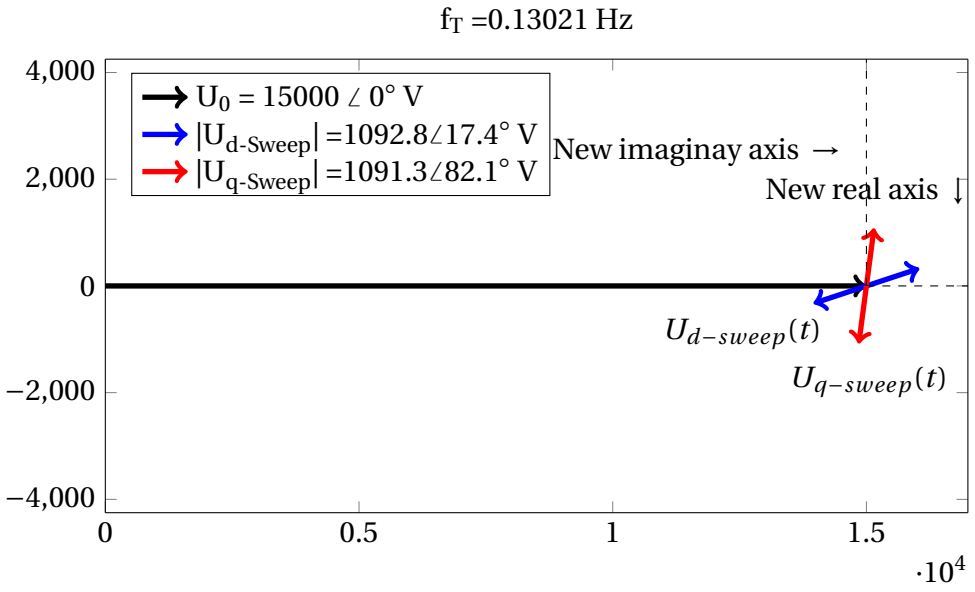

Figure 5.2: This plot illustrate the phasor plot which focus on the 'modulation-diretion'. Notice that the d-sweep and q-sweep is not lined perfectly in direct- and quadrature direction

In spite of static modulation direction for a specific modulation frequency, the modulation direction vary a bit for different modualtion frequencies. This is not the case for the fundamental component which is static[1] for different modulation frequencies. Since U_0 is static, and $U_{d,sweep}$ and $U_{q,sweep}$ are not, the next plot ignores U_0, and focus only on the modulation components. The new imaginary- and real axis are marked in Figure 5.2. The result is shown in Figure 5.3:

[1]The amplitude may vary a bit depending on the amplitude of the 15 kV line during the test. Its phase is per definition lined along the real axis.

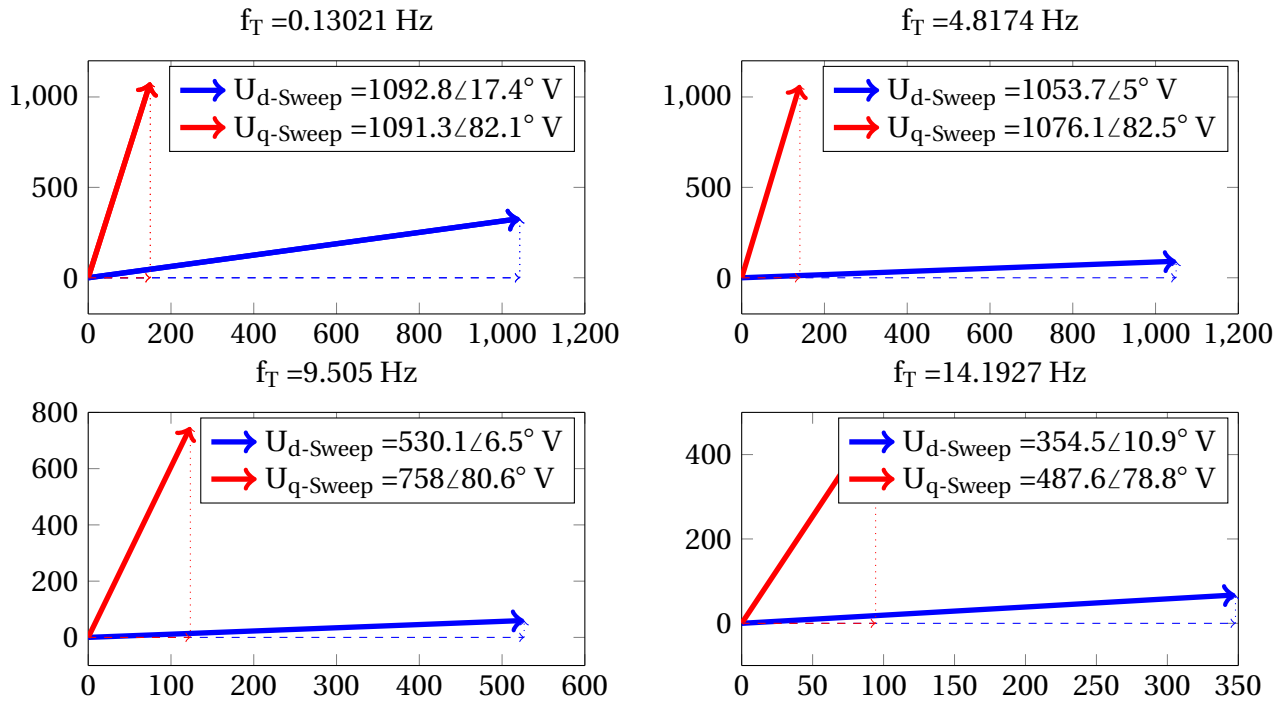

Figure 5.3: $|U_d|$ (dashed), $j|U_q|$ (dotted) and $|U_d| + j|U_q|$ (thick, filled) for both d-sweep (blue) and q-sweep (red). Plotted as as phasors where the j operator determines if the voltage is direct modulated (real) or quadrature modulated (imaginary).

The phasor plots in Figure 5.3 highlight the 'modulation-direction'. The voltage for the d-sweep and q-sweep are both described as $U = |U_d| + j|U_q|$. This plot ignores the phase of the modulation.

Since the direct- and quadrature components are represented with their absolute values, the components will always be equal or more than zero. The angel between the d-sweep and q-sweep will therefore always be equal or less than 90 degrees.

5.2.3 'Modulation-phase' of the voltages

The phasor plots in Figure 5.4 highlight the 'modulation-phase'. The voltage for the d-sweep and q-sweep are both described by its direct component and quadrature component. The direct component and quadrature component are both described by phasors, so the 'modulation-phase' is described. The imaginary operator j is therefore used for determining a modulation

phase of 90 modulation degrees. In opposite to the phasors of type 'modulation-direction', the direct and quadrature component can not be summed, as explained in Section 2.2.6. The plots do not visualize the phasor components exactly as the output of the time-2-dq transformation gives. Two modifications are done:

- The quadrature components are not plotted from zero, but from the end of a direct component of the same sweep.

- The quadrature components is multiplied with the imaginary operator j.

These modifications are done in order to spread the phasors from the orgin and from the real axis. A perfect d-sweep (only direct modulated voltage) with modulation angle equal zero, will therefore be perfectly lined along the real axis. A perfect q-sweep (only quadrature modulated voltage) with modulation angle equal zero, will therefore be perfectly lined along the imaginary axis.

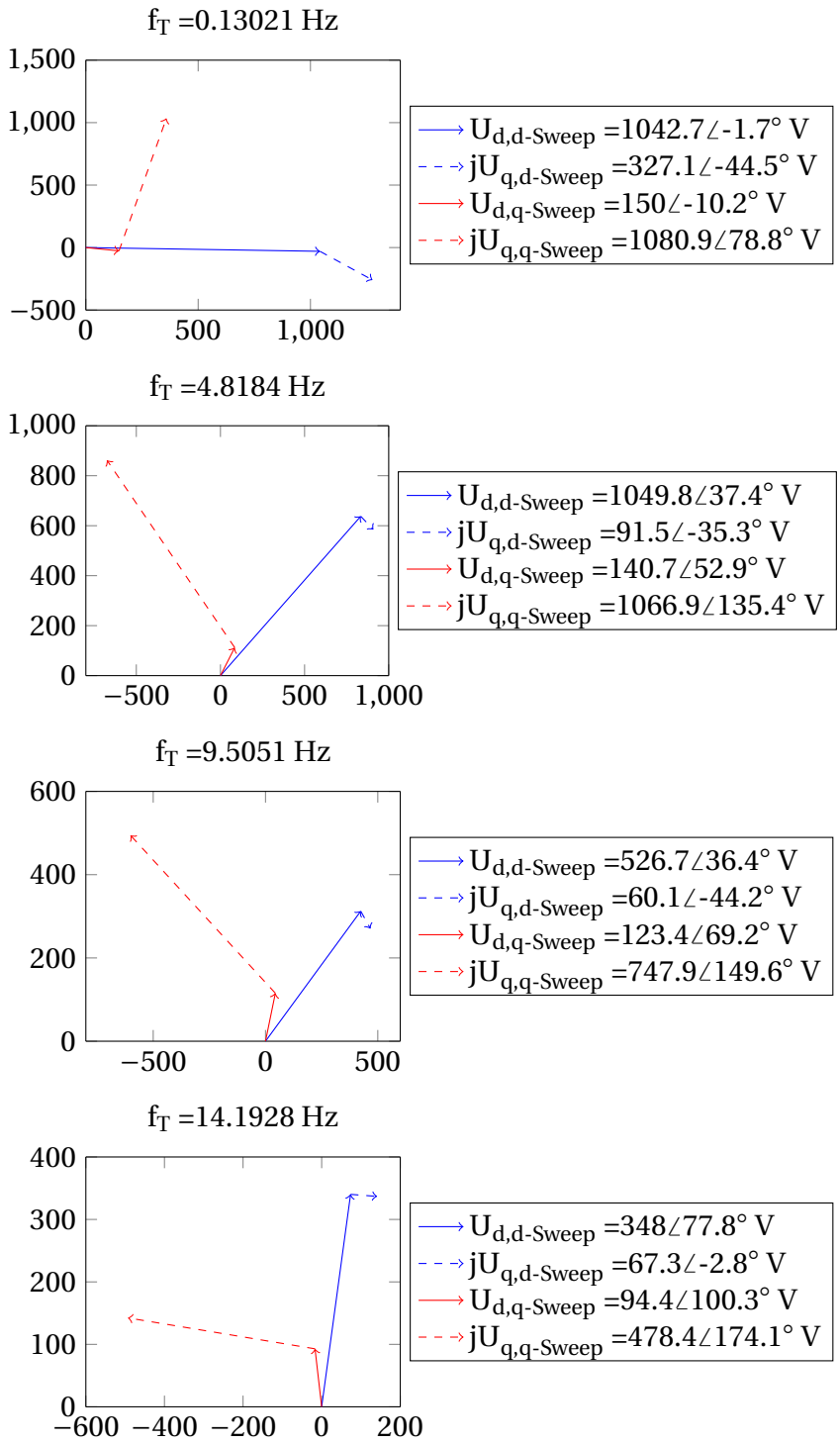

Figure 5.4: Phasor plot for four chosen modulation frequencies. Both direct- and quadrature components of the voltages, for both the direct and quadrature sweeps, are presented in each plot. Notice that the quadrature components are multiplied by the imaginary operator *j*.

5.2.4 Time-phasor combination

Figure 5.5 displays the measured direct and quadrature voltage components in the time domain. The presentation is given for four modulation frequencies. These frequencies are the same as the four given for the phasor plots (Figure 5.4). Thus, comparisons of the frequency and time domain can be conducted. The plots' time axes are limited to one modulation period. To make the modulation components more visible, the fundamental voltage and fundamental frequency is modified. Thus, this is not a presentation of the time dependent measurements, but a way to present the measured frequency components in the time domain. For real time domain measurements, check appendix of the project from fall 2014 by the author[1] or the test report from Alnabru by S. Pika[16].

- The *fundamental frequency is changed* to keep the ratio between the fundamental frequency and modulation frequency constant. A constant ratio ease comparisons between different modulation frequency. A well-chosen ratio makes the characteristics of both the direct modulation and the quadrature modulation visible.

- The *amplitude of the fundamental voltage is changed* in order to visualize the smaller amplitudes of the modulations.

The direct modulation is visible for the d-sweep as the amplitude of the voltage is not constant, but vary with the time (the modulation period). The quadrature modulation is noticeable by considering the phase of the q-sweep in relation to the d-sweep: In the start of the plot ($\theta_{modulation} \approx 0$), the q-sweep is leading a bit. Halfway in th plot ($\theta_{modulation} \approx 180°$), the q-sweep is lagging a bit. This is the result of the quadrature modulation. A larger version with just two subplots is attached in Fig. C.1 in Appendix C.

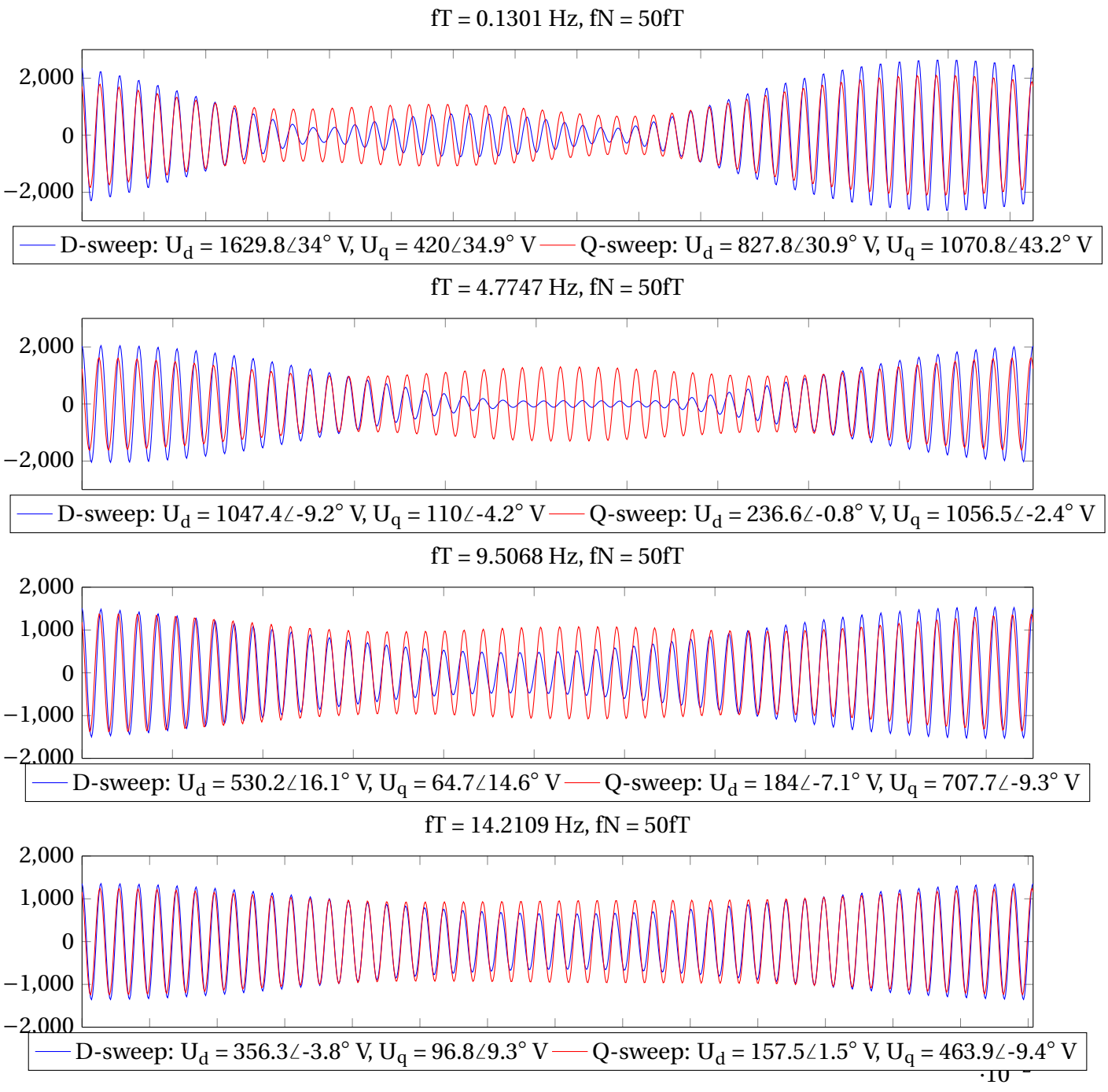

Figure 5.5: Time domain presentation of the frequency components from measurements of test ID33d and ID33q at Alnabru[16]. The fundamental voltage and fundamental frequency is modified in order to make the modulation components more visible. Each plot last for one modulation period.

5.2.5 Conclusion

- The frequency responses of the amplitude and phase presents every modulation frequencies in one figure.
- Both phasor presentations gives detailed information for chosen modulation frequencies. This information is given both numerically and visually. The visual presentation shows relations of angels and magnitudes in the complex plane. The two plots highlight two different aspects of the modulation voltage: The 'modulation-phase' and the 'modulation-direction'.
- The time domain presentation shows detailed information for chosen modulation frequencies as well. This presentation explains the physical interpretation of direct- and quadrature modulated sweeps in the time domain.

5.3 Test specifications at Alnabru

The measured voltage presented in the previous section is based on the "DQ tests" at Alnabru. These "DQ tests" has their specification for the excitation voltage. This section presents these specifications. Further the specifications are compared with the actual measured response.

5.3.1 Test specifications

The test specifications for the excitation voltage is given by Table 5.1. The specifications are given as time constant corresponding to the time equation for the modulation voltage (Equation 2.3). This equation is also shown in the figure for the test setup; Figure 1.2 in Section 1.2.4. The reference for these test specification is the test report from Alnabru[16].

Table 5.1: Test specifications - time constants

ID	Sweep	U_{d0}	U_{q0}	U_{da}	U_{db}	U_{qa}	U_{qb}	f_T
ID33d	d Sweep	15750 V	0 V	750 V	0 V	0 V	0 V	$\frac{(1...110)}{128} f_N$
ID33q	q Sweep	15750 V	0 V	0 V	0 V	750 V	0 V	$\frac{(1...110)}{128} f_N$

5.3.2 Expected results and actually results

According to the test specification, the expected excitation voltage for the d-sweep is a clean direct modulated sweep with modulation phase equals zero ($U_d = \sqrt{2} \cdot 750 \angle 0° V$ and $U_q = 0V$). The expected excitation for the q-sweep is a clean quadrature modulated sweep with modulation phase equals zero ($U_d = 0V$ and $U_q = \sqrt{2} \cdot 750 \angle 0° V$).

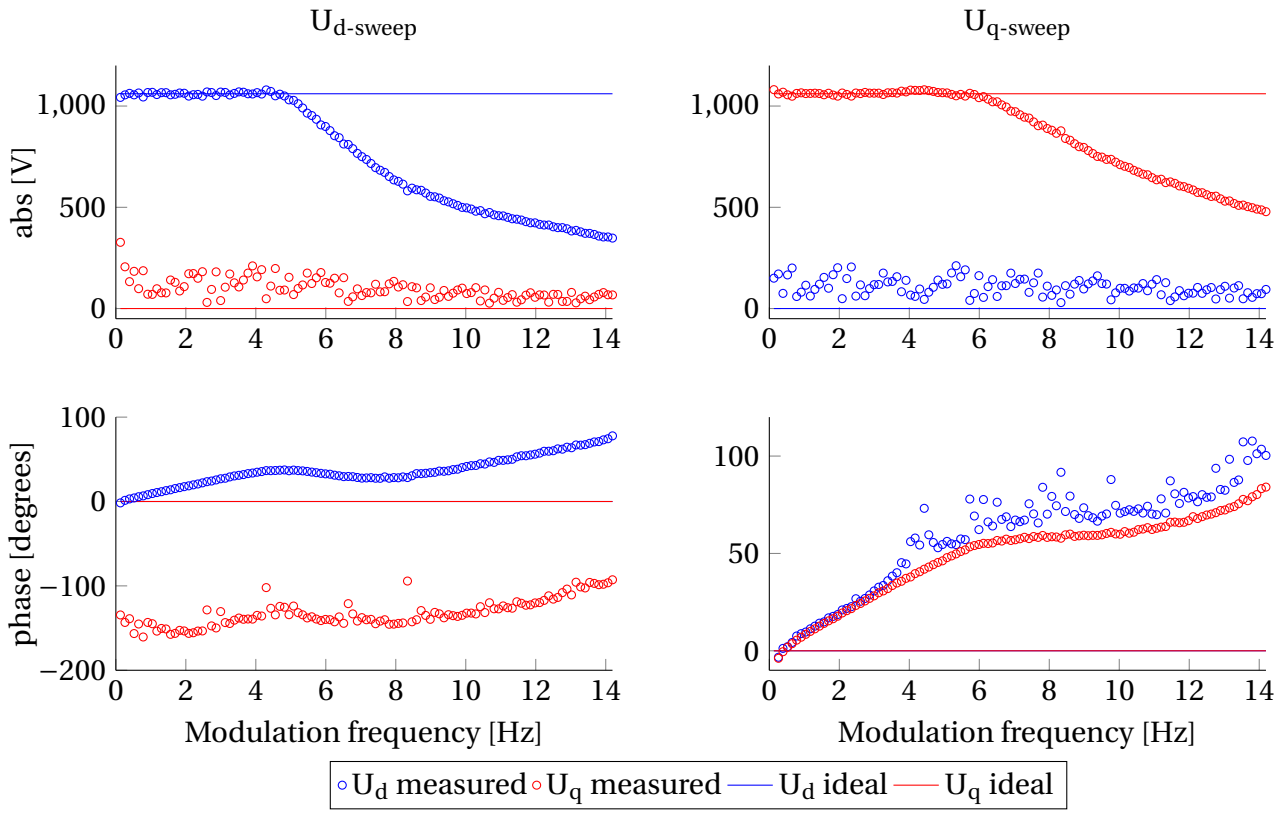

Figure 5.6: Comparing the voltage of the output of a assumed ideal converter with the measured voltage on the 15-kV line

In Figure 5.6, the measured voltage is compared with the ideal voltage on the output of the static converter. The observations are summed up below, where they are categorized in Expected behavior, Unexpected behavior and Other observations:

Expected behavior

- Values $|U_{d,d-sweep}|$ and $|U_{q,q-sweep|}$ is as specified for modulation frequencies up to ≈ 5 Hz.
- $\underline{/U_{d,d-sweep}}$ and $\underline{/U_{q,q-sweep}}$ starts at approximately zero degrees.
- Both phase and absolute values for $U_{d,d-sweep}$ and $U_{q,q-sweep}$ have a smooth behavior.

Unexpected behavior

- The decreasing values of $|U_{d,d-sweep}|$ and $|U_{q,q-sweep|}$ for increasing modulation frequencies.
- $|U_{q,d-sweep}|$ and $|U_{d,q-sweep}|$ are not zero

Other obeservations

- The phase deviation of $\underline{/U_{d,d-sweep}}$ and $\underline{/U_{q,q-sweep}}$.
- Since $U_{q,d-sweep}$ and $U_{d,q-sweep}$ should be zero, their angles do not have any expected value. Anyway, it is observed that $\underline{/U_{d,q-sweep}} \approx \underline{/U_{q,q-sweep}}$ and $\underline{/U_{q,d-sweep}} \approx \underline{/U_{d,d-sweep}} - 150°$.

5.4 Voltage drop over transformer

As stated in Section 5.3.2, the measurements deviate from the test specifications. This deviation might be because of the the voltage drop of the transformer. The voltage drop over the transformer will be calculated in this section.

5.4.1 Fundamental voltage and modulation voltage

As shown in Figure 3.7, the modulation circuit(s) and the fundamental circuit are decoupled. In spite of same physical path, the different electric components might have different influence on

the modulation components and the fundamental components. Therefore the voltage drop for both the modulation voltages and the fundamental voltage is calculated.

Both calculations will be performed in order to explain the behavior of the measured modulation voltage. Therefore, the motivation for calculating the modulation voltage is clear. The fundamental voltage and the modulation voltage do not have, or have small, influence on each other, as discussed in Section 3.1. However, the fundamental component is directly connected to the reference of the modulation angle. The modulation components are generated from the converter with the phase reference inside the converter, lined with the fundamental voltage. The modulation components on the line is measured with reference of the fundamental voltage on the line. Therefore, the phase of the fundamental voltage on the line is important.

5.4.2 Model

The topology at Alnabru is presented in Fig. 5.7. The transformer and grid filter is modeled as given in Fig. 5.7. The specifications for the transformer and grid filer, with their references, is found in Appendix B, and Figure B.1 and B.2, respectively. The electric traction vehicle, in series with the line and the cable, is modeled with frequency dependent admittance.

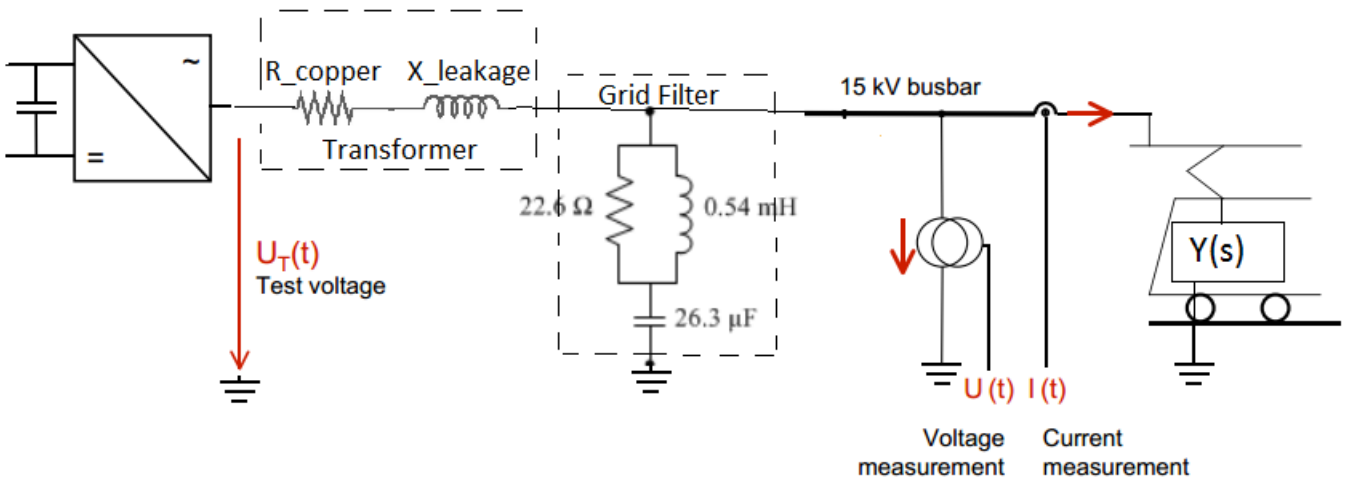

Figure 5.7: The complete topology used for calculating the voltage drop. Original figure by Emkamatik[9], but modified.

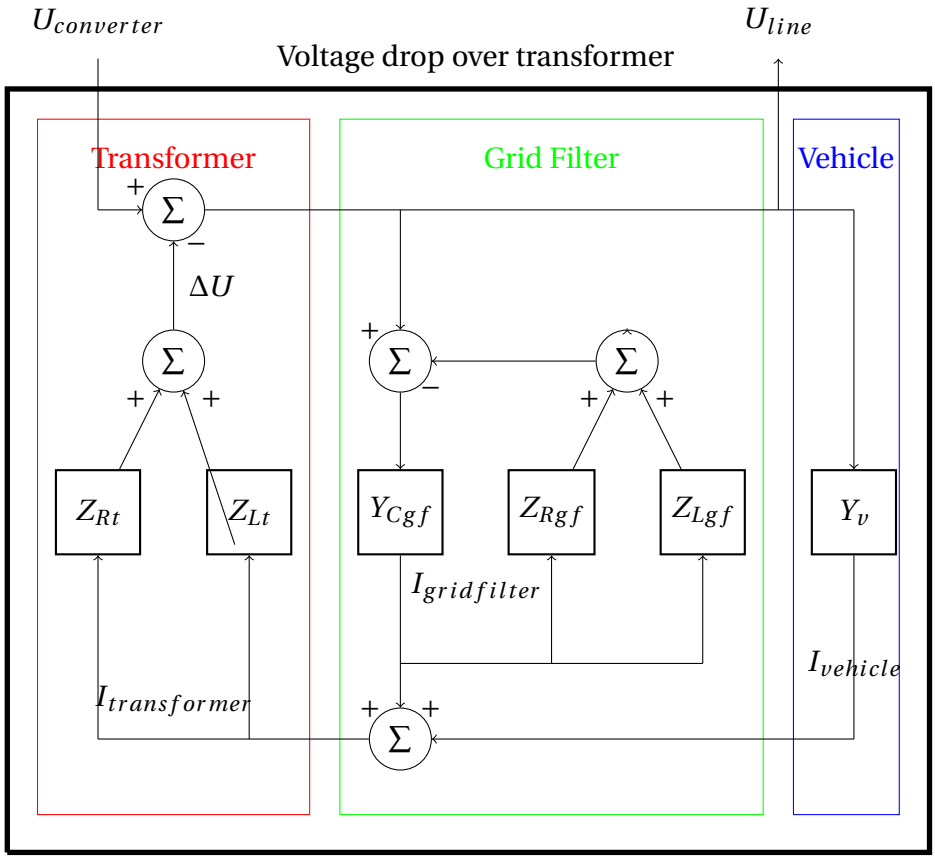

Figure 5.8: Voltage drop over transformer represented by blocks

5.4.3 Calculations

Calculations of the modulation components

This section will briefly explain how the voltage drop over the transformer is calculated. Since this calculation deals with currents and voltages in both direct- and quadrature direction, impedances for each component must be expressed as dq-matrix-impedances. Such impedances for an inductor, a capacitance and a resistor is derived in Section 3.3, and presented by Equation 3.12, 3.14 and 3.16, respectively. Further, simple circuit analysis is applied on the given topology (Figure 5.7) and solved by using linear algebra. The result is given by Equation 5.1:

$$\begin{bmatrix} U_d \\ U_q \end{bmatrix}_{line} = (I - Z_{trans} Y_{tot}) \begin{bmatrix} U_d \\ U_q \end{bmatrix}_{statConv} \tag{5.1}$$

The elements in Equation 5.1:

- $\begin{bmatrix} U_d \\ U_q \end{bmatrix}_{line}$ is the result of direct- and quadrature modulated components of the voltage on the 15-kV line (point of measurement).
- $\begin{bmatrix} U_d \\ U_q \end{bmatrix}_{statConv}$ is the direct- and quadrature modulated components of the generated voltage on the terminals of the static converter. In this example it is assumed that these voltages equals the specified voltages (Table 5.1).
- I is the 2×2-identity matrix.
- Z_{trans} is the impedance of the transformer on the dq-matrix-form.
- Y_{tot} is the total impedance of the total topology on the dq-matrix-form:

  $Y_{tot} = \frac{1}{Z_{trans} + \frac{1}{Y_{GridFilter} + Y_{vehicle}}}$

Calculation of the fundamental voltage

As the fundamental components can be decoupled as explained in Section 3.2, the drop of the fundamental voltage can be calculated isolated. The principals of phasor calculations is therefore applied on the simple circuit in Figure 5.7. The admittance of the vehicle of the circuit in

Figure 5.7, is replaced with the current source. The effective frequency of the modulation frequency is assumed to be $f = f_N + f_T$. This assumption is not verified, but chosen in order to give the results a wider range if possibilities. There do not exist any easy measurable data for the current. Such data requires a time to fundamental frequency transformation, which is time demanding to develop. The amplitude is approximated to 4 A, and the calculations will be performed for the phase equal -90, 0, 90 and 180 degrees. Again, this is to get a wider range of possibilities. The measurements will not be exact anyway, therefore the whole specter of possibilities are searched. Maybe one of the possibility might be interesting.

5.4.4 Results and discussion, modulation voltage

$M = (I - Z_{trans} Y_{tot})$

$M = (I - Z_{trans} Y_{tot})$ gives the relation between the input voltage and output voltage, for a given modulation frequency, and is plotted in Fig. 5.9.

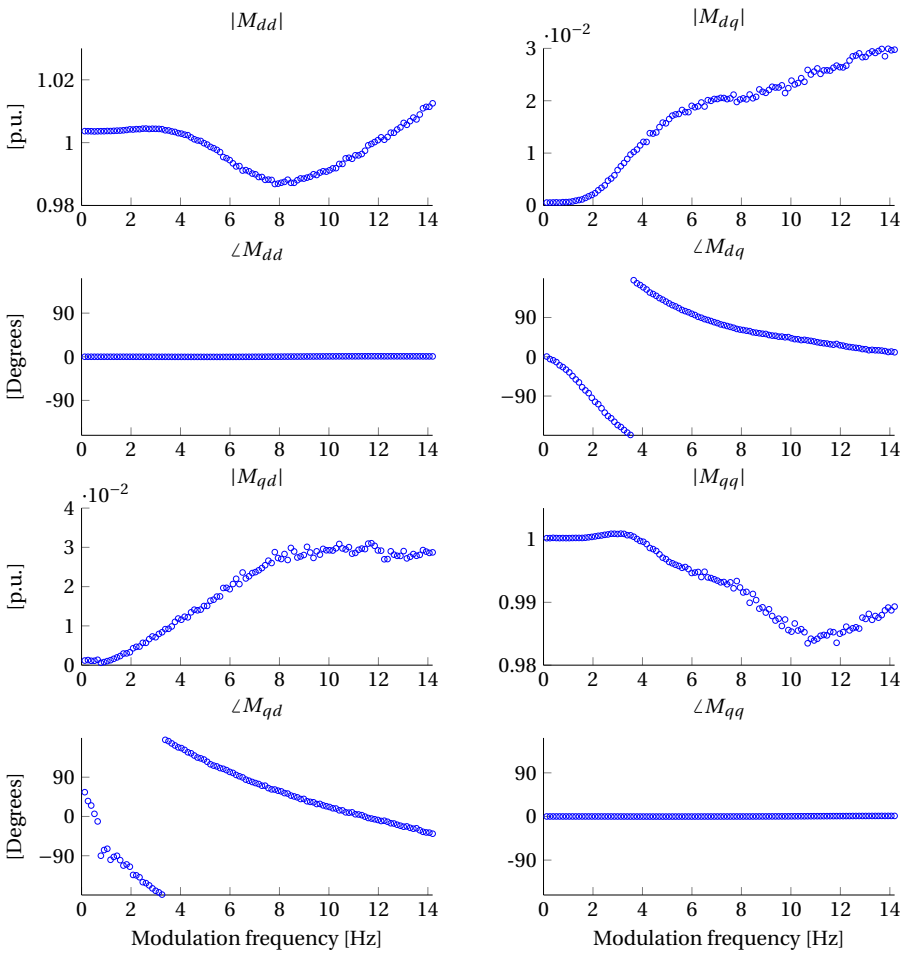

Figure 5.9: $M = (I - Z_{trans}Y_{tot}) \rightarrow U_{measure}(j\omega) = M(j\omega) \cdot U_{statConv}(j\omega)$

As seen from Figure 5.9, the transformer in combination with the rest of the topology, gives a small voltage drop. No voltage drop is determined by $M_{dd} = M_{qq} = 1\underline{/0°}$ and $M_{dq} = M_{qd} = 0$. The actual results are close to these values: The direct coupled components (M_{dd} and M_{qq}) vary within a range of ±2% from one. The cross coupled components (M_{dq} and M_{qd}) vary with a range of ±3% from zero. This is expected since the voltage drop over a transformer should be low for power systems in regular operation.

Notice that the matrix is close to symmetric, but not exactly due to the no-symmetric impact of the admittance of the electric vehicle. If the electric vehicle had been modeled as a RLC-load, and not a no-symetric admittance, the M-matrix would have been completely symmetric.

Is the calculation method valid?

The calculation method are considered to be valid. The arguments are as follows:

- The calculations is in accordance with the rules presented in Section 3.4.
- The system is small, and an equal method is considered to be valid by the author in the project from fall 2014[1]. This is briefly discussed in Section 4.3.2.
- Expected result. It is not expected any large voltage drop over the transformer. This is not expected due to the low impedance of the transformer compared to the large impedance of the grid filter and the electric vehicle.

5.4.5 Results and consequences, fundamental voltage

The voltage drop of the fundamental voltage is intersting as this change the reference phase of the modulation components. This reference is defined by the phase of the voltage. As the voltage is measured on the 15 kV line, this is the reference for the dq transformed data. However, the reference of the voltage excitation is at the static converter. This might give deviation between the dq transformed data and the test specification. The phase of the voltage on the 15 kV line is presented in Figure 5.10 with zero degrees in the static converter as the reference. The amplitude is ignored, as this will have no effect on the reference of the modulation components.

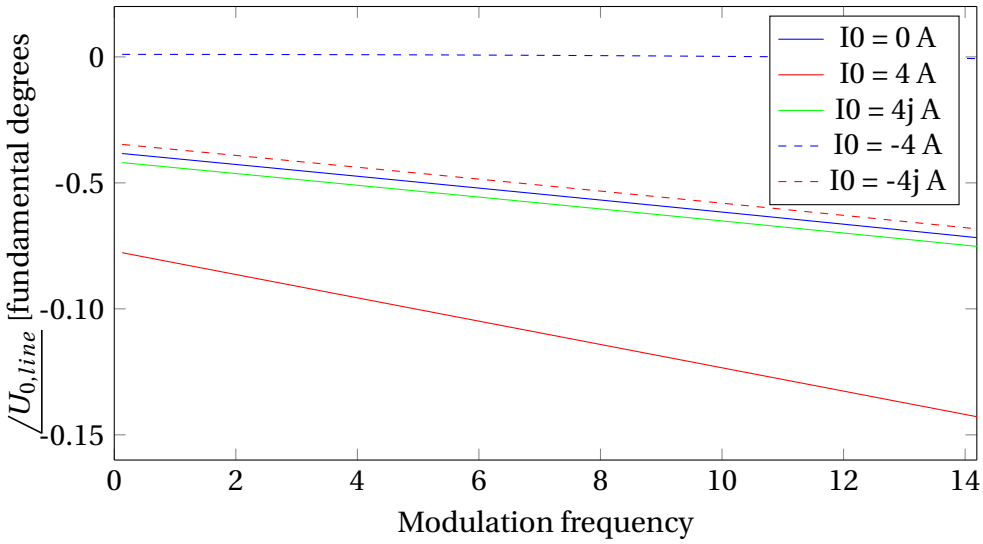

Figure 5.10: The phase of the fundamental voltage at the line (point of measurements). Since the $I0$ may vary, and is hard to measure exactly, several phases of $I0$ is calculated.

The result reveals a low phase deviation of the fundamental voltage. As seen, the choice of $f_{effective} = f_T + f_N$, and the choice of different phases of I_0, gives different phase deviation. Non of these deviations are large. It is still some uncertainty related to the series impedance of the transformer. If this impedance had been ten times larger, the maximum phase deviation still would have been no larger than two fundamental degrees. The results shows a phase deviation also with no current conducted by the electric vehicle ($I0 = 0$). This is due to the grid filter current.

In spite of small voltage deviations, this might have larger consequences for the calculations of the modulation components. The phase shift of the fundamental voltage ($\Delta\theta_{fund}$) causes a shift in the modulation angel reference ($\Delta\theta_{ref} = \Delta\theta_{fund}$). In Appendix A, the consequences of this change in reference is calculated, form a mathematically perspective. The result is a change in the modulation direction and a change in the modulation phase. The change in modulation direction will cause a leakage from the direct component to the quadrature component; $U_q(\Delta\theta_{ref}) = \sin(\Delta\theta_{ref})U_{d,\Delta\theta=0} + \cos(\Delta\theta_{ref})U_{q,\Delta\theta=0}$. the corresponding change from quadrature component to direct component is $U_d(\Delta\theta_{ref}) = \cos(\Delta\theta_{ref})U_{d,\Delta\theta=0} + \sin(\Delta\theta_{ref})U_{q,\Delta\theta=0}$ The change in modulation phase, due to a change in the fundamental phase is given by $\Delta\theta_{mod} = \frac{\omega_T}{\omega_N}\Delta\theta_{ref}$

Since $\Delta\theta_{ref} = \Delta\theta_{fund}$ is so small, it is clear that the small phase deviations calculated from the voltage drop, presented in Figure 5.10, will have a small effect on the change of modulation phase and modulation direction.

5.5 Numeric issues

The voltage in the frequency domain, is a result of a challenging time to dq transformation. The most challenging part of such a transformation is the conditioning of the time domain data. Time data needs to be conditioned before it is sufficiently decomposed for the Fourier transform. Conditioning of the signal is a quite large topic, which is a bit out of scope for this master thesis. However, one of the issues of the time to dq transformation is highlighted. Further, investigations of how this issue can be related to the voltage measurements, are conducted.

5.5.1 Conditioning of time domain data

Performance of a successful time to dq transformation when Fourier transformation is applied, has the following requirements:

- The fundamental frequency must be known before starting the transformation.
- The modulation frequency must be known before starting the transformation.
- The signal must contain an integer of fundamental periods.
- The signal must contain an integer of modulation periods.

The two first requirements is quite straight forward as the fundamental frequency is constant and as $\omega_{modulation}$ is measured at the "DQ tests" at Alnabru[16]. The two last requirements are a bit more challenging. Challenging in terms of the performance of the pre-conditioning, and challenging in terms of what is possible, given a short test period (ten seconds) for each modulation frequency. The last of these challenges is discussed in Section 5.5.2.

5.5.2 Fit between T_T and T_N

A successful time to dq transformation of a signal requires the signal's duration to be exactly an integer times the modulation period (T_T) and exactly an integer times fundamental period (T_N). Since this must happen at the same time, and the duration of the signal is limited to ten seconds[2], the two periods will rarely match 100%. When they do not match, this happens with a phase deviation $\Delta\theta$ from the optimal matching. This non-optimal fit might be a limitation of the accuracy of the time to dq transformations.

5.5.3 Correlations of data

As the frequency-fit might be a limitation of the accuracy, there might be some correlation between the fit of the frequencies and the accuracy of the transformed dq voltages. In Figure 5.11, the least phase deviation for each set of T_T and T_N (or f_T and f_N) is plotted. This phase deviation is not calculated by use of the measurements: It is an isolated algorithm with T_T and T_N as input, and the frequency-fit as output. This phase deviation is given in the modulation frame. In the same plot, the "accuracy" of the voltage amplitudes of the d-sweep and q-sweep, are plotted. More specific: the "accuracy" is the deviation from; the instant voltage amplitude for a modulation frequency, to the average voltage amplitude. The plots are carried out for modulation frequencies up to 4 Hz due to the decreasing voltage.

[2]The test time for each each modulation frequency is ten seconds. In order to avoid transient switching responses, the "effective" time is less than ten seconds.

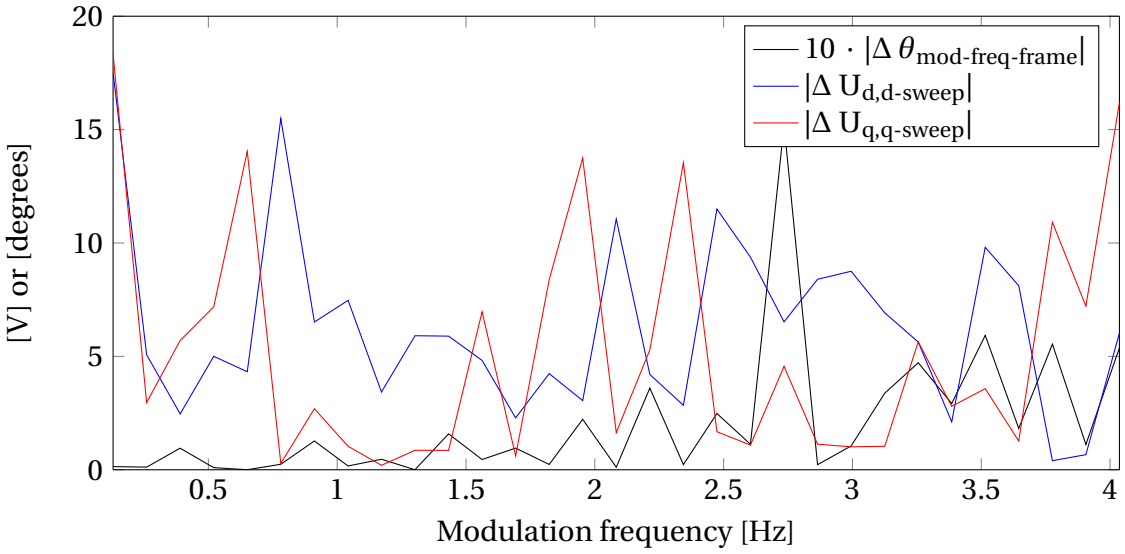

Figure 5.11: Fit between f_T and f_N compared with deviation of voltage from the average value.

Figure 5.11 shows that it is a small correlation between the voltage deviation and the 'frequency-fit'. This indicates that the voltage deviation is not determined by the *theoretic optimal* 'frequency-fit'. However, the deviation might still be related to the 'frequency-fit': The performance of the conditioning is then the limitation of the resulting 'frequency-fit', not the theoretic limitation.

Other correlation is also checked:

- $\Delta|U_{d,d-sweep}|$ between $\Delta|U_{q,q-sweep}|$
- $|U_{q,d-sweep}|$ between $|U_{d,q-sweep}|$
- $|U_{q,d-sweep}|$ between 'frequency-fit'
- $|U_{d,q-sweep}|$ between 'frequency-fit'

None of these combinations gave any significantly large correlation factor.

5.5.4 Correlation between voltage current

The correlation between the current and voltage should also be checked. The quadrature component of the d-sweep, and the direct component of the q-sweep, are the two components of the voltage with the largest possibility to be exposed for numeric issues. Therefore, it should

be tested if the deviations in $|U_{q,d-sweep}|$ and $|U_{d,q-sweep}|$ can be found as deviation in the currents. If this is the case, the deviation in $|U_{q,d-sweep}|$ and $|U_{d,q-sweep}|$ have a larger probability to be result of non ideal converter, not numeric issues. However, all the current components are both dependent of the direct and quadrature component of the voltage, through the cross components of the admittance (Y_{dq} and Y_{qd}), and therefore it is hard to investigate the correlations. One way of checking the correlation between current and voltage is simply to check the smoothness of the elements the frequency dependent admittance matrix, Y. As seen in Figure 4.1, the admittance is smooth, but is probably dominated of the large values of $|U_{d,d-sweep}|$ and $|U_{d,d-sweep}|$, so the impact of $|U_{q,d-sweep}|$ and $|U_{d,q-sweep}|$ drowns. Therefore; no conclusion can be drawn.

To compare $|U_{q,d-sweep}|$ with $|I_{q,d-sweep}|$, and $|U_{d,q-sweep}|$ with $|U_{d,q-sweep}|$, will not be sufficient due to the cross components (Y_{dq} and Y_{qd}) of the admittance, given in Equation 6.1. Actually a smart method of checking the correlation between the voltage and current is to check the frequency dependent admittance, Y. The frequency dependent admittance is actually smooth, as seen in Figure 4.1, and gives a large correlation between the voltage current.

5.5.5 Time to dq transformation on artificial signals

There are some uncertainties regarding numeric issues of time to dq transformation since the signal to be transformed is not known. In other words: Deviation from the optimal dq components might be caused by the signal, and not by any numeric issue. To test the performance of the time to dq transformation, an artificial signal is generated and transformed:

Artificial voltage sweeps are generated by use of Equation 2.3. The signal is perfectly generated as specified by the test specifications (Table 5.1) at Alnabru[16]. The perfect signal is transformed from the time frame to the dq frame by the t2dq-function by Meyer[11]. The same modulation frequencies as for the test at Alnabru is used. The resulting modulation components are not perfect. This is because of limited length (time) of the signal and therefore not optimal frequency fit for many pairs of modulation- and fundamental frequencies. The length of the signal that is transformed is $t_n = round(n \cdot \frac{f_N}{f_T})$[3]. Larger n means better accuracy as the ratio between the modulation period and the fundamental period is closer to an integer. In Fig-

[3]Where $round(x)$ gives the closest integer to x

ure D.1 - D.4 in Appendix D, the modulation components are plotted for $n = 1, 10, 100$ and 1000. In Figure 5.12 the modulation components is ploted for $n = 1$:

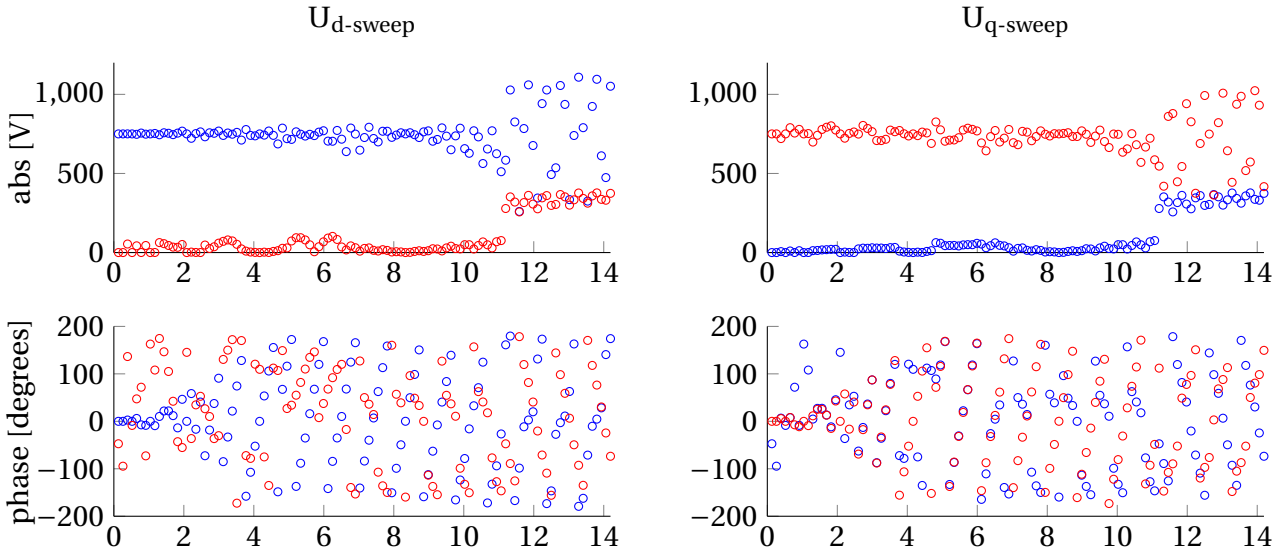

Figure 5.12: Time to dq transformation on artificial signal. $n = 1$

For this plot, it is observed that the amplitude of the voltage component are quite accurate, and the accuracy of the phase of the components is very low. This indicates that the accuracy of the phase might be less accurate than the amplitude for the real transformation as well.

5.6 Decreasing amplitude: Non ideal converter?

From e.g. Figure 5.6, it is observed that direct component for the voltage for the d-sweep and the quadrature component of the q-sweep is decreasing with higher modifications. The reduction is large; a relative reduction from one to half. The reduction has a smooth and clear behavior and is present for both sweeps: Therefore it is probably not caused by any numeric issues, but is a result of the nature of the system. As this reduction is so large, and attacks suddenly for certain modulation frequencies, it is not related to any impedance considerations in the distribution systems. This statement is supported by the result of the voltage drop, which is of a very small magnitude, discussed in Section 5.4.

The decreasing amplitude could be a result of a no ideal converter. The sudden attack of the decreasing amplitude, and its smooth linear behavior, reminds of some saturation related to (a) conflict(s) for higher modulation frequencies. It is not put any more effort into investigating this topic.

5.7 'Modulation-direction'

The infiltration of quadrature modulated voltage in the d-sweep, and vice versa, are presences for all modulation frequencies for both sweeps. The size of the infiltrations vary a lot and it seems to have no dependency of the modulation frequency.

The infiltration might be dependent of an error in the reference of the modulation angel. In that case, there is a deviation in the modulation angel $\Delta\theta_{mod}$. This deviation will cause a leakage of voltages between the direct and quadrature component. This is shown as a mathematically derivation in Appendix A. The change in modulation direction will cause a leakage from the direct component to the quadrature component; $U_q(\Delta\theta_{mod}) = \sin(\Delta\theta_{mod})U_{d,\Delta\theta=0} + \cos(\Delta\theta_{mod})U_{q,\Delta\theta=0}$. The corresponding change from quadrature component to direct component is $U_d(\Delta\theta_{mod}) = \cos(\Delta\theta_{mod})U_{d,\Delta\theta=0}+\sin(\Delta\theta_{mod})U_{q,\Delta\theta=0}$. Since $\sin^2(\Delta\theta_{mod})+\cos^2(\Delta\theta_{mod}) = 1$, $\sqrt{|U_d|^2+|U_q|^2}$ will stay constant no matter of the size of $\Delta\theta_{mod}$. In Figure 5.13, $\sqrt{|U_d|^2+|U_q|^2}$ is plotted for both the d-sweep and the q-sweep. This plot shows that $\sqrt{|U_d|^2+|U_q|^2}$ stay quite constant, while $|U_d|$ and $|U_q|$ fluctuate much. This indicates that there is a deviation in the modulation reference $\Delta\theta_{mod}$, which cause $|U_d|$ and $|U_q|$ to deviate from their specified values.

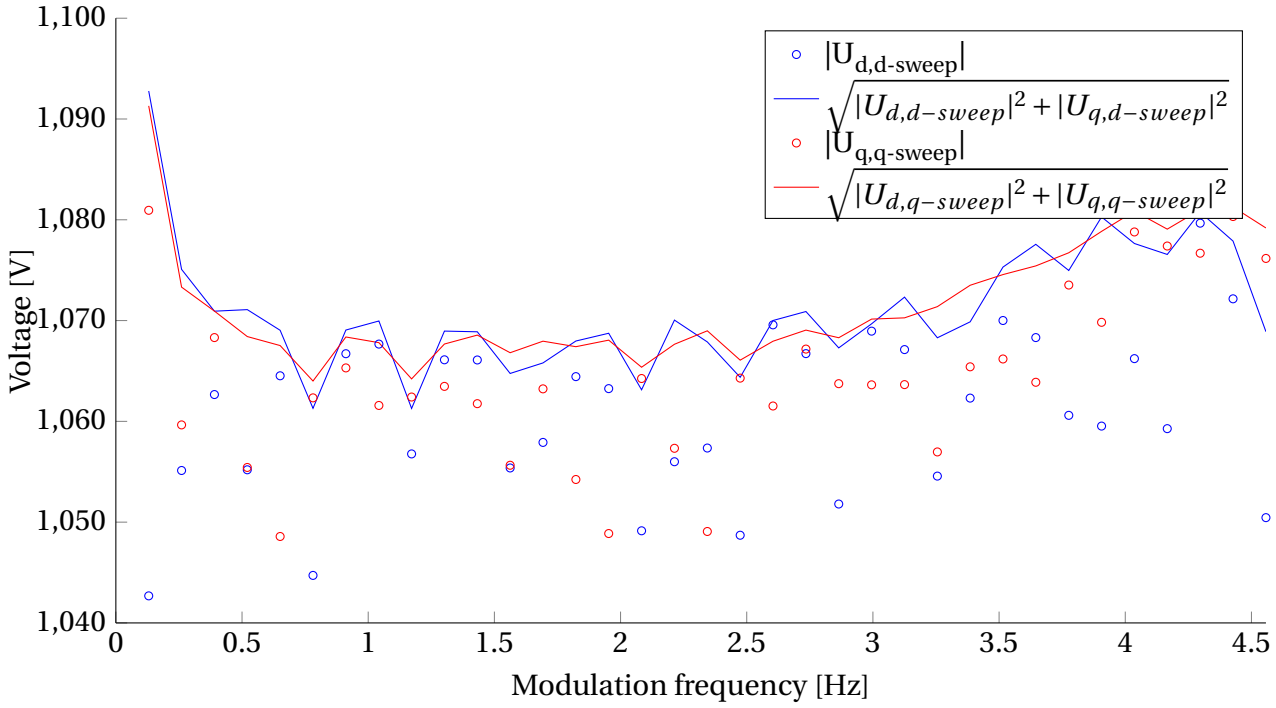

Figure 5.13: Deviation of $|U_d|$ and $|U_q|$, for both sweep are not randomly as $\sqrt{|U_d|^2+|U_q|^2}$ is quite constant. Indicates a deviation of the modulation angle, $\Delta\theta_{mod}$.

The deviation of the modulation $\Delta\theta_{mod}$ vary for each modulation frequency and is thereby not caused by any impedance consideration. This was discussed in Section 5.4.5 when the voltage drop over the transformer was calculated. The deviation in the modulation reference might be caused by the time to dq transformation or the the performance of the sweeps in the static converter.

5.8 Phase deviation

The response of the phase still needs some analysis before its behavior can be understood. Some analysis thats explain some of the behavior will be conducted in this section.

5.8.1 Data

For this analysis, data that seems to have a correct frequency response is selected for closer studies. This data is the quadrature modulation of the voltage during test ID33q, for a selected interval of the modulation frequency. This interval is indicated with vertical lines in Fig. 5.14 and spans from $f_T \approx 1$ Hz to $f_T \approx 5$ Hz. This data has a nice frequency response, shown by the following observations:

- U_d and U_q are in phase ($\angle U_d = \angle U_q$).
- The phase increases linearly without any numeric deviation.
- The amplitude of U_d is quite constant, and its value ($\approx \sqrt{2} \cdot 750V$) is in accordance with the test specifications for ID33q (Table 5.1).

Due to these reasons, the phase of U_q for this interval has most likely a characteristic determined by the nature of the system, and not by any numeric issues or unknown influence.

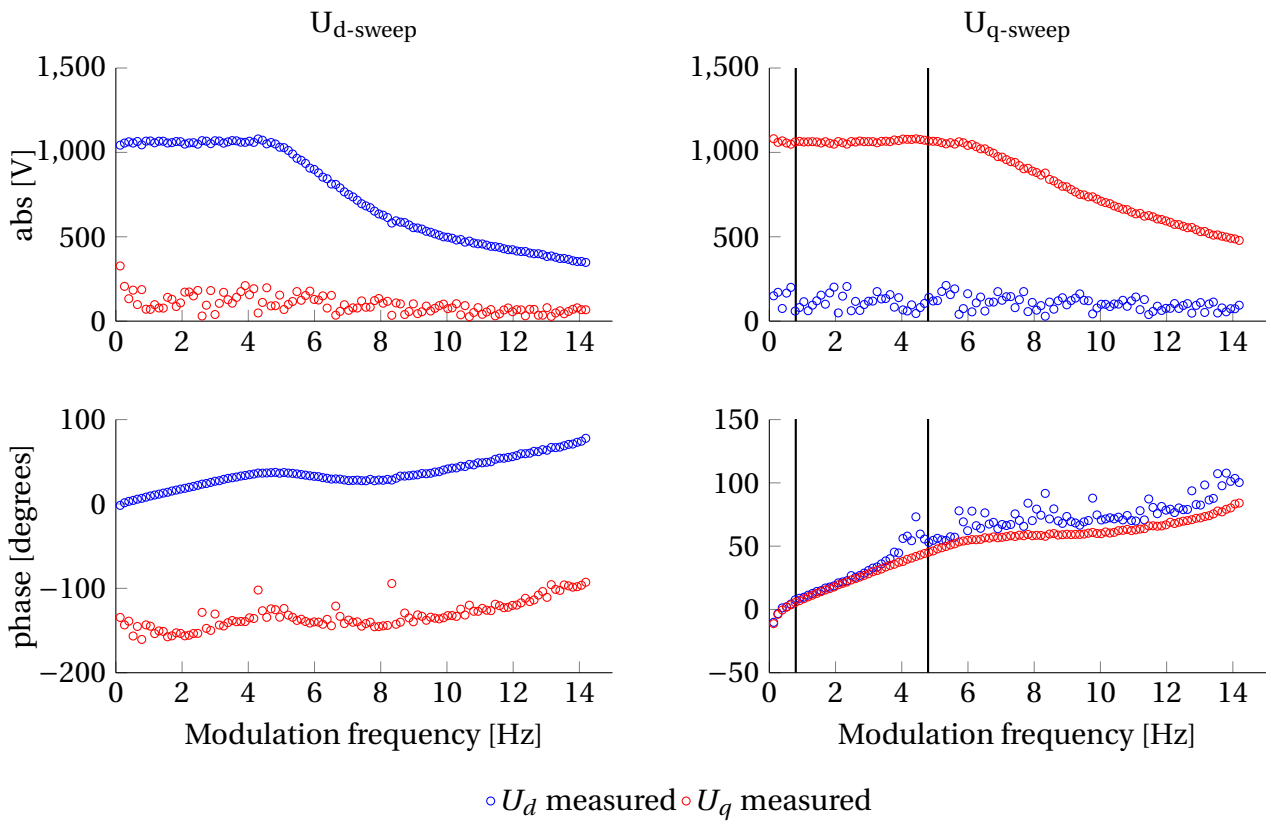

Figure 5.14: Frequency response of the modulation voltage in the dq-frame on the 15-kV line during sweep ID33d and ID33q. Notice the interval between the vertical lines: the phase of both U_d and U_q are equal, the phase is increasing linearly and the amplitude of the q-component is constant.

5.8.2 Converting from modulation- to fundamental degrees

As explained in Section 2.2.3, the phase of the direct- and quadrature modulation voltage are related to the phase in the modulation domain. This phase can also be given in the the time domain and in the fundamental frequency domain. Figure 5.15 illustrates how the phase deviation between the modulation of two signals can be given in different domains.

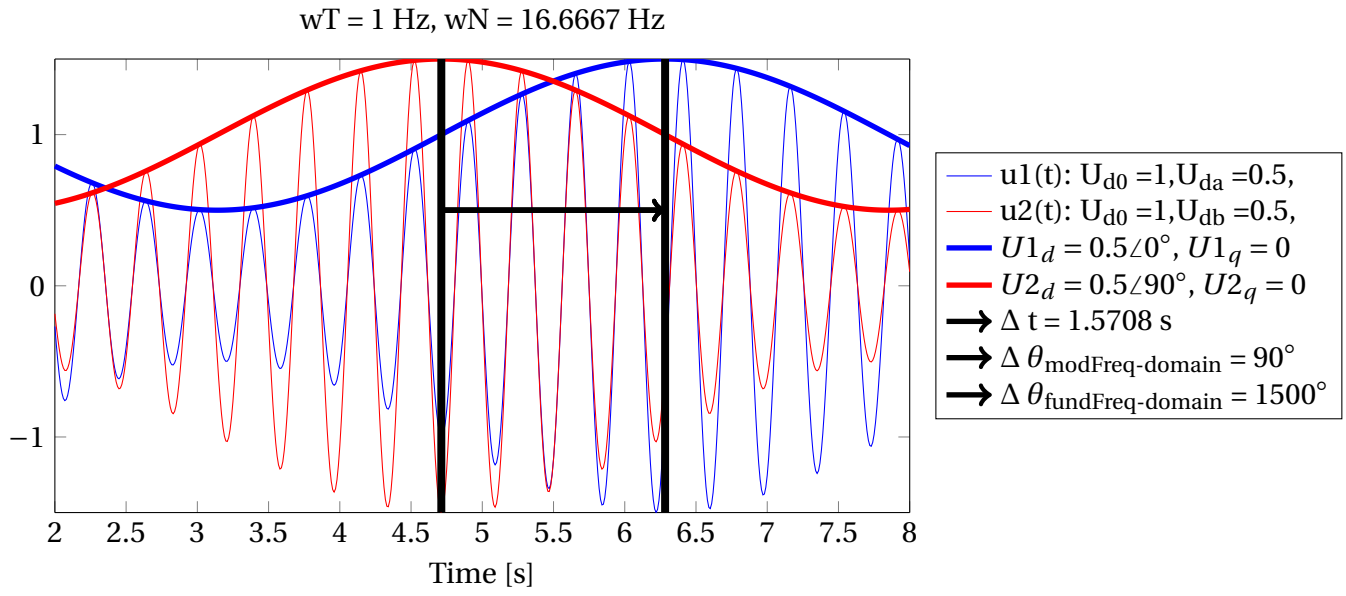

Figure 5.15: The illustartion shows the phase difference in the modulation of signal $u1(t)$ and $u2(t)$. This phase deviation is given in the time-domain, modulation-frequency-domain and the fundamental-frequency-domain.

As the modulation frequency vary, angular deviations across different modulation frequencies might not be comparable. By converting the phase deviation to a time deviation, comparison of the deviation across different modulation frequencies makes more sense. Such a translation is given by Equation 5.2 and is shown in Figure 5.16. As seen in Figure 5.16, the time deviation is actually constant within the highlighted frequency interval.

$$\Delta t = \underline{/X_y(\omega_T)} \cdot \frac{1}{\omega_T} \tag{5.2}$$

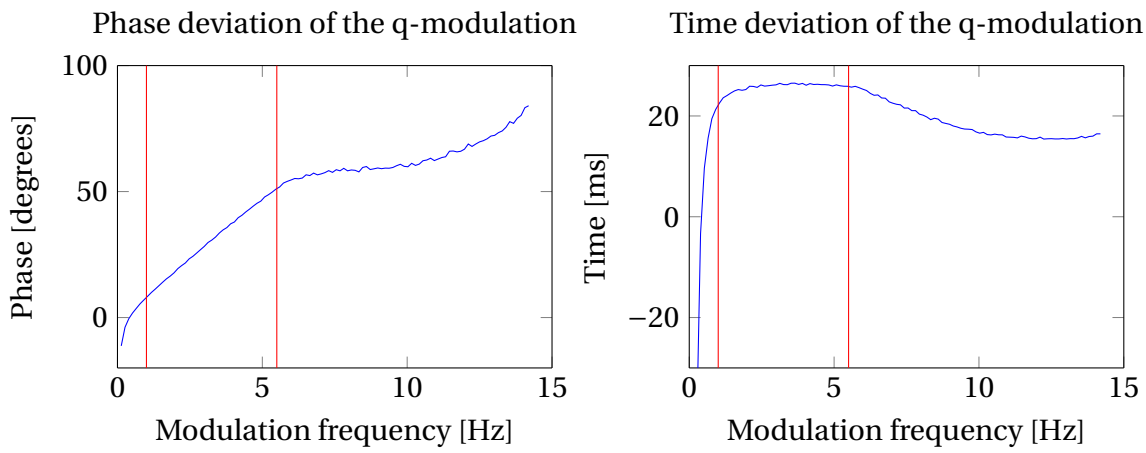

Figure 5.16: The plot shows the phase of the q-component of the measured voltage during ID33q. The linear increasing phase, given in the modulation frame, gives a constant deviation in the time domain.

The phase deviation related to the modulation frequency can also be converted to a phase deviation in relation to the fundamental frequency. This conversion is given by Equation 5.3 and is plotted for all voltage measurements in Fig. 5.17.

$$\angle X_y(\omega_T)|_{N-domain} = \angle X_y(\omega_T)|_{T-domain} \cdot \frac{\omega_N}{\omega_T} \tag{5.3}$$

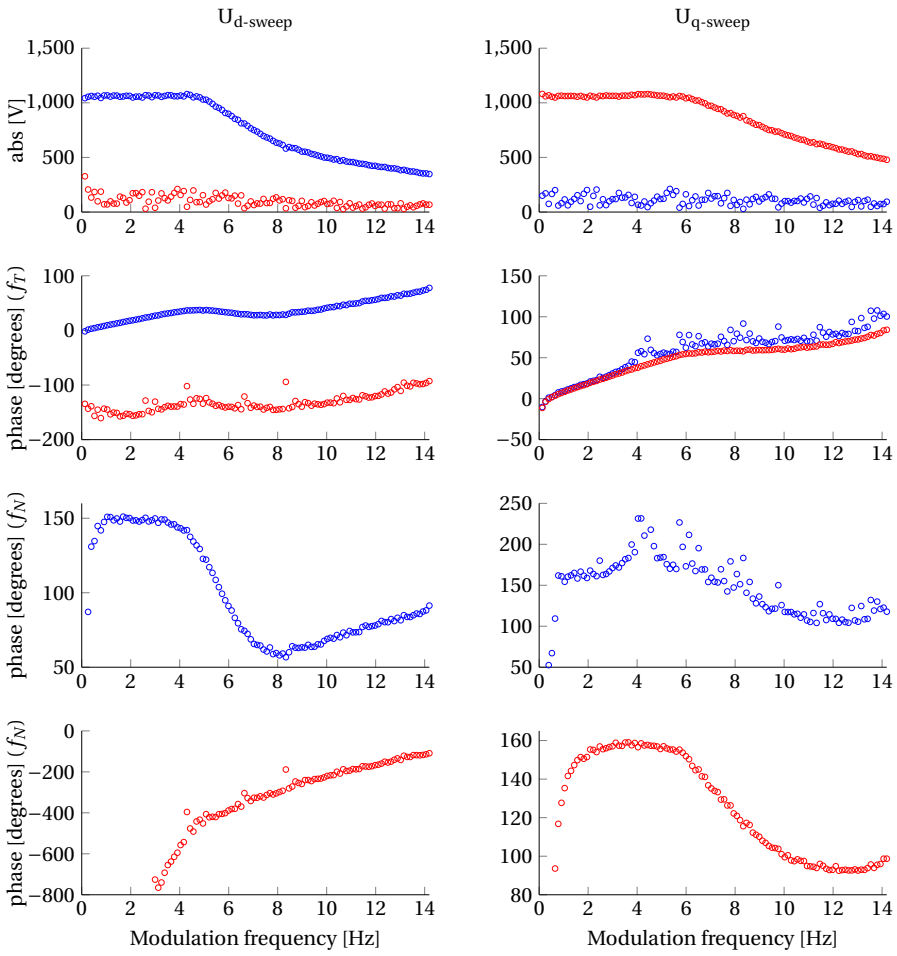

Figure 5.17: The plots shows the phase in both relation to f_T and f_N during sweep ID33d and ID33q.U_d is blue and U_q is red.

5.8.3 Discussion of the phase

This discussion is based on measurements of the plots in Figure 5.17, in the light of the test specifications for the ID33d and ID33q (Table 5.1).

Tendency

From Figure 5.17 a clear tendency is observed: The voltage has more or less the same phase response for every components. However, there are some exceptions:

- Some numeric/source issues on the phase of $U_{q,d-sweep}$ and $U_{d,q-sweep}$. Those issues are found for the corresponding absolute values as well.

- The frequency response for the phase of $U_{q,d-sweep}$ is not in accordance with the tendency for the first half of the sweep.
- $U_{q,d-sweep}$ has the same tendency for the last half of the sweep, but is lagging approximately 130 modulation degrees.

In spite of these exceptions, there are some factors which really support the observed tendency:

- The frequency responses of the phase of $U_{d,d-sweep}$ and $U_{q,q-sweep}$ are similar.
- Both the phase and amplitude responses of $U_{d,d-sweep}$ and $U_{q,q-sweep}$ are smooth.
- In spite of the poor numeric/converter accuracy on $U_{q,d-sweep}$ and $U_{d,q-sweep}$, they both follow the same tendency quite well.
- The amplitude of $U_{q,d-sweep}$ and $U_{d,q-sweep}$ seems to not have any relation to the modulation frequency. Still, the phase of the same components do have a clear dependency to the modulation frequency. When this poor data still have a significant relation to the tendency, the existence of the tendency is strengthened.

Four stages of the frequency reponse of the phases

By observing the frequency responses of the phases of $U_{d,d-sweep}$ and $U_{q,q-sweep}$, four stages can be detected. They are now discussed in the terms of fundamental degrees:

- **Stage 1: Increasing phase** ($f_t \approx 0-1Hz$)
- **Stage 2: Constant phase** ($f_t \approx 2-5Hz$)
- **Stage 3: Decreasing phase** ($f_t \approx 6-8Hz$)
- **Stage 4: Constant phase** ($f_t \approx 9-14Hz$)

Stage 2 and Stage 4: Constant fundamental phase is expected for $U_{d,d-sweep}$ and $U_{q,q-sweep}$. This is due to no phase deviation for direct coupled elements of M (M_{dd} and M_{qq}) in Figure 5.9, which states no phase deviation caused by voltage drop. Due to numeric issues, and limitation of performing the tests, a small phase deviation is inevitable. Given this small deviation, it

makes sense that this deviation is constant in the time frame, rather than constant in the modulations frame. This is the case for Stage 2 and Stage 4. This is observed as constant phase in the fundamental phase domain, and as a linear smooth increasing phase in the modulation phase frame.

Stage 1 and Stage 3: The increasing/decreasing of phase might be connected to the current amplitude. Before stating this as the only reason, some other possibilities are checked:

- Not caused by the voltage drop over the transformer. No phase deviation for direct coupled elements of M (M_{dd} and M_{qq}) in Figure 5.9. A voltage drop would not appear so strongly for just a short interval of modulation frequencies.

- Not caused by numeric issues. If that was the case, the angel would not be so smooth.

- The running modulation frequency, $\theta_m od$, measured from the static converter, is investigated and no suspiciously behavior is detected.

Investigations of the current during sweep ID33d and ID33q, attached in Appendix F; Figure F.1, shows some correlation to the four stages of phase response. These correlations are ploted in Figure 5.18, and described as follows:

- The interval of close-to-zero current for $I_{d,d-sweep}$, correspond to the interval of Stage 1 for the d-sweep.

- The interval of close-to-zero current for $I_{q,q-sweep}$, correspond to the interval of Stage 1 for the q-sweep.

- The interval of maximum current for $I_{d,d-sweep}$ correspond to the interval of Stage 3 for the q-sweep.

- The interval of maximum current for $I_{q,q-sweep}$ correspond to the interval of Stage 3 for the q-sweep.

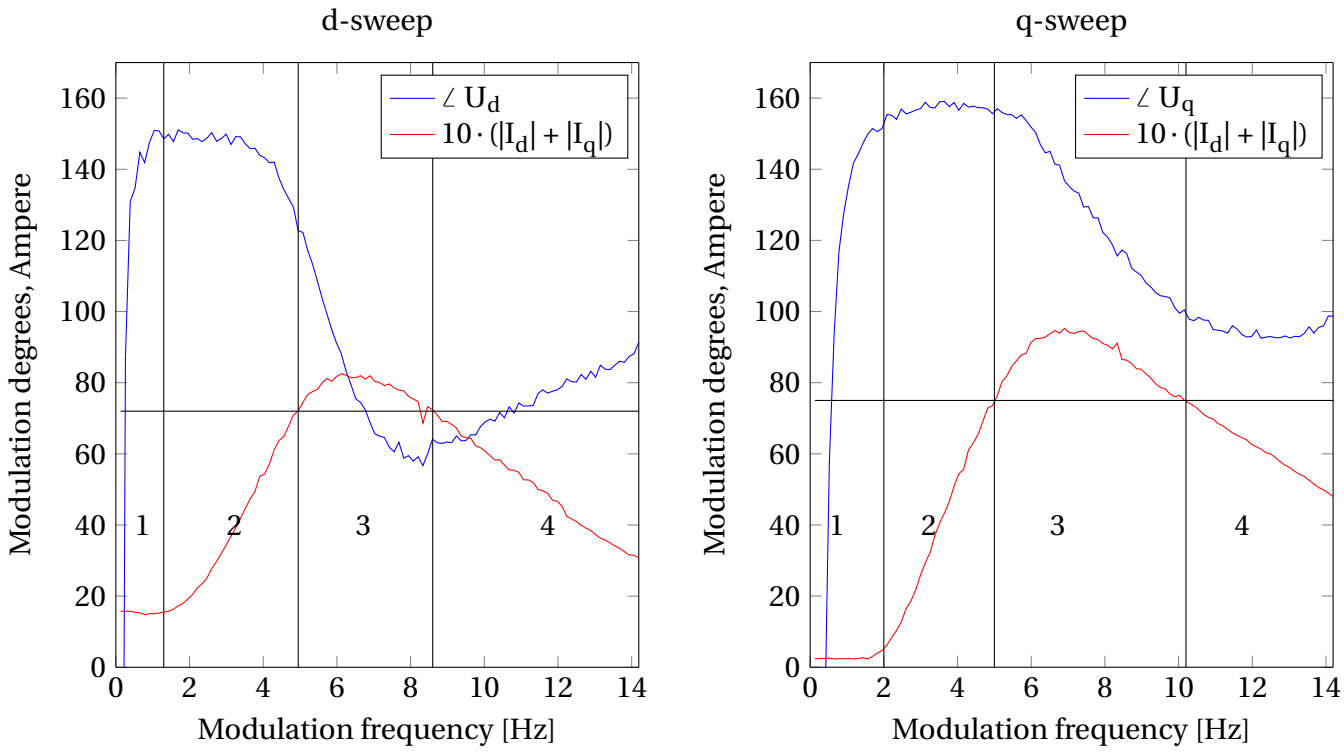

Figure 5.18: The four stages of the behavior of $\angle U_{d,d-sweep}$ and $\angle U_{q,q-sweep}$ do have some correlation to the total current ($|U_d| + |U_q|$) of each sweep. In other words: the operation of the static converter, related to the phase, might be affected of the level of the supplying current.

5.9 Conclusion

Different presentation methods

Different presentation methods of modulation components should be used depending on the reason for the presentation. The four methods presented here are: frequency response of phase and amplitude, phasor plot in relation to the 'modulation-direction', phasor plot in relation to the modulation phase, and modulation components in the time frame. In addition, the phase is plotted in both modulation degrees (default) and fundamental degrees.

Measurements deviate from test specifications

The voltage measured on the 15 kV line differs from the specifications of the "DQ tests" at Alnabru: Amplitude for higher modulation frequencies for $U_{d,d-sweep}$ and $U_{q,q-sweep}$ decrease. The voltage is not pure direct modulated for the d-sweep, and it is not pure quadrature modulated for the q-sweep. The modulation phase deviates from zero.

Voltage drop over the transformer

The test setup at Alnabru is modeled with a voltage source, a transformer, a grid filter and an electric traction vehicle. The transformer and grid filter is modeled by using the 2×2 dq impedance matrices for a resistor, inductor and a capacitor, derived and presented in Section 3.3.2. The electric traction vehicle is modeled with frequency response of the 2×2 admittance. The voltage drop over the transformer is small, but noticeable. This result is expected as the voltage drop over a transformer should be very small. The voltage drop is to small to explain any of the measured voltage deviation from the test specifications. It does not explain the tendency either.

Numeric issues

To obtain the frequency dependent modulation components, from the time dependent measurements, is not straight forward. As this topic is a bit out of scope of the research questions of this thesis, and the topic's complexity is large, just some of the many issues is highlighted: The optimal 'frequency-fit' for different modulation frequencies is calculated. Further, different correlations to the measurements is checked, without any significant results.

Voltage amplitude

A smooth linear and large (relatively from one to half) deviation of the voltage, is observed for higher frequency modulations, for both d-sweep and q-sweep. This deviation is probably caused by no ideal static converter, rather than numeric issues. This is concluded with background in the relatively smooth phase response of the components, and the fact that the phase response might be harder to calculate accurate, as discussed in Section 5.5.5. However, these

statements is not verified and further investigations must be carried out for a complete confirmation.

'Modulation-direction'

The infiltration of quadrature modulated voltage in the d-sweep, and vice versa, are presented for all modulation frequencies for both sweeps. The size of the infiltrations vary a lot and it seems to have no dependency of the modulation frequency.

However an interesting observation is made: $\sqrt{|U_d|^2 + |U_q|^2}$ is constant in spite of the very fluctuating components of $|U_d|$ and $|U_q|$. This is seen in relation to the consequences of a change in the modulation reference $\Delta\theta$: The change in modulation direction will cause a leakage from the direct component to the quadrature component; $U_q(\Delta\theta_{mod}) = \sin(\Delta\theta_{mod})U_{d,\Delta\theta=0} + \cos(\Delta\theta_{mod})U_{q,\Delta\theta=0}$. The corresponding leakage is presence for leakage from quadrature to direct. Since $\sin^2(\Delta\theta_{mod}) + \cos^2(\Delta\theta_{mod}) = 1$, $\sqrt{|U_d|^2 + |U_q|^2}$ will stay constants. This is the case for voltage measurements. The leakage of the two sweeps are therefore probably caused by a change in the modulation reference. This change may be from the static converter. It has simply problems by hitting the exact modulation angel, and might be missing by $\Delta\theta$. It can also be numeric issues related to the time to dq transformation.

Phase deviation

The phase deviation of all the voltage components do have more or less the same tendency. The tendency is a clear and smooth frequency response for the direct component of the voltage in the d-sweep, and the quadrature component of the voltage in the q-sweep.

The phase of the modulation is "given" as complex numbers in the *modulation frequency domain*. "Given" in terms of the output of the time-to-dq-transformation, and thus the frequency responses that is plotted throughout this thesis and the test report from Alnabru[16]. As the modulation frequency vary during the test, angles in the modulation frequency domain might not be comparable across different modulation frequencies. The phase deviation is therefore transformed into angles in the *fundamental frequency domain*, which is static. The results reveal that some smooth *linear increasing* angel deviations, given in the modulation frequency frame, are transformed to *constant* phase deviations in the fundamental frequency frame.

Still, the phase do not correspond completely to the specified "DQ tests". This deviation might be related to both numeric issues and non ideal voltage source. However, the phase deviation in the fundamental frequency frame, are compared with the absolute value of the current. There are some vague correlations. These correlations indicate that the phase deviation is caused by the voltage source, and is further dependent of the operation state of it.

Chapter 6

How do imperfect sweeps affect further calculations?

This chapter discuss how imperfect "DQ tests" affects the resulting frequency response. The mathematical description of the system states that imperfect tests are sufficient for achieving the correct frequency responses. However, the excitation voltage can not be in conflict with the linearization point.

6.1 'Modulation-direction'

The two sweeps was specified (Table 5.1) to be a clean d-sweep and a clean q-sweep: The 'modulation-direction' of the two sweep was specified to be orthogonal sweeps. However, the measurements was not in accordance with the specifications and the sweeps was not orthogonal. Therefore the following research question is raised: Are not orthogonal sweeps sufficient for identifying the correct frequency responses of electric components?

6.1.1 Orientations of the 'modulation-direction' of the sweeps

Figure 5.3 in Section 5.2.2 shows phasor plots of the 'modulation-directions' for the measured modulation components at Alnabru[16]. These phasor plots can be categorized among "Othogonal. dq-lined", "Orthogonal. Not dq-lined" and "Not Orthogonal. Not dq-lined" as shown in

Figure 6.1:

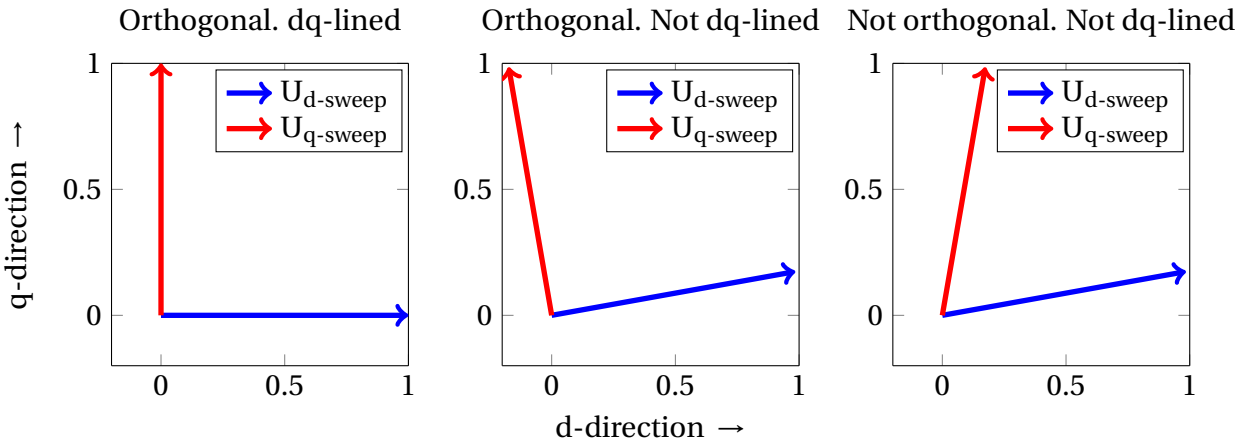

Figure 6.1: Orientations of the 'modulation-direction' of the sweeps

dq-sweeps according to the test specifications (Table 5.1), gives dq-sweeps of the cathegory "Orthogonal. dq-lined". Sweeps of the cathegory "Orthogonal. Not dq-lined" are not possible with the phasor system described in Section 5.2.2, as explained in the same section. "Not orthogonal. Not dq-lined" is the the case of all measurements at Alnabru[16].

6.1.2 The equations takes care of not-orthogonal cases

Equation 6.1, presented in Section 3.1.2, states the relation between the current ΔI, the admittance Y and the voltage U given in Figure 3.1:

$$\begin{bmatrix} \Delta I_d \\ \Delta I_q \end{bmatrix} = \begin{bmatrix} Y_{dd} & Y_{dq} \\ Y_{qd} & Y_{qq} \end{bmatrix} \begin{bmatrix} U_d \\ U_q \end{bmatrix} \tag{6.1}$$

The current and voltage are measurable, unlike the admittance which not can be measured directly. Thus, Matrix Equation 6.1 have four unknown variables (Y_{dd}, Y_{dq}, Y_{qd} and Y_{qq}), but only two equations. A single set with measurements are therefore not enough to unveil the four unknown parameters. However, if two set of measurements are used, e.g. *Set 1* and *Set 2*, the matrix equation 6.1 can be used two times as Equation 6.2 shows:

$$\begin{bmatrix} \Delta I_{d,Set1} & \Delta I_{d,Set2} \\ \Delta I_{q,Set1} & \Delta I_{q,Set2} \end{bmatrix} = \begin{bmatrix} Y_{dd} & Y_{dq} \\ Y_{qd} & Y_{qq} \end{bmatrix} \begin{bmatrix} U_{d,Set1} & U_{d,Set2} \\ U_{q,Set1} & U_{q,Set2} \end{bmatrix} \tag{6.2}$$

If both *Set 1* and *Set 2* are based on the same voltage level and state of operation, Equation 6.2 will be valid for any set of currents and voltages[1]. If *Set 1* and *Set 2* are linear independent, Equation 6.2 are solvable for Y_{dd}, Y_{dq}, Y_{qd} and Y_{qq}. Since two equations do not have to be orthogonal in order to be linear independent, *Set 1* and *Set 2* do not need to be orthogonal. The only requirement for being linear independent is that the two sets must have elements that can be orthogonal projected.

Thus, mathematically, the two voltage sweeps do not need to be orthogonal. From an electric power view, the author does not see any reasons that the two sweeps needs to be orthogonal either. However, there might be several factors that motivate to perform orthogonal sweeps:

- When the sweeps are orthogonal, they are guaranteed to be linear independent.
- The accuracy might be larger. The orthogonal projection are larger when the sweeps actually are orthogonal.
- From an Electric Power view, there might be easier, both practically and educationally, to perform sweeps in the direct- and quadrature direction, thus orthogonal sweeps.

6.2 Modulation phase

As discussed in Section 2.2.3, the modulation phase is not as specified in the "DQ tests". As for the 'modulation-direction', the not perfect modulation phase is also handled by Equation 6.2: A change in the modulation phase for the voltage will cause a change in the modulation phase for the current. This change will be the same for both the voltage and the current. The resulting admittance is therefore not effected of the phase of the modulation signals.

[1] The same voltage level and state of operation is required since the model is based on linearization of a voltage level during one state of operation

6.3 Amplitude

As Figure 5.1 shows, the amplitude of the modulation voltage measured on the 15 kV line decrease a lot during both "dq sweeps". The amplitudes of the modulation components do actually has maximum values twice their minimum values.

6.3.1 Varying amplitude is in conflict with the linearization

Linearization of a nonlinear model requires operation around this operation point. Since the measurment is not performed within one operation point, the model build on this system will loose accuracy. The loss of accuracy is depended on the nonlinear behavior of the system: If $f_{sys}(x) = a \cdot x^{1.1}$ represent the nonlinear physical system, the linearization $f_{model}(x) = a \cdot x$ will not be very bad although x escape a bit from the linearization point.

Chapter 7

Extracting transfer functions and application of them

This chapter presents a set of extracted transfer functions from the numeric frequency response of the electric traction vehicle. Application of these transfer functions in a larger electric system during stability analysis is presented.

7.1 Motivation

During this thesis, most of the calculations has been conducted numeric. In these cases; matrix operations has been performed for every frequency available. By extracting the frequency responses to transfer functions, further usage can be conducted analytically. This is very handy because software often supports calculations with transfer functions on matrix form.

Stability analysis of the electric traction system might be performed in a larger system than only one vehicle and one static converter. In this chapter an extension of the simple system is shown.

Both the extraction and the application in a larger system will be shown without much explanation. The two sections should be used more for inspiration to further work.

7.2 A set of extracted transfer functions

Given a numeric frequency response, there are many methods for extracting transfer function to fit the numeric frequency response. Theory regarding this operation is out of scope of this thesis. A set of transfer functions will be presented to show that this extraction is possible, and that the result is quite good. Matlab System Identification Toolbox^{TM} is applied for the extractions. The numbers of poles and zeros can be chosen before starting the extraction. Higher number of poles and zeros gives larger accuracy of the specified interval. If there are problems by reaching high accuracy in some areas, and these areas are important for the stability analysis, these frequency ranges can be set to higher priority of the extraction. In Figure 7.1 a set of transfer functions is presented. These are plotted together with the numeric frequency responses.

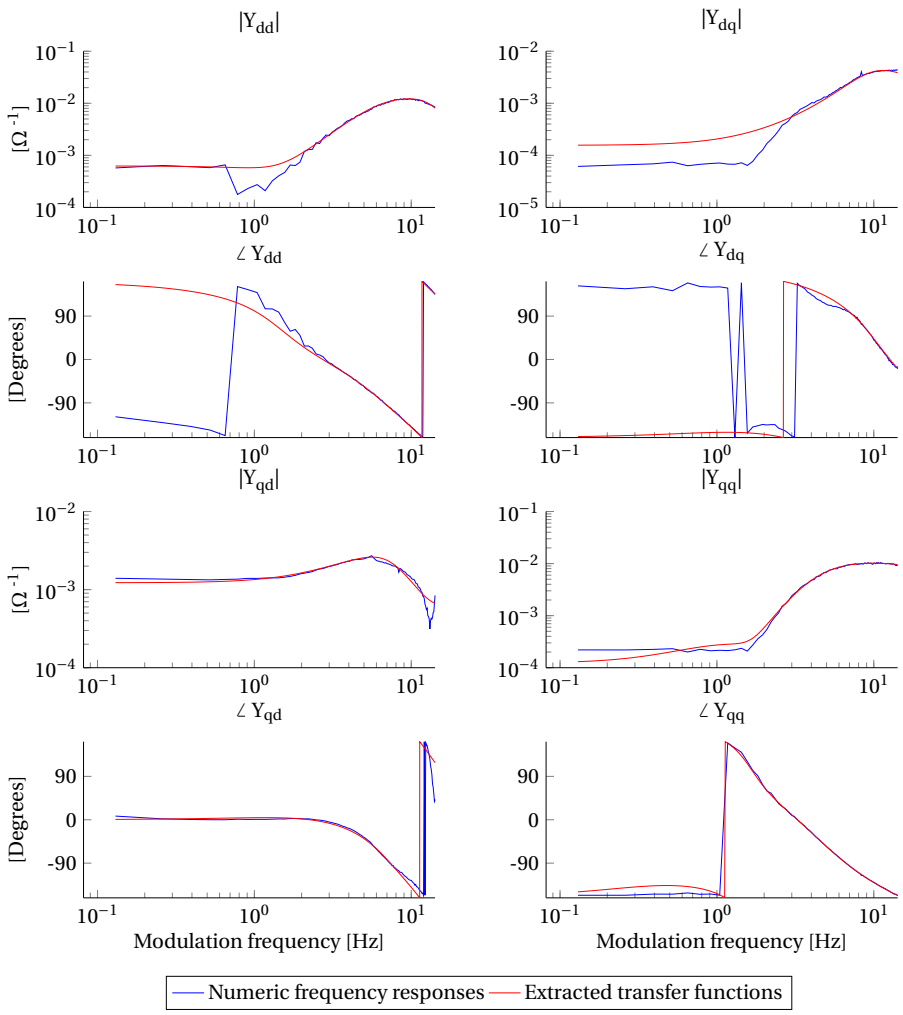

Figure 7.1: The numeric frequency response of the electric traction vehicle from test ID33d and ID33q at Alnabru, and a corresponding set of extracted transfer functions.

The transfer function on analytic form:

- $Y_{dd}(s) = \frac{-0.005693s^4 - 0.1522s^3 - 90.95s^2 + 925.9s - 7936}{s^4 + 123.6s^3 + 1.296e04s^2 + 5.126e05s + 1.267e07}$
- $Y_{dq}(s) = \frac{-0.0233s^3 + 35.57s^2 - 490.1s - 6328}{s^4 + 183.8s^3 + 2.151e04s^2 + 1.084e06s + 4.054e07}$
- $Y_{qd}(s) = \frac{0.0008975s^3 - 0.04443s^2 + 5.984s + 88.54}{s^3 + 78.93s^2 + 3564s + 7.223e04}$
- $Y_{qq}(s) = \frac{-1.347s^3 + 5.653s^2 - 127.4s - 318.5}{s^4 + 166.6s^3 + 8828s^2 + 2.214e05s + 2.59e06}$

7.3 Application in larger systems

The "DQ approach" allows usage of traditional linear system modeling. This is because the output and input of the components are clearly defined and independent of the rest of the system given operation around the linearization point. This was discussed, and some simple rules was given in Section 3.4. Thus, a further expansion of the system can be done: Figure 7.2 shows a system with two vehicles, two lines and one source exposed for a disturbance. The two lines and two vehicles can easily be reduced to one block. This block represent the whole load. The system is then consisting of just two blocks. This is useful, as the stability criterion for a double feedback loop system then can be applied. This criterion is derived from the Nyquist stability criterion by e.g. S. Pika and S. Danielsen[18]

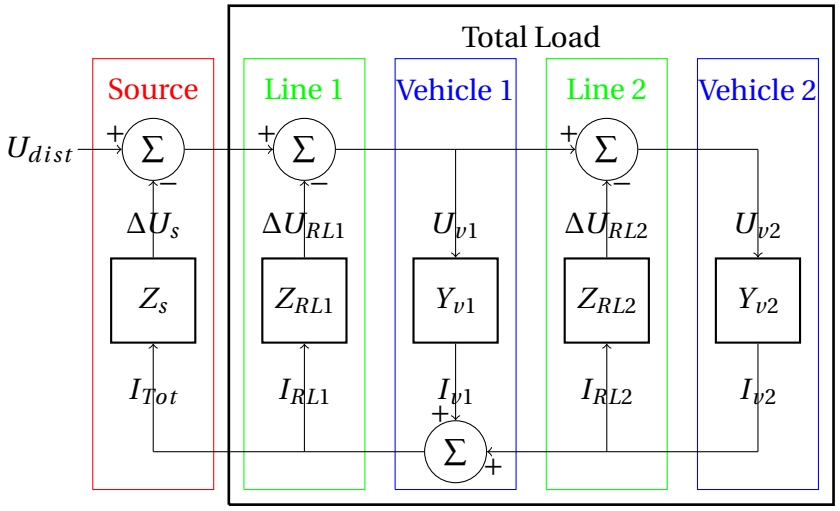

Figure 7.2: A system with two vehicles, two lines, one cable and one disturbance. The two lines and two vehicles can easily be reduced to one block; total load

In addition to analytic stability analysis, time dependent analysis can be conducted easily in simulation tools. In that case, the transfer functions can be directly implemented. And the electric traction system can be disturbed by any signal, $U_{dist} = \begin{bmatrix} U_d \\ U_q \end{bmatrix}_{dist}$.

A model with several disturbances, static converters and rotary converters can also be made. The static- and rotary converters can be included as regular frequency responses. Several disturbances can be included by either; make several inputs to the system, or use principles of

superposition. The principle of superposition is probably the easiest since the block diagram must be modified when the location of the disturbance vary. This is because the disturbance must see its Thévenin impedance in front. In case of several disturbances the linear assumption must be taken into account.

Chapter 8

Conclusion and further work

This chapter makes conclusions of the discoveries made in this thesis. Later, proposals to further work is suggested.

8.1 Conclusion

The conclusions of this section will follow the structure of the research questions, presented in Chapter 1:

- How does the test infrastructure affect the test results?
- During the tests, the excitation voltage was deviating from its test specifications. Why?
- How truthful will the developed frequency responses be?
- How can the resulting frequency responses be applied for stability analysis?

8.1.1 How does the test infrastructure affect the test results?

Three issues are under concern related to the infrastructure: The idle current, other infrastructure inside the test terminals, and infrastructure between test excitation and measurements. The conclusions related to these concerns will now be presented:

The idle current is considered as test infrastructure, and not a part of the test component. This is because the idle current is not related to the dynamics of the vehicle. However, it might

affect the resulting frequency responses. Since the frequency responses only represent the dynamics of a system, only the modulated components of the current and voltage should be included when calculating the frequency responses. This is achieved in the calculations since the time to dq transformation filters the fundamental components. Thus, the measured steady state current will disappear during the time to dq transformation.

To avoid misunderstanding of this topics in the future, this master thesis suggest a correction to the "DQ approach". This suggestions requires that the fundamental components and the modulation components are isolated when they are presented as phasors. This is supported by the fact that the phasor domains of fundamental-, direct modulated-, and quadrature modulated components differ. In spite of the ignorance of the fundamental component, they are still included as the model is based on a fixed operation point, determined by the fundamental voltage and current.

Since a line and a cable was included inside the test terminals, they are affecting the measured frequency response. Compensations for this infrastructure has to be done in order to isolate the frequency response of the electric vehicle. The analytic frequency responses of an inductor, a capacitor and a resistor is presented. When these are given as 2×2 frequency response matrices, well known circuit calculations can be applied on the modulation domain of the system. Regular phasor calculations is then performed by vectors and matrices for the whole range of the frequencies. As the parameters for the topology is given, the frequency responses of the electric vehicle is found by compensating for a short line and cable. The result of the compensation shows that the short cable and line hardly affect the frequency responses of the system. This is expected as the impedance of the line is much lower than the "impedance approach " of the vehicle's regulation system.

The test infrastructure between the voltage excitation and the measurements might give distorted test voltages. In addition, imperfect "dq sweeps" during the "dq tests" was observed. The distortion from the infrastructure will be included in this larger issue of imperfect sweeps, and will be discussed in the two next sections.

8.1.2 During the tests, the excitation voltage was deviating from its test specifications. Why?

The excitation voltage measured at the line at Alnabru does not correspond to the test specifications. The deviation is recognized in the modulation phase, modulation direction, and the modulation amplitude. These deviation are illustrated with plots.

In order to investigate the deviation, many analyzes was performed. The most important discoveries are:

- The deviations are not caused by the voltage drop over the transformer.

- Linear smooth increasing phase deviations in the modulation domain are transformed to constant phase deviations in the fundamental domain.

- The tendency of all phase deviations are equal. This tendency has some correlation with the tendency of the current. The responses themselves are not directly correlating, but the four stages of the tendencies have some interesting relations. Therefore the phase deviation might be a result of the operation mode of the static converter.

- The leakage of direct modulated voltage to quadrature modulated voltage during the d-sweep, and vica versa, might be related to the modulation angel reference. This deviation might be related to numeric issues during time to dq transformation, but is probably related to non ideal converter.

- The decreasing voltage amplitude for increasing modulation voltage is most likely caused by non ideal static converter.

These discoveries do not only explain the behavior of some isolated tests: They explain some fundamental characteristic of an oscillating system modeled with modulation component. Some of the behavior of this "dq tests" might therefore appears on later "dq test". This is probably the case for e.g. the linear increasing modulation phase.

8.1.3 How truthful will the developed frequency responses be?

The reliability of the frequency responses will be discussed in light of the imperfect voltage sweep and sources of other possible issues. The affect of the rest of the topology can be removed by compensations, as concluded earlier. The linearization needs to be taken into account, as earlier concluded.

The imperfect voltage sweep is recognized by the modulation phase, modulation direction and the amplitude. It is shown that the modulation phase and the modulation direction probably have no affect on the resulting frequency responses. This can be explained by support of the matrix equation that show the relation between the vehicle's admittance, the test voltage and the resulting current: The matrix equation solves the system, in respect of the vehicle's admittances, by using two datasets. These two datasets are measured during two sweeps. There are just one requirement for the linear system to be solved: The voltage sweeps can not be performed in the same modulation direction. The mathematical approach claims linear independent voltage sweeps: The voltage matrix can not be invertible or nonsingular. On the other hand, the modulation amplitude affects the result of frequency response due to the nonlinear system. If the voltage amplitude deviates from the linear operation point, the accuracy of the model will loose accuracy. The accuracy is dependent of the nonlinear behavior. This behavior can be investigated by comparisons of the frequency responses of different linearization points.

Other possible limitations for achieving the correct frequency response might be numeric issues or limitation of the current supplement from the static converter. The numeric issues are considered to be small. The dq transformed measurements looks like they are prone to numeric issues. However, the most of the behavior is explained during investigations of imperfect voltage. The current supplement might be limited by the static converter. Thus, the non optimal static converter might not be sufficient to achieve correct test result from the "dq test". However, the size of the current are always small, which ease the operation of the static converter. If the static converter has to decrease the supplement of current. The voltage will probably follow as well. This could be the case for the decreasing voltage for higher frequencies. In that case, the current limit cause no problems since the equation will take into account the lower voltage.

8.1.4 How can the resulting frequency responses be applied for stability analysis?

The "DQ approach" describes the behavior of the systems components by an input-output-approach in the dq system. Thus, the facilities for performing stability analysis are quite good. Each component creates a *multiple input multiple output system* and can be decoupled from the rest of the system. The same rules as for regular linear state space modeling are applicable. Regular circuit analysis, but on matrix and vector form, is also applicable. Analytically derived components and test derived components can be combined in the same system. In case of numeric frequency response extracted from measurements, the response can further be extracted to transfer functions, as conducted in this thesis. When the system is modeled with several components, the components can easily be combined to new components. As shown, a system with multiple vehicles with multiple lines can be combined into one single load component that interacts with a source. In that case the stability criterion for MIMO-system can be used or simulation can be conducted. Notice that the system is nonlinear and just valid for given operation point(s) and limited disturbances.

8.2 Futher work

The goal of this master thesis was to achieve a model of the dynamic behavior of an electric traction system. This goal was set in order to come one step closer to solve problems related to low frequency power oscillation of the electric traction system.

In more detail; this thesis was supposed to do analysis related to the "DQ approach", so the dynamics of the electric vehicle could be modeled in the dq-frame without knowing the inner topology of the vehicle. This has been achieved by extracting a set of frequency responses from measurements on a vehicle. Further, these frequency responses have been modified to be independent of the test topology. They are verified as correct, but with some limitation. The verification is based on analysis of the excitation voltage, and studies of the mathematically formulation of the "DQ approach". Some of the strange behavior of the excitation voltage is explained, and the mathematically description shows that the frequency responses are inde-

pendent of the modulation direction and modulation phase. However, limitations are related to the linearization. This is because the excitation voltage was variating and escaping from the linearization point.

I recommend in further work to complete the modeling of the vehicle. The modeling can be considered as finished for ID33d and ID33q, which represent one linearization point and one operation point. If frequency responses are achieved for the other tests, two further tasks can be conducted: Comparisons of the frequency responses can be conducted in order to exclude some possible errors. In spite of nonlinear behavior and different responses for different operation points, the sets of frequency responses have probably much of the same responses. This is a great opportunity to detect errors. The other task I want ot recommend, is to establish methods to model the nonlinear behavior. Linear modeling of nonlinear systems is widely applied, so this will be a solvable task. In both cases, the extraction of the numeric frequency response will probably be a powerful tool. Such an extraction have been fast and successfully performed in this thesis.

When a robust model, or models, of the vehicle is established, stability analysis can be conducted. The analytic frequency response of an inductor, a resistor and a capacitor is given in this thesis. Methods so these components can be combined to larger RLC components is also presented. In this way, the frequency responses of much infrastructure can be modeled. This infrastructure includes lines, cables, grid filter and transformers. More advance components, such as other vehicles, static converters or rotary converter, can both be modeled analytically or by performing "DQ tests".

The modeling of the larger system should be achievable when each component is presented by its frequency responses. As each component are clearly defined by its input and output, and independent from the rest of the system, standard linear state space modeling can be used to model the traction system. This is briefly presented in this thesis. When models are established, the reasons for the low frequency instability issues might be detected. When the issues are detected, the low frequency instability problem can be solved by better regulation of the vehicle, static converter, or rotary converter. As the advance traction vehicle probably has most of the fault of the instability, requirements of the frequency response of the vehicle can be made. The manufactures of the vehicle know the inner topology of it, and should therefore known how to

satisfy these requirements.

In the end I hope that the work will be a contribution to solve the issues related to electric traction system instability. The methods presented here may be adaptable to other systems as well. I also hope that this thesis has inspired to further work in the field of dynamic modeling of electric systems.

Bibliography

[1] Alstad, O. (2015). Frequency reponse Presentation in the dq-frame for Power Systems Components.

[2] Danielsen, S. (2010). *Electric Traction Power System Stability*. PhD thesis.

[3] Danielsen, S. and Pika, S. Measurments from DQ-sweep test preformed at Alnabru, 28th of June, 2014. In this project measurments ID33d and ID33q is studiet.

[4] der Linden, T. V. (2012). Dynamic control of static converters. Master's thesis, Norwegian University of Science and Technology.

[5] Gonzalez, M., Cardenas, V., and Pazos, F. (2004). Dq transformation development for single-phase systems to compensate harmonic distortion and reactive power. In *Power Electronics Congress, 2004. CIEP 2004. 9th IEEE International*, pages 177–182.

[6] Harnefors, L. (2007). Modeling of three-phase dynamic systems using complex transfer functions and transfer matrices. *Industrial Electronics, IEEE Transactions on*, 54(4):2239–2248.

[7] Kiessling, F., Puschmann, R., Schmieder, A., and Schneider, E. (2009). *Contact Lines for Electric Railways. Planning, Design, Implementation, Maintenance*.

[8] Kreyszig, E. (1988). *Advanced engineering mathematics*. John Wiley & Sons.

[9] Menth, S. and Meyer, M. *Results of pilot measurment with...* Technical report, Document 14-0561, emkamatik GmbH.

[10] Menth, S. and Meyer, M. (2006). Low frequency power oscillations in electric railway systems. *ELEKTRISCHE BAHNEN-CHARLOTTENBURG THEN BERLIN THEN MUNCHEN-*, 104(5):216.

[11] Meyer, M. Function for calculating low frequency (subharmonic) modulation signals for voltage and current domain signals.

[12] Meyer, M. (2012). Concepts for measurements of "dq" frequency responses. (12-0459).

[13] Nilsson, J. W. and Riedel, S. A. (2009). *Electric circuits*, volume 8. Prentice Hall.

[14] Östlund, S. (2005). Electrical traction (original title in swedish). *KTH, Stockholm*, 153:154.

[15] Park, R. H. (1929). Two-reaction theory of synchronous machines generalized method of analysis-part i. *American Institute of Electrical Engineers, Transactions of the*, 48(3):716–727.

[16] Pika, S. Test report alnabru 2014-06. Technical report, Jernbaneverket.

[17] Pika, S. (2015). Description of dq approach to stability of electric traction system.

[18] Pika, S. and Danielsen, S. (2010). Understanding of the stability criterion for a double-feedback loop system. In *Electrical Systems for Aircraft, Railway and Ship Propulsion (ESARS), 2010*, pages 1–5. IEEE.

[19] Steimel, A. (2008). *Electric traction-motive power and energy supply: basics and practical experience*. Oldenbourg Industrieverlag.

Appendix A

Change of modulation reference

The modulation components are dependent of the reference phase of the system. If the modulation phase is static in relation to a time reference, the modulation components still will change if the reference of the modulation change. This section takes into account a change of reference equal $\Delta\theta$, which might be caused by a change of the fundamental phase; $\Delta\theta = \Delta\theta_{fund}$. This is discussed in the light of the equation for a modulated signal in the time frame, given Equation 2.3. This equation is repeated in A.1, where just the modulation components is included. Phases in the modulation frame is highlighted with blue text, and phases in the fundamental frame is highlighted with red text.

$$\begin{aligned} u_{mod}(t) = \\ U_{da}\cos(\omega_N t)\cos(\omega_T t) - U_{db}\cos(\omega_N t)\sin(\omega_T t) \\ -U_{qa}\sin(\omega_N t)\cos(\omega_T t) + U_{qa}\sin(\omega_N t)\sin(\omega_T t) \end{aligned} \tag{A.1}$$

Futher, clean direct sweep with modulation phase equals zero, is assumed, as shown in Equation A.2:

$$u_{mod}(t) = U_{da}\cos(\omega_N t)\cos(\omega_T t) \tag{A.2}$$

Now, the change of reference, $\Delta\theta$, is included. $\Delta\theta$ is given in fundamental degrees. Therefore $\Delta\theta$ is just added in the red cosine argument, which is given in fundamental degrees. In the blue

cosine argument, which is given in modulation degrees, the change of reference is converted to modulation degrees by the factor $\frac{\omega_T}{\omega_N}$. The result of the change of the reference is given by Equation A.3:

$$u_{mod}(t) = U_{da}\cos(\omega_N t + \Delta\theta)\cos(\omega_T t + \frac{\omega_T}{\omega_N}\Delta\theta) \tag{A.3}$$

The addition formula for cosine expressions, $\cos(ax+b) = \cos(b)\cos(ax) - \sin(b)sin(ax)$, is applied on both terms of Equation A.3. The result after the multiplication is shown in Equation A.4:

$$\begin{aligned} u_{mod}(t) = \\ U_{da}\cos(\Delta\theta)\cos(\frac{\omega_T}{\omega_N}\Delta\theta)\cos(\omega_N t)\cos(\omega_T t) + U_{da}\cos(\Delta\theta)\sin(\frac{\omega_T}{\omega_N}\Delta\theta)\cos(\omega_N t)\sin(\omega_T t) \\ +U_{da}\sin(\Delta\theta)\cos(\frac{\omega_T}{\omega_N}\Delta\theta)\sin(\omega_N t)\cos(\omega_T t) + U_{da}\sin(\Delta\theta)\sin(\frac{\omega_T}{\omega_N}\Delta\theta)\sin(\omega_N t)\sin(\omega_T t) \end{aligned} \tag{A.4}$$

The change of modulation direction and modulation phase is then shown in Equation A.4. By assuming $\cos(\frac{\omega_T}{\omega_N}\Delta\theta) \approx 1$ and $\sin(\Delta\theta)\sin(\frac{\omega_T}{\omega_N}\Delta\theta) \approx 0$, and consider Equation A.4, the leakage from the direct component modulation to the quadrature modulation is given by Equation A.5:

$$|U_{q,d-sweep}| = \sin(\Delta\theta)|U_{d,d-sweep}| \tag{A.5}$$

The corresponding same equation is valid for leakage to the direct component for a q-sweep. In general, the correction of the direct component and quadrature component, after a change in reference $\Delta\theta$, is given by Equation A.6 and Equation A.7, respectively:

$$U_d(\Delta\theta) = \cos(\Delta\theta)U_{d,\Delta\theta=0} + \sin(\Delta\theta)U_{q,\Delta\theta=0} \tag{A.6}$$

$$U_d(\Delta\theta) = \sin(\Delta\theta)U_{d,\Delta\theta=0} + \cos(\Delta\theta)U_{q,\Delta\theta=0} \tag{A.7}$$

The change of phase of the direct modulated voltage is given by Equation A.8:

$$\Delta\theta_{mod} = \frac{\omega_T}{\omega_N}\Delta\theta_{fund} \tag{A.8}$$

Appendix B

Data of topology

Table B.1: Line parameters of the line at Alnabru

Parameter	**Unit**	**Value**	**Reference**
r_{line} - Resistance per length	Ω/km	0.19	Danielsen, Appendix B1, [2]
x_{line} - Reactance per length	Ω/km	0.21	Danielsen, Appendix B1, [2]
l_{line} - Length of the line	km	0.500	[9]

Table B.2: Cable parameters of the cable at Alnabru

Parameter	**Unit**	**Value**	**Reference**
r_{cable} - Resistance per length	Ω/km	0.107	JBV [**?**]
x_{cable} - Reactance per length	Ω/km	0.21	JBV [**?**]
C'_{cable} - Shunt capacitance per length	$\mu F/km$	0.15	No data availbl.
l_{cable} - Length of the cable	km	0.510	JBV [**?**]

Parameter	Value	Unit
Rated power	12.510	[MVA]
Primary voltage	16.5	[kV]
Secondary voltage	4	[kV]
Leakage reactance	0.1183	[pu]
Copper resistance	0.011	[pu]
Connection type	i-i	

Figure B.1: The 16 2/3 Hz power transformer used in calculation. Collected from the master thesis of T.v.d.Linden[4]

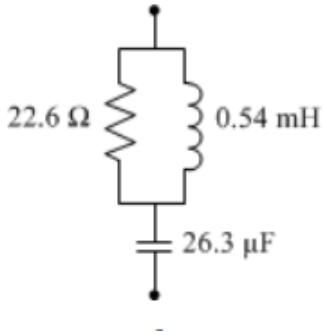

Figure B.2: The 16 2/3 Hz power grid filter used in calculation. Collected from the master thesis of T.v.d.Linden[4]

Appendix C

Measured voltage modulation, time frame

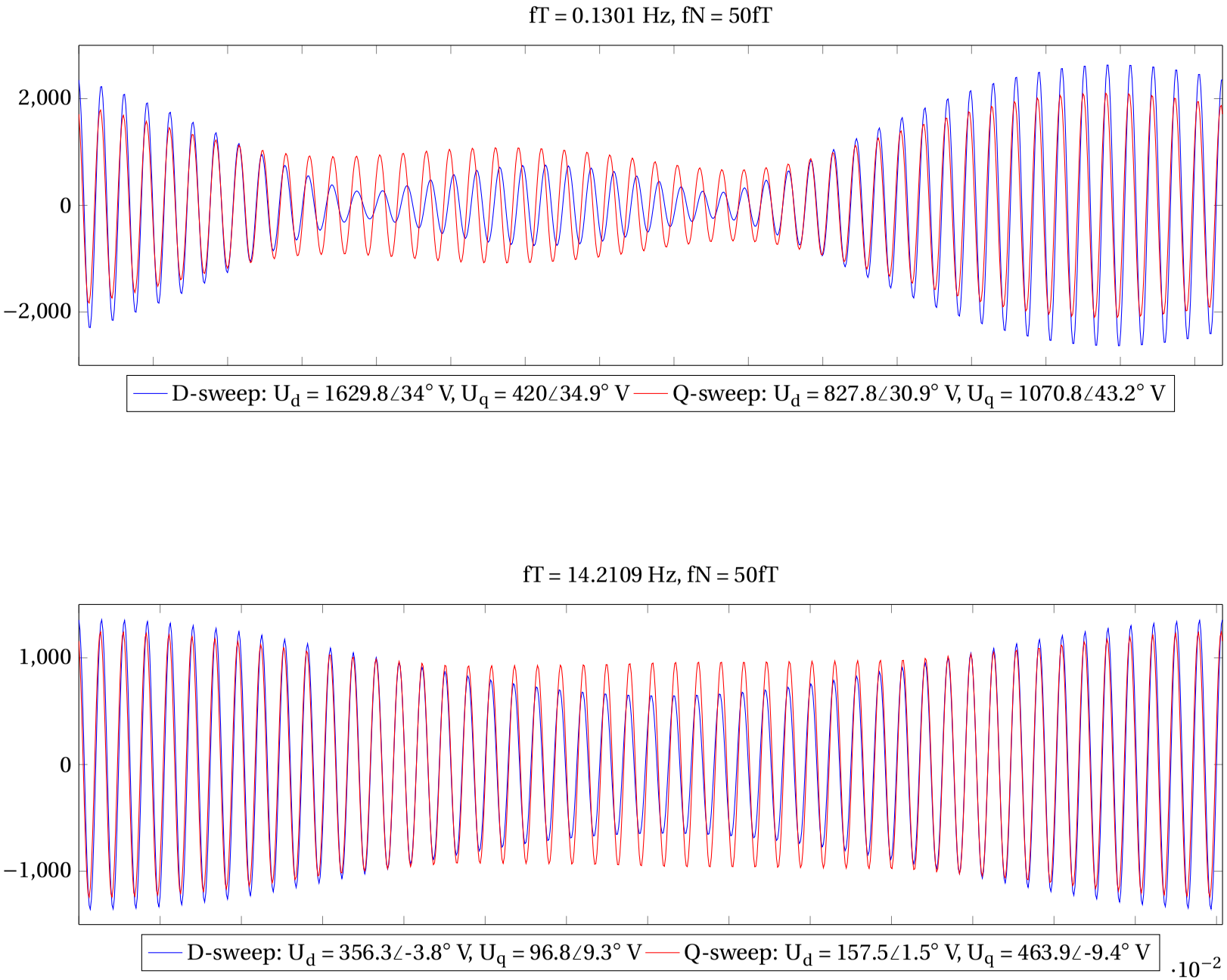

Figure C.1: Time domain presentation of the frequency components from measurements of test ID33d and ID33q at Alnabru[16]. The fundamental voltage and fundamental frequency is modified in order to make the modulation components more visible. Each plot last for one modulation period. More information in Sec. 5.2.4

Appendix D

Time to dq transform of artificial signals

Artificial voltage sweeps are generated by use of Equation 2.3. The signal is perfectly generated as specified by the test specifications (Table 5.1) at Alnabru [16]. The perfect signal is transformed from time frame to the dq frame by the t2dq-function by Meyer[11]. The same modulation frequencies as for the test at Alnbru is used. The resulting modulation components are not perfect. This is because of limited length (time) of the signal and therefore not optimal frequency fit for many pairs of modultion- and fundamental frequencies. The length of the signal that is transformed is $t_n = round(n \cdot \frac{f_N}{fT})$. Larger n gives better accuracy as the ratio between the modulation period and the fundamental period is closer to an integer. In Figure D.1 - D.4 in Appendix D, the modulation components are plotet for $n = 1, 10, 100 and 1000$.:

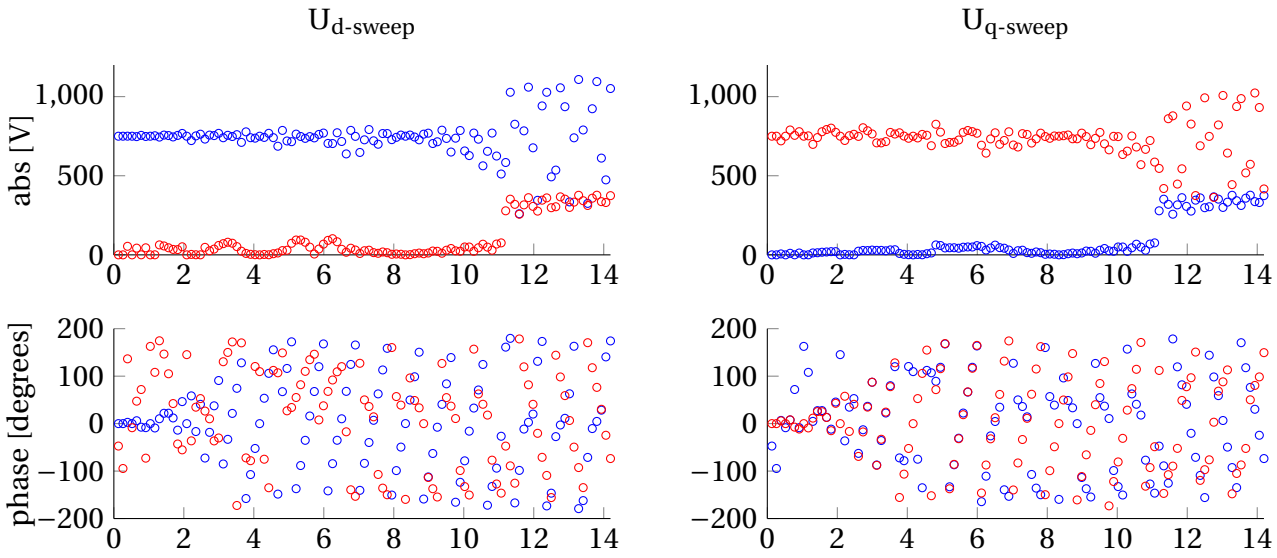

Figure D.1: Dq transformation on artificial signal. $n = 1$

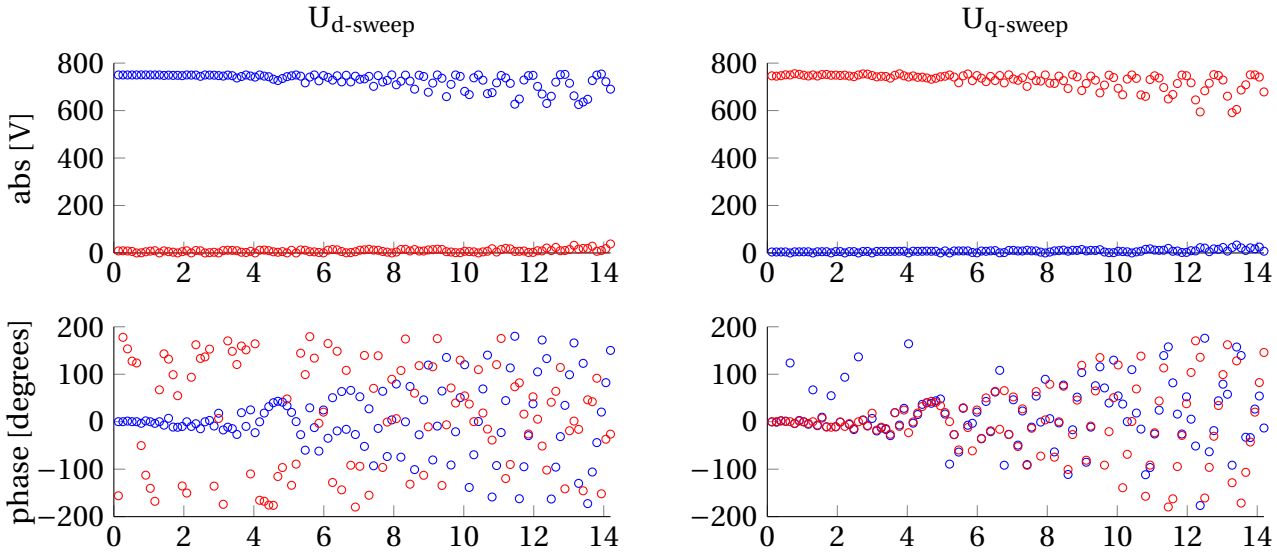

Figure D.2: Dq transformation on artificial signal. $n = 10$

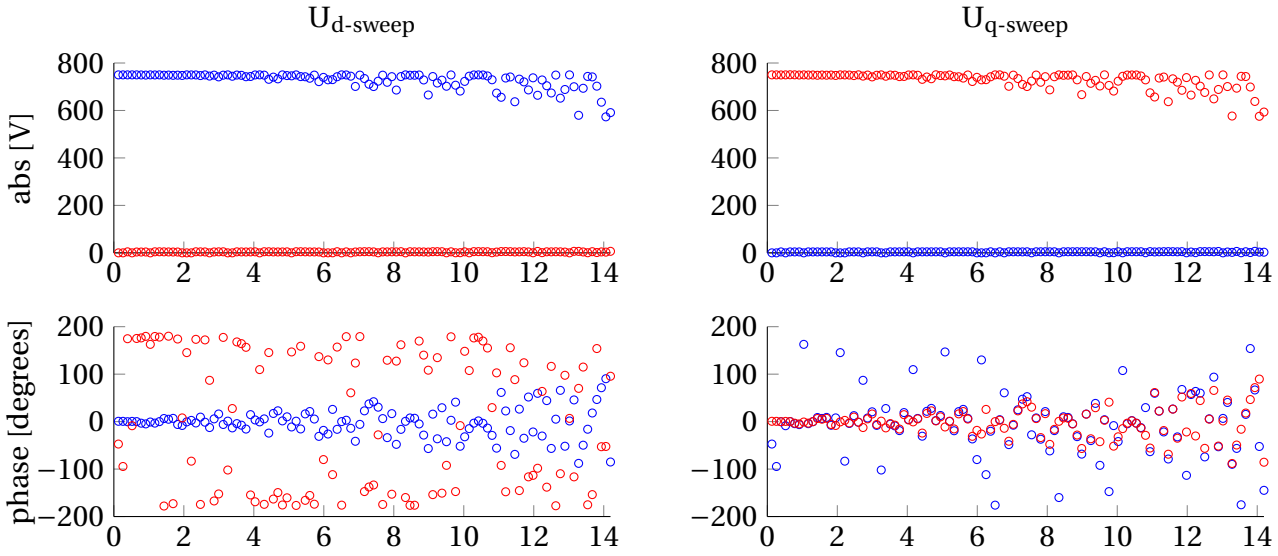

Figure D.3: Dq transformation on artificial signal. $n = 100$

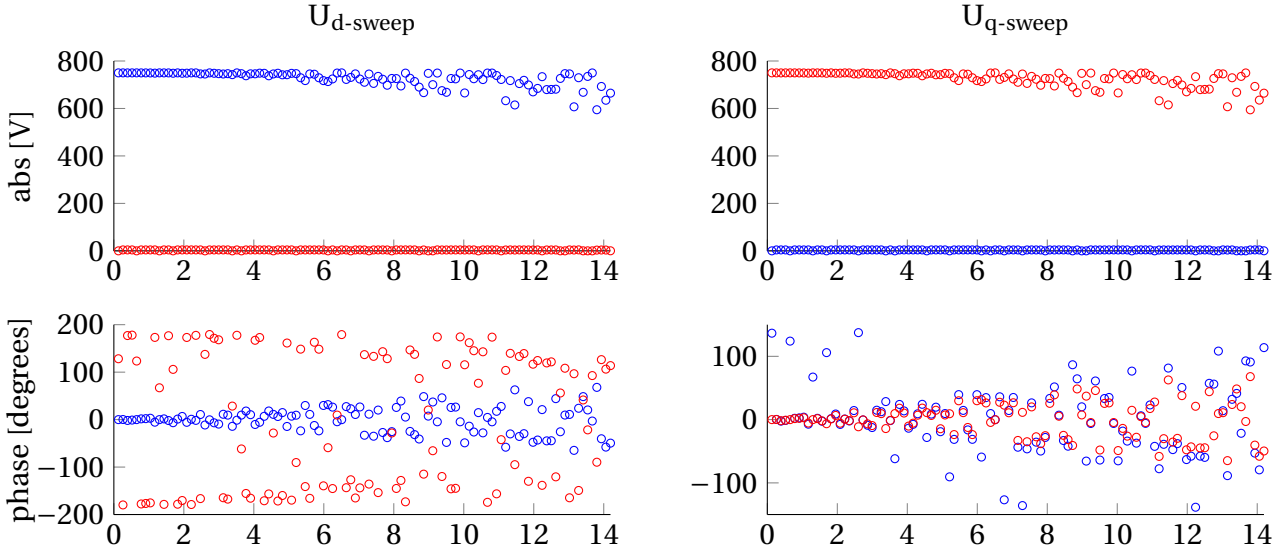

Figure D.4: Dq transformation on artificial signal. $n = 1000$

Appendix E

Phasors to dq matrix

In Section 3.3.2, Equation E.1 where derived to be valid for a voltage described by a phasor $\bar{U} = U_d + jU_q$, and a current described by a phasor $\bar{I} = I_d + jI_q$.

$$\begin{bmatrix} U_d(s) \\ U_q(s) \end{bmatrix} = \begin{bmatrix} Ls & -\omega_s L \\ \omega_s L & Ls \end{bmatrix} \begin{bmatrix} bI_d(s) \\ I_q(s) \end{bmatrix}, s = \omega_{osc} \tag{E.1}$$

The same system is also valid for voltage described by $\bar{U} = U_d + kU_q$ and $\bar{I} = I_d + iI_q$, where the i is an operator that determines 90 *fundamental degrees* phase deviation. By assuming linear behavior of the inductor, it is clear that E.1 is valid for two other pairs of voltages and currents: $\bar{U}_{Re} = U_{d,Re} + iU_{q,Re}$ and $\bar{I}_{Re} = I_{d,Re} + iI_{q,Re}$, and $\bar{U}_{Im} = U_{d,Im} + iU_{q,Im}$ and $\bar{I}_{Im} = I_{d,Im} + iI_{q,Im}$:

$$\begin{bmatrix} U_{d,Re}(s) \\ U_{q,Re}(s) \end{bmatrix} = \begin{bmatrix} Ls & -\omega_s L \\ \omega_s L & Ls \end{bmatrix} \begin{bmatrix} I_{d,Re}(s) \\ I_{q,Re}(s) \end{bmatrix}, s = \omega_{osc} \tag{E.2}$$

$$\begin{bmatrix} U_{d,Im}(s) \\ U_{q,Im}(s) \end{bmatrix} = \begin{bmatrix} Ls & -\omega_s L \\ \omega_s L & Ls \end{bmatrix} \begin{bmatrix} I_{d,Im}(s) \\ I_{q,Im}(s) \end{bmatrix}, s = \omega_{osc} \tag{E.3}$$

As the inductor is assumed linear, the components can be any voltages and currents, also the modulation components of a voltage and current. In that case the i operator determines *90 fundamental degrees*, and the j operator determines *90 modulation degrees*. Equation E.2 and j times Equation E.3 can be added together, and creates into Equation E.4 ($E.4 = E.2 + jE.3$):

$$\begin{bmatrix} U_{d,Re}(s) + jU_{d,Im}(s) \\ U_{q,Re}(s) + jU_{q,Im}(s) \end{bmatrix} = \begin{bmatrix} Ls & -\omega_s L \\ \omega_s L & Ls \end{bmatrix} \begin{bmatrix} I_{d,Re}(s) + jI_{d,Im}(s) \\ I_{q,Re}(s) + jI_{q,Im}(s) \end{bmatrix}, s = \omega_{osc} \tag{E.4}$$

By applying $\overline{U}_x = U_{x,Re} + jU_{x,Im}$, Equation E.4 can be described by Equation E.5:

$$\begin{bmatrix} \bar{U}_d(s) \\ \bar{U}_q(s) \end{bmatrix} = \begin{bmatrix} Ls & -\omega_s L \\ \omega_s L & Ls \end{bmatrix} \begin{bmatrix} \bar{I}_d(s) \\ \bar{I}_q(s) \end{bmatrix} = \begin{bmatrix} Z_{dd}(s) & Z_{dq}(s) \\ Z_{qd}(s) & Z_{qq}(s) \end{bmatrix} \begin{bmatrix} \bar{I}_d(s) \\ \bar{I}_q(s) \end{bmatrix}, s = \omega_{osc} \tag{E.5}$$

Appendix F

Current plots

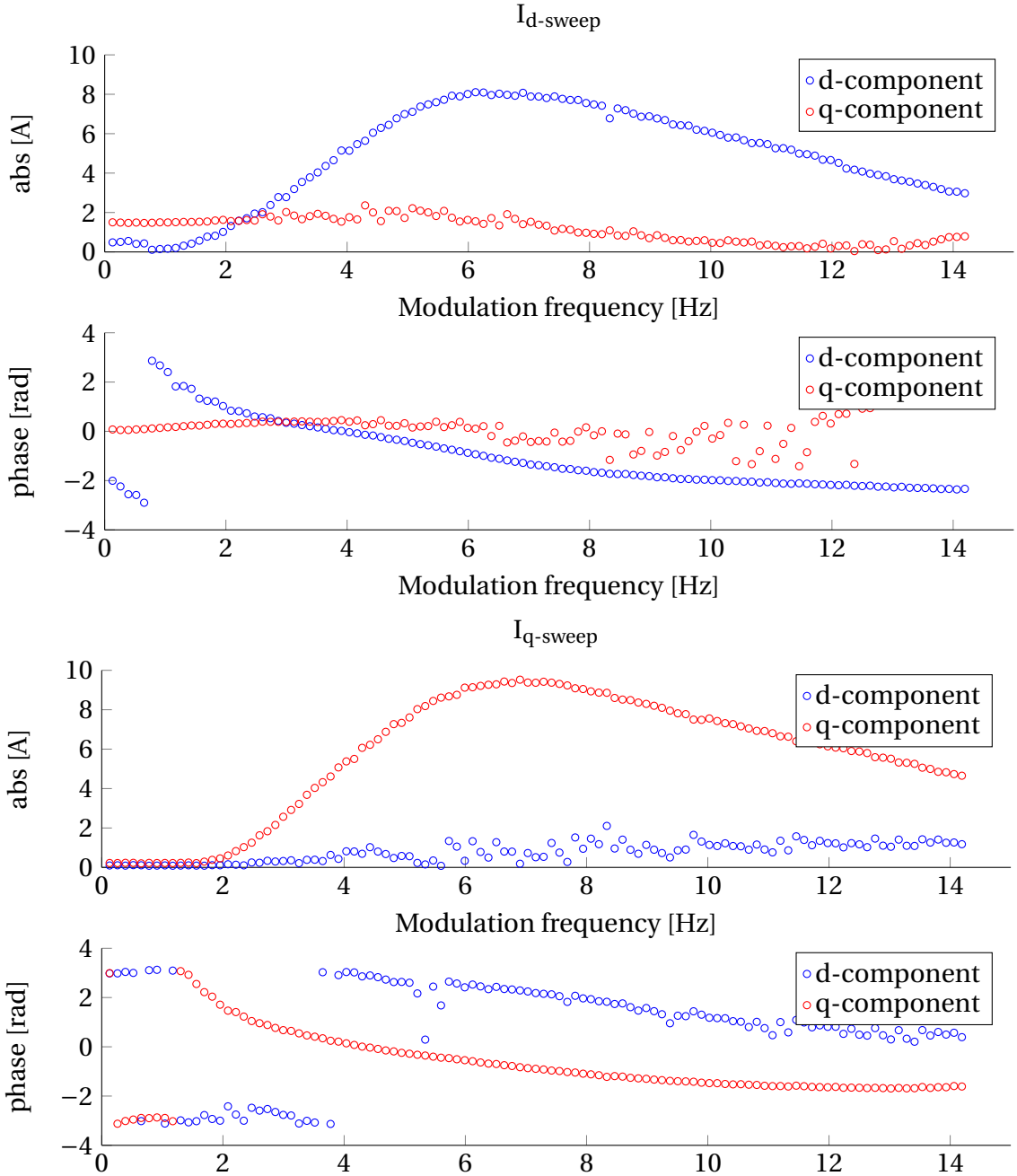

List of Figures

List of Tables